European Journal of Taxonomy 949: 1–96
https://doi.org/10.5852/ejt.2024.949.2641
ISSN 2118-9773
www.europeanjournaloftaxonomy.eu
2024 · Borrero-Pérez G.H. *et al.*

Monograph

urn:lsid:zoobank.org:pub:EA45BD5E-98F7-4229-A4FD-E377D6BC8591

Understanding the color variability and resolving taxonomic confusion in the sea cucumber *Isostichopus badionotus* (Echinodermata, Holothuroidea): a revision of the genus *Isostichopus*

Giomar H. BORRERO-PÉREZ [1,*], Francisco A. SOLÍS-MARÍN [2] & Harilaos LESSIOS [3]

[1]Current affiliation: independent researcher, Santa Marta, Magdalena, Colombia.
[1]Instituto de Investigaciones Marinas y Costeras – Invemar, Calle 25 No. 2–55, Playa Salguero, Rodadero, Santa Marta, Colombia.
[2]Instituto de Ciencias del Mar y Limnología, Universidad Nacional Autónoma de México, 04510, Ciudad de Mexico, México.
[1,3]Smithsonian Tropical Research Institute – STRI, BOX 0843-03092, Balboa, Panama.

[*]Corresponding author: giomarborrero@gmail.com
[2]Email: fasolis@cmarl.unam.mx
[3]Email: lessiosh@si.edu

[1]urn:lsid:zoobank.org:author:987B3945-3A71-4DF0-B860-F23CC231F34C
[2]urn:lsid:zoobank.org:author:A2417F0D-CA2A-4BE2-A6F0-C8991F4B90EA
[3]urn:lsid:zoobank.org:author:B59566D2-3326-4026-B9B6-9AB12A3EB140

Abstract. *Isostichopus badionotus* (Selenka, 1867) is distributed in the Atlantic Ocean. It has been recognized as a species with highly variable intraspecific coloration. To clarify taxonomic confusion and show the characters for correct identification of this valuable species, mitochondrial DNA (16S and COI), color patterns, external and internal morphology, ossicles, and habitat were examined in specimens from museum collections and from original sampling. As part of the revision, *I. fuscus* (Ludwig, 1875) from the Eastern Pacific Ocean and *I. macroparentheses* (Clark, 1922) from the Caribbean Sea, the only other two species currently recognized in the genus *Isostichopus*, were included. It was concluded that *I. fuscus* and *I. macroparentheses* are distinct and valid species, and that *I. badionotus* consists of two species: *I. badionotus* and *I. maculatus* (Greeff, 1882), previously synonymized as *I. baqdionotus* by Clark (1922). *Isostichopus maculatus* includes two subspecies, the nominal *I. maculatus maculatus* (Greeff, 1882) and *I. maculatus phoenius* (Clark, 1922), described as *Stichopus badionotus* var. *phoenius* Clark, 1922. *Isostichopus maculatus maculatus*, distributed in the East Atlantic, is very similar to *I. maculatus phoenius*, but differs in DNA characters, color pattern, and the size and shape of the tables in the dorsal papillae. *Isostichopus maculatus phoenius*, widely distributed in the Caribbean Sea and the Gulf of Mexico, is sympatric with *I. badionotus*, has similar ossicles but is clearly distinguished by its DNA sequences, color patterns, and habitat preferences. For the first time, ossicles from internal organs are described for *Isostichopus*, enhancing original species descriptions. Distribution maps, habitat, biology, conservation status, and a taxonomic key for distinguishing these species to aid their fishery management and aquaculture are presented.

Keywords. Integrative taxonomy, Atlantic, Eastern Pacific, commercially important, conservation status.

Borrero-Pérez G.H., Solís-Marín F.A. & Lessios H. 2024. Understanding the color variability and resolving taxonomic confusion in the sea cucumber *Isostichopus badionotus* (Echinodermata, Holothuroidea): a revision of the genus *Isostichopus*. *European Journal of Taxonomy* 949: 1–96. https://doi.org/10.5852/ejt.2024.949.2641

Table of contents

Introduction

The genus *Isostichopus*, erected by Deichmann (1958) and distributed in the Eastern Pacific and the Atlantic Ocean, is easily recognized by external morphology and ossicles. However, identifying the species within the genus is not easy because of their similarity in ossicle shape and their ontogenetic variation. Currently, *Isostichopus* includes three species: *I. badionotus* (Selenka, 1867), *I. macroparentheses* (Clark, 1922), and *I. fuscus* (Ludwig, 1875). Molecular phylogeny of the family Stichopodidae has recovered the genus as a monophyletic clade, sister to all species of *Stichopus* Brandt, 1835 (Byrne *et al.* 2010), a mainly Indo-West Pacific genus, with some species in the Eastern Pacific (Uthicke *et al.* 2010; Wen *et al.* 2011).

The "tree-rowed", "four-sided", or "chocolate chip" sea cucumber *Isostichopus badionotus*, previously *Stichopus badionotus*, has been the subject of extensive taxonomic confusion that involves the other two species, *I. macroparentheses*, and *I. fuscus*. Clark (1922) synonymized all eight species of *Stichopus* described at that time in the West and East Atlantic Ocean under a single name, *Stichopus badionotus.* On the basis of his detailed revision, *I. badionotus* has been recognized and accepted as a highly color variable species widely distributed in the Atlantic Ocean, including Angola (Bell 1883; Théel 1886, previously described as *Stichopus assimilis* Bell, 1883), the Gulf of Guinea (Greeff 1882; described as *Stichopus maculatus* Greeff, 1882; Cherbonnier 1975, as *Stichopus badionotus*), Ascension Island (as *Isostichopus badionotus* Pawson 1978, Cape Verde Island (also as *I. badionotus* Pérez-Ruzafa *et al.* 1999, 2003; Entrambasaguas 2008; Entrambasaguas *et al.* 2008), Bermuda, east coast of United States from North Carolina to Florida, Haiti (Semper 1868, originally described as *Stichopus haytiensis* Semper, 1868), the Virgin Islands (Sluiter 1910, as *Stichopus haytiensis*), Bermuda (Heilprin 1888 and Clark 1899, described as *Stichopus diaboli* Heilprin, 1888 and *Stichopus xanthomela* Heilprin, 1888),

Gulf of Mexico, Caribbean Sea, and the subtropical Atlantic (Brazil) (Deichmann 1957, as *Stichopus badionotus*; Miller & Pawson 1984; Hendler *et al.* 1995; Cutress 1996; Pawson *et al.* 2010; Borrero-Pérez *et al.* 2012; Purcell *et al.* 2012; Toral Granda *et al.* 2013; Prata *et al.* 2014, as *I. badionotus*).

Clark (1922) assigned a single specimen collected on Buccoo Reef (Tobago) to *Stichopus badionotus* var. *phoenius* (see also Clark 1933: 1909). He thought that it was justifiable to recognize a separate variety for this specimen because of its bright carmine-red color in life. However, this variety has not been noted since Clark (1933). Clark (1922) described *Stichopus macroparentheses* (currently *I. macroparentheses*) as a new species based on two juvenile specimens; Deichmann (1957) synonymized *I. macroparentheses* (as *S. macroparentheses*) with *I. badionotus* (as *S. badionotus*). Since then, some authors have considered *I. macroparentheses* as a subjective junior synonym of *I. badionotus* (Miller & Pawson 1984; Cutress 1996; Pawson *et al.* 2010), whereas others continued to consider it as a valid species, but without a morphological description that includes adult specimens to identify diagnostic characters (Pawson 1976; Laguarda-Figueras *et al.* 2005; Alvarado & Solís-Marín 2013). In addition, Clark (1922) considered *Isostichopus fuscus* from the Eastern Pacific as a form that "had never been adequately diagnosed or associated with any well-known holothurians". Deichmann (1958) clarified the taxonomic status of *I. fuscus*, recognizing part of Selenka's cotypes of *I. badionotus* as *I. fuscus* and proposing morphological characters for distinguishing them.

Isostichopus, especially *I. badionotus* and *I. fuscus*, can be considered as the most valuable species in the holothuroid fishery industry of the Caribbean Sea and the Eastern Tropical Pacific, respectively (Purcell *et al.* 2012). Indiscriminate and illegal exploitation occurs in many Caribbean and Pacific regions (Toral-Granda 2008a, 2008b; Rogers *et al.* 2017). An extreme exploitation case was reported for *I. fuscus* in the Galapagos Islands, which led to the inclusion of this species in the IUCN red list of threatened species in the category of "Endangered" and Appendix III of CITES (Toral-Granda 2008b; Mercier *et al.* 2013). *Isostichopus badionotus* is included in the IUCN red list in the category of "Least Concern" (Toral-Granda *et al.* 2013). Because of the increasing value of *I. badionotus* in the fishery industry in the Caribbean Sea, efforts to characterize natural populations for fishery management and to farm it have been developed in many countries (Guzmán & Guevara 2002; Guzmán *et al.* 2003; Alfonso *et al.* 2004; Lacerda-Miceli & Scott 2005; Toral-Granda 2008a; Invemar 2013, 2014, 2015; Rodríguez-Forero *et al.* 2013; Rogers 2013; Zacarías-Soto *et al.* 2013; Agudelo & Rodríguez 2015). Associated with the fisheries, a new misperception has surfaced: *Stichopus herrmanni* Semper, 1868, *S. variegatus* (= *Stichopus herrmanni variegatus* Semper, 1868) and three morphotypes of *Stichopus* sp. have been reported from the Colombian Caribbean Sea by Rodríguez-Forero *et al.* (2013), Agudelo & Rodríguez (2015) and Koike *et al.* (2015), even though the genus does not occur in the Atlantic and the mentioned species have an Indo-Pacific distribution. To increase the confusion, an unidentified *Isostichopus* sp. (Wen *et al.* 2011; Vergara & Rodríguez 2015, 2016; Acosta *et al.* 2020, 2021) and *Isostichopus* sp. aff *badionotus* (Agudelo-Martínez & Rodríguez-Forero 2017; Arias-Hernández *et al.* 2017) have been reported. Accurate species delineation, coupled with correct nomenclature, is essential for the success of any conservation or aquiculture and fishery effort.

To clarify the taxonomic status of species of *Isostichopus*, including the three currently recognized species and their synonyms, we present new evidence obtained from mitochondrial DNA, description of coloration patterns, external and internal morphology, and ossicle morphology and habitat preferences.

Material and methods

Sampling of taxa, color patterns, and habitat preference

Approximately 400 specimens of *Isostichopus badionotus* were collected or observed in situ, together with approximately 270 museum specimens (including types) from across the range of the species. Samples of *I. fuscus* and *I macroparentheses* were collected or examined from museum material from

the tropical eastern Pacific and western Atlantic respectively. Sampling was conducted by snorkeling and SCUBA diving at depths from 1 to 25 m. Specimens were photographed, recording their live appearance and habitat. Representative individuals were collected, relaxed in ~10% $MgCl_2$ solution, and preserved in 70% ethanol and/or subsampled in 96% ethanol for sequencing.

Collection acronyms, museum vouchers and type material

Acronyms of collections where specimens were examined or where specimens and tissues collected were deposited:

ICML-UNAM	=	Colección Nacional de Equinodermos, "Dra. Ma.E. Caso M.", Instituto de Ciencias del Mar y Limnología, Universidad Nacional Autónoma de México, México
INV EQU	=	Echinoderm collection, Museo de Historia Natural Marina de Colombia, Invemar, Colombia
INV TEJ	=	Tissue collection, Museo de Historia Natural Marina de Colombia, Invemar, Colombia
MBMLP	=	Museo de Biología Marina y Limnología, Universidad de Panamá, Panamá
MCZ	=	Museum of Comparative Zoology, Harvard University, USA
TbBT0002	=	This type of code indicates the tissues deposited in the Smithsonian Tropical Institute (Panama) (contact the first author)
UF	=	Florida Museum of Natural History, University of Florida, USA
USNM	=	National Museum of Natural History, Smithsonian Institution, USA
ZMH	=	Zoologisches Museum zu Universität Hamburg, Germany
ZMMU	=	Moscow Museum., Russia
ZOO	=	Natural History Museum of London, UK

Types examined

Stichopus badionotus Selenka, 1867. Syntype: MCZ HOL-509, designated here as lectotype.
Stichopus badionotus var. *phoenius* Clark, 1922. Holotype: MCZ HOL-1182.
Stichopus macroparentheses Clark, 1922. Holotype: MCZ HOL-921; ossicles plate MCZ HOL-225; paratype: MCZ HOL-1214.
Stichopus assimilis Bell, 1883. Holotype: Natural History Museum of London (ZOO) 1873.7.29.1.

Types examined through photos (at http://www.echinodermata.be/, currently disabled)
Stichopus haytiensis Semper, 1868. Holotype: ZMMU.
Stichopus moebii Semper, 1868. Holotype: ZMH.
Stichopus fuscus Ludwig, 1875. Syntype: ZMH E.2689.

Type material of *Stichopus maculatus* Greeff, 1882; *Stichopus errans* Ludwig, 1875; *Stichopus diaboli* Heilprin, 1888 and *Stichopus xanthomela* Heilprin, 1888 was not located. We designated a neotype (USNM E16150) and neoparatype (USNM E16151) for *I. maculatus maculatus* (Geeff, 1882).

Morphological description and terminology

External morphology

We recorded body cross-section; shape (described as "loaf-like" when body length <4× diameter); firmness, rugosity and average thickness of body wall; tentacle size, shape, and number; collar around the mouth; position of mouth and anus; shape and arrangement of dorsal papillae and ventral pedicels.

Color

Color variation was binned into 12 color patterns and coded accordingly (Fig. 1). They are explained and presented in detail in the taxonomic description of each species and in figures in the systematic account (Figs 8, 14, 17, 21, 24).

Internal morphology

We examined the shape and size of the calcareous ring (radial and interradial plates); the size of tentacle ampullae; number, shape, and length of Polian vesicles; number, shape, length, and attachment of stone canal; shape and size of madreporite; gonads; respiratory trees and longitudinal muscles.

Ossicles

Terminology of ossicle types for tables, rods, perforated plates, and end-plates is that proposed by Samyn *et al.* (2006) (Fig. 2). *Isostichopus* also contains some tridimensional spheres, not recorded previously (Fig. 2). Presence, size, and morphology of each type of ossicle were recorded from each body region. They were obtained from tentacles, dorsal and ventral body wall, dorsal papillae, ventral tube feet, longitudinal muscles, anterior and posterior cloaca (anterior part closest to the intestine and posterior part to de anus), respiratory trees, and gonads. Ossicles from specimens of comparable sizes from each species, as well as juveniles (body length <40 mm), were analyzed when possible. Ossicles were extracted with sodium hypochlorite, observed with light microscopy and photographed; a minimum of 10 ossicles per type were measured using ImageJ software (Schneider *et al.* 2012). For scanning electron microscopy (SEM), ossicles were washed with distilled water, then with 70%, 80%, 95% and 100% ethanol, mounted on stubs, coated with gold, and observed with a Zeiss Evo 40 VP scanning electron microscope at the Laboratory of Electron and Confocal Microscopy of the Smithsonian Tropical Research Institute, Panamá.

Table disc diameter (from bottom or top views, and from lateral view), pillar height and width of spire just below the crown was recorded. Tables were coded as high when height>disc diameter, medium when height = diameter, and low when height < diameter (Fig. 2). The maximum length was recorded for the rods and perforated plates.

DNA extraction, amplification, sequencing, and analysis

Mitochondrial sequences were obtained from 95 specimens previously identified as *Isostichopus badionotus*, 13 *I. fuscus* and six *I. macroparentheses* (Table 1). DNA was extracted using the QIAGEN DNeasy Blood & Tissue kit following the manufacturer's instructions. Partial fragments of two mitochondrial genes, the large ribosomal subunit (16S) and the cytochrome oxidase subunit 1 (COI), were amplified with primers 16SAR 5′-CGCCTGTTTATCAAAAACAT-3′ and 16SBR 5′-CTCCGGTTTGAACTCAGATCA-3′ (Palumbi 1996); COIceF 5′-ACTGCCCACGCCCTAGTAATGATATTTTTTATGGTNATGCC-3′ and COIceR 5′-TCGTGTGTCTACGTCCATTCCTACTGTRAACATRTG-3′ (Hoareau & Boissin 2010) and COI5r-5′-TTGRTTYTTTGGTCAYCCWGARGTYTA-3′ and COI5rd 5′-TCAGARTAWCGYCGWGG-3′ (A. Hiller unpubl. data). PCRs were carried out following Hoareau & Boissin (2010) for both 16S and COI. PCR products were purified using Exo/SAP and sequenced using BigDye ver. 3.1 (Applied Biosystems) technology. The nucleotide sequences were edited using Sequencher ver. 5.1.

In COI, we analyzed one fragment of 572 bp from 58 specimens (including outgroups and GenBank sequences) obtained with primers COIceF-COIceR (COI-Fr1). This fragment is located at positions 288 to 859 of the complete COI gene of *Apostichopus japonicus* (Selenka, 1867) (GenBank Accession no. NC012616.1). We also sequenced a second fragment of 455 bp of COI from 75 specimens with primers COI5r-COI5rd (COI-Fr2) located at positions 858 to 1312 bp of *A. japonicus*. In 16S, we sequenced a fragment of 468 bp from 116 specimens. All sequences were submitted to GenBank (Table 1). Unpublished sequences from other projects as well as from GenBank are part of the data set, including the outgroups (Table 1). The sequences of COI and of 16S were analyzed separately or concatenated. 16S sequences were aligned using the L-INS-i method implemented in MAFFT 6 (Katoh *et al.* 2002) and of COI with Clustal W (Thompson *et al.* 1994). Kimura (1980) 2 Parameter distances were calculated using Mega 7 (Kumar *et al.* 2016). Phylogenetic relationships were inferred using Bayesian inference

Table 1 (continued on next six pages). Specimens of *Isostichopus* Deichmann, 1958 analyzed for the partial regions of cytochrome oxidase subunit 1 (COI-Fr1-Barcoding region, COI-Fr2) and 16S genes. Catalog number column includes voucher specimens or tissues from where the sequences were obtained. Field numbers used in phylogenetic trees correspond to the initial letter of the locality, the code and the color patterns in Fig. 1. Contractions in locality column: Mexico: Yuc = Yucatán; Belize: TC = Tobacco Cay; CBC = Carrie Bow Cay; Panama: BT = Bocas del Toro; Ga = Galeta; Ta = Taboguilla Island (Pacific); IP = Perlas Islands (Pacific); Colombia: SM = Santa Marta; MSM = Morro de Santa Marta; MPA = Morritos de Punta Aguja; Ne = Bahía Neguanje; LG = La Guajira; BA = Banco de las Ánimas; Prov = Providencia Island; Ch = Choco (Pacific); Ecuador: Gal = Galapagos; U.S. Virgin Islands: SCI = St. Croix; British Virgin Islands: GI = Guana Island; Curaçao: Cu = Curaçao; Cu-CMRS = Curaçao-Carmabi Marine Research Station; Brazil: SC = Santa Catalina; Cape Verde: SV = Sao Vicente Island; SI = Santiago Island; Senegal: DÎM = Dakar-Îles Madeleines; Liberia: K = Kligba, Rivercess County; AB = Artah Beach, Sasstow Grand Kru County; Ascension Island: EB = English Bay; G = Georgetown. Photo ID: figure number in the present paper or the process ID in the BOLD database. GenBank accession numbers in parentheses denote sequences by other authors. *Astichopus multifidus* (Sluiter, 1910), *Stichopus horrens* Selenka, 1867, and *Apostichopus japonicus* (Selenka, 1867) were used as outgroups in the phylogenetic analyses. An asterisk (*) in the species column indicates that the species ID in GenBank was changed from a previous name (shown in parentheses).

Species	Museum Catalog number	Field Number	Locality	Photo	GeneBank Acc. No. COI-Fr1	GeneBank Acc. No. COI-Fr2	GeneBank Acc. No. 16S	Reference
I. badionotus	TbBT0002	BT2-R	Panama-BT	8C’	–	–	MK477775	This study
I. badionotus	USNM 1659459	BT14-CH	Panama-BT	8A	–	MK477909	MK477776	This study
I. badionotus	TbBT0016	BT16-CH	Panama-BT	8B	–	–	MK477777	This study
I. badionotus	USNM 1659460	BT20-R	Panama-BT	1F–G	MK477881	–	MK477778	This study
I. badionotus	USNM 1659461	BT45-U	Panama-BT	8V	MK477882	MK477910	MK477779	This study
I. badionotus	USNM 1659462	BT48-U	Panama-BT	8W	MK477883	MK477911	MK477780	This study
I. badionotus	USNM 1659463	BT55-CH	Panama-BT	8C	MK477884	–	MK477781	This study
I. badionotus	USNM 1659464	BT62-CH	Panama-BT	8D	MK477885	–	MK477782	This study
I. badionotus	TbBT0067	BT67-BY	Panama-BT	–	–	MK477912	MK477783	This study
I. badionotus	USNM 1659465	BT69-BY	Panama-BT	–	MK477886	–	MK477784	This study
I. badionotus	TbBT0071	BT71-BY	Panama-BT	–	–	MK477913	MK477785	This study
I. badionotus	TbBT0073	BT73-BY	Panama-BT	–	–	MK477914	MK477786	This study
I. badionotus	MBMLP BT75	BT75-R	Panama-BT	–	MK477887	MK477915	MK477787	This study
I. badionotus	TbBT0083	BT83-R	Panama-BT	–	–	MK477916	MK477788	This study
I. badionotus	USNM 1659466	BT98-R	Panama-BT	8E’	MK477888	MK477917	MK477789	This study
I. badionotus	MBMLP BT106	BT106-CH	Panama-BT	8E	MK477889	–	MK477790	This study
I. badionotus	USNM 1659467	BT107-CH	Panama-BT	8F	MK477890	–	MK477791	This study

Table 1 (continued). Specimens of *Isostichopus* Deichmann, 1958 analyzed for the partial regions of cytochrome oxidase subunit 1 (COI-Fr1-Barcoding region, COI-Fr2) and 16S genes. Catalog number column includes voucher specimens or tissues from where the sequences were obtained. Field numbers used in phylogenetic trees correspond to the initial letter of the locality, the code and the color patterns in Fig. 1.

Species	Museum Catalog number	Field Number	Locality	Photo	GeneBank Acc. No. COI-Fr1	GeneBank Acc. No. COI-Fr2	GeneBank Acc. No. 16S	Reference
I. badionotus	USNM 1659454	BT111-CH	Panama-BT	8G	MK477891	MK477918	MK477792	This study
I. badionotus	USNM 1659455	BT112-U	Panama-BT	8X	MK477892	MK477919	MK477793	This study
I. badionotus	USNM 1659456	BT115-CH	Panama-BT	6H	MK477893	MK477920	MK477794	This study
I. badionotus	USNM 1659457	BT116-BY	Panama-BT	8L'	MK477894	MK477921	MK477795	This study
I. badionotus	USNM 1659458	BT118-CH	Panama-BT	8I	MK477895	MK477922	MK477796	This study
I. badionotus	INV TEJ1167	SM4-R	Colombia-SM	1H–I	–	–	MK477797	This study
I. badionotus	INV TEJ1168	SM5-R	Colombia-SM	8G'	–	–	MK477798	This study
I. badionotus	INV TEJ1170	SM7-R	Colombia-SM	8H'	–	MK477923	MK477799	This study
I. badionotus	INV TEJ1172	SM9-R	Colombia-SM	8H' right	–	MK477924	MK477800	This study
I. badionotus	INV TEJ1173	SM10-R	Colombia-SM	8H'	–	MK477925	MK477801	This study
I. badionotus	INV TEJ1176	SM13-BY	Colombia-SM	1J	–	MK477926	MK477802	This study
I. badionotus	INV TEJ1178	SM15-R	Colombia-SM		–	–	MK477803	This study
I. badionotus	INV EQU4572 INV TEJ1987	MSM16-U	Colombia-MSM	BECSC73-20	OL989848	–	–	This study
I. badionotus	INV EQU4573 INV TEJ1988	MPA17-R	Colombia-MPA	BECSC74-20	OL989849	–	–	This study
I. badionotus	INV TEJ1179	Ne1-CH	Colombia-Ne	–	–	MK477927	MK477804	This study
I. badionotus	INV TEJ1184	Ne6-CH	Colombia-Ne	8J	–	MK477928	MK477805	This study
I. badionotus	INV TEJ1193	Ne15-CH	Colombia-Ne	8K	–	–	MK477806	This study
I. badionotus	INV TEJ1194	Ne16-CH	Colombia-Ne	–	–	–	MK477807	This study
I. badionotus	INV TEJ1196	Ne18-CH	Colombia-Ne	8L	–	MK477929	MK477808	This study
I. badionotus	INV TEJ1267	GV93-CH	Colombia-LG	8M	–	MK477930	MK477809	This study
I. badionotus	INV TEJ1268	GV100-CH	Colombia-LG	8N	–	MK477931	MK477810	This study

Table 1 (continued). Specimens of *Isostichopus* Deichmann, 1958 analyzed for the partial regions of cytochrome oxidase subunit 1 (COI-Fr1-Barcoding region, COI-Fr2) and 16S genes. Catalog number column includes voucher specimens or tissues from where the sequences were obtained. Field numbers used in phylogenetic trees correspond to the initial letter of the locality, the code and the color patterns in Fig. 1.

Species	Museum Catalog number	Field Number	Locality	Photo	GeneBank Acc. No. COI-Fr1	GeneBank Acc. No. COI-Fr2	GeneBank Acc. No. 16S	Reference
I. badionotus	INV TEJ1292	GV155-U	Colombia-LG	8Y	–	–	MK477811	This study
I. badionotus	INV TEJ1294	GV157-R	Colombia-LG	8J'	–	MK477932	MK477812	This study
I. badionotus	INV TEJ1301	GV236-R	Colombia-LG	8K'	–	MK477933	MK477813	This study
I. badionotus	INV TEJ1306	GV250-CH	Colombia-LG	8O	–	MK477934	MK477814	This study
I. badionotus	INV TEJ1310	GV300-CH	Colombia-LG	8P	–	MK477935	MK477815	This study
I. badionotus	INV TEJ1125	Ma10-CH	Colombia-LG	1C–D	–	–	MK477817	This study
I. badionotus	INV EQU3046	EQU3046-CH	Colombia-LG	8Q	–	–	MK477816	This study
I. badionotus	INV EQU3089	EQU3089-R	Colombia-SM	BECSC49-20	–	–	OL989879	This study
I. badionotus	INV TEJ2052	Pr29-R	Colombia-Prov	BECSC71-20	OL989773	–	–	This study
I. badionotus	INV TEJ2056	Pr38-R	Colombia-Prov	BECSC72-20	OL989774	–	–	This study
I. badionotus		Cu1-BY	Curaçao-Cu	8M'	–	MK477940	MK477821	This study
I. badionotus		Cu2-U	Curaçao-Cu	8Z	–	MK477941	MK477822	This study
I. badionotus		Br1	Brazil-SC	–	–	MK477936	MK477818	This study
I. badionotus		Br6	Brazil-SC	–	–	MK477937	MK477819	This study
I. badionotus		Br9	Brazil-SC	–	–	MK477938	–	This study
I. badionotus		Br15	Brazil-SC	–	–	MK477939	MK477820	This study
I. maculatus phoenius	USNM 1659468	BT5-LSD	Panama-BT	17T	–	–	MK477823	This study
I. maculatus phoenius	MBMLP IpBT7	BT7-DW	Panama-BT	–	MK477896	MK477942	MK477824	This study
I. maculatus phoenius	USNM 1659473	BT21-DW	Panama-BT	–	MK477897	–	MK477825	This study
I. maculatus phoenius	USNM 1659474	BT22-DW	Panama-BT	17O	MK477898	MK477943	MK477826	This study
I. maculatus phoenius	USNM 1659475	BT23-DW	Panama-BT	17G	MK477899	–	MK477827	This study
I. maculatus phoenius	USNM 1659476	BT25-DW	Panama-BT	17F	MK477900	MK477944	MK477828	This study
I. maculatus phoenius	USNM 1659477	BT43-DW	Panama-BT	1ST/18A	MK477901	MK477945	MK477829	This study
I. maculatus phoenius	USNM 1659478	BT44-DW	Panama-BT	17E/18E	MK477902	MK477946	MK477830	This study
I. maculatus phoenius	USNM 1659479	BT53-LSD	Panama-BT	17A'	MK477903	MK477947	MK477831	This study
I. maculatus phoenius	USNM 1659469	BT131-DW	Panama-BT	17N/18H	MK477904	MK477948	MK477832	This study

Table 1 (continued). Specimens of *Isostichopus* Deichmann, 1958 analyzed for the partial regions of cytochrome oxidase subunit 1 (COI-Fr1-Barcoding region, COI-Fr2) and 16S genes. Catalog number column includes voucher specimens or tissues from where the sequences were obtained. Field numbers used in phylogenetic trees correspond to the initial letter of the locality, the code and the color patterns in Fig. 1.

Species	Museum Catalog number	Field Number	Locality	Photo	GeneBank Acc. No. COI-Fr1	GeneBank Acc. No. COI-Fr2	GeneBank Acc. No. 16S	Reference
I. maculatus phoenius	USNM 1659470	BT190-DW	Panama-BT	18L	MK477905	MK477949	MK477833	This study
I. maculatus phoenius	USNM 1659471	BT191-DW	Panama-BT	17M	MK477906	–	MK477834	This study
I. maculatus phoenius	USNM 1659472	BT192-DW	Panama-BT	17R/18I	MK477907	MK477950	MK477835	This study
I. maculatus phoenius	TpGa0008	Ga8-U	Panama-Ga	1K	–	MK477951	MK477836	This study
I. maculatus phoenius	TpGa0011	Ga11-LBD	Panama-Ga	17U	–	MK477952	MK477837	This study
I. maculatus phoenius	TpGa0209	Ga209-LSD	Panama-Ga	–	–	MK477953	MK477838	This study
I. maculatus phoenius	USNM 1659480	Ga223-LSD	Panama-Ga	17S	–	MK477954	MK477839	This study
I. maculatus phoenius	USNM 1659481	Ga224-DW	Panama-Ga	17I	–	MK477955	MK477840	This study
I. maculatus phoenius	INV EQU4144 INV TEJ1333	BA313-LBD	Colombia-BA	17V	–	MK477956	MK477841	This study
I. maculatus phoenius	INV EQU4146 INV TEJ1334	BA314-LBD	Colombia-BA	17W	–	MK477957	MK477842	This study
I. maculatus phoenius	INV TEJ1336	BA319-U	Colombia-BA	1L	–	MK477958	MK477843	This study
I. maculatus phoenius	INV TEJ1257	GV82-DW	Colombia-LG	17J	–	–	MK477844	This study
I. maculatus phoenius	INV TEJ1258	GV83-DW	Colombia-LG	17K	–	MK477959	MK477845	This study
I. maculatus phoenius	INV TEJ1259	GV84-DW	Colombia-LG	17P	–	MK477960	MK477846	This study
I. maculatus phoenius	INV TEJ1261	GV86-DW	Colombia-LG	17L	–	MK477961	MK477847	This study
I. maculatus phoenius	INV TEJ1265	GV90-LSD	Colombia-LG	17X	–	MK477962	MK477848	This study
I. maculatus phoenius	INV TEJ1269	GV108-DW	Colombia-LG	17Q	–	MK477963	MK477849	This study
I. maculatus phoenius	INV TEJ1272	GV117-LSD	Colombia-LG	17Y	–	MK477964	MK477850	This study
I. maculatus phoenius	INV TEJ1113	GCV1-LBD	Colombia-LG	–	–	–	MK477851	This study
I. maculatus phoenius	INV TEJ1115	GCV3-U	Colombia-LG	17C	–	–	MK477852	This study
I. maculatus maculatus		CV1-DW	Cape Verde-SVI	14A	–	MK477965	MK477853	This study
I. maculatus maculatus		CV7-LSD	Cape Verde-SI	14G	–	MK477971	MK477859	This study
I. maculatus maculatus		CV10-LSD	Cape Verde-SI	14E	–	MK477974	MK477862	This study
I. maculatus maculatus		ASI1-LSD	Ascension Is.-EB	–	–	MK477975	MK477863	This study

Table 1 (continued). Specimens of *Isostichopus* Deichmann, 1958 analyzed for the partial regions of cytochrome oxidase subunit 1 (COI-Fr1-Barcoding region, COI-Fr2) and 16S genes. Catalog number column includes voucher specimens or tissues from where the sequences were obtained. Field numbers used in phylogenetic trees correspond to the initial letter of the locality, the code and the color patterns in Fig. 1.

Species	Museum Catalog number	Field Number	Locality	Photo	GeneBank Acc. No. COI-Fr1	GeneBank Acc. No. COI-Fr2	GeneBank Acc. No. 16S	Reference
I. maculatus maculatus		ASI2-LSD	Ascension Is.-EB	–	–	MK477976	MK477864	This study
I. maculatus maculatus		ASI4-LSD	Ascension Is.-EB	–	–	MK477978	MK477866	This study
I. maculatus maculatus	USNM E16150	E16150-LSD	Ascension Is.-EB	12A	–	MK477980	MK477867	This study
I. maculatus maculatus	UF 16295	UF16295-LSD	Senegal-DÎM	14L	OM056886	–	–	Florida Museum, unpubl.
I. maculatus maculatus		FAOLIB08-LSD	Liberia-K	14N–O	MZ742160	–	MZ743890	González-Wangüemert *et al*. in prep.
I. maculatus maculatus		FAOLIB09-LSD	Liberia-K	14N–O	MZ742161	–	MZ743891	González-Wangüemert *et al*. in prep.
I. maculatus maculatus		FAOLIB10-LSD	Liberia-AB	14N–O	MZ742162	–	MZ743892	González-Wangüemert *et al*. in prep.
I. fuscus	TfTa0210	Ta210-R	Panama-Ta	21A	MK477908	MK477981	MK477869	This study
I. fuscus	USNM 1659483	Ta211-R	Panama-Ta	1L'–M'	–	MK477982	MK477870	This study
I. fuscus	USNM 1659482	IP322-R	Panamá-IP	21B	–	MK477983	MK477871	This study
I. fuscus	INV EQU4323	EQU4323-R	Colombia-Ch	21D–E	–	MK477984	MK477872	This study
I. fuscus	INV EQU4324	EQU4324-BR	Colombia-Ch	21D–E	–	MK477985	MK477873	This study
I. fuscus	INV EQU2746	EQU2746-R	Colombia-Ch	21C	–	–	MK477875	This study
I. fuscus	INV TEJ1960	Ri54C1-R	Colombia-Ch	–	–	MK477986	MK477874	This study
I. fuscus	INV TEJ1923	TEJ1923-R	Colombia- Ch	BECSC75-20	OL989775	–	–	This study
I. fuscus	INV EQU4229	EQU4229	Colombia- Ch	21M, BECSC52-20	–	–	OL989880	This study
I. fuscus	INV EQU4230	EQU4230-BU	Colombia- Ch	BECSC53-20	–	–	OL989881	This study
I. fuscus	UF 9112	Ga UF 9112	Ecuador-Ga		PP093756			Florida Museum, unpubl.
I. fuscus	UF 9651	Ga UF 9651	Ecuador-Ga		PP093755			Florida Museum, unpubl.
I. fuscus	UF 9672	Ga UF 9672	Ecuador-Ga		PP093757			Florida Museum, unpubl.

Table 1 (continued). Specimens of *Isostichopus* Deichmann, 1958 analyzed for the partial regions of cytochrome oxidase subunit 1 (COI-Fr1-Barcoding region, COI-Fr2) and 16S genes. Catalog number column includes voucher specimens or tissues from where the sequences were obtained. Field numbers used in phylogenetic trees correspond to the initial letter of the locality, the code and the color patterns in Fig. 1.

Species	Museum Catalog number	Field Number	Locality	Photo	GeneBank Acc. No. COI-Fr1	GeneBank Acc. No. COI-Fr2	GeneBank Acc. No. 16S	Reference
I. macroparentheses	USNM E40833	E40833	U.S. Virgin Islands-SCI	24G	–	MK477987	MK477876	This study
I. macroparentheses	USNM E47624	E47524	British Virgin Islands-GI	1Q'/24F	–	MK477988	MK477877	This study
I. macroparentheses	USNM 1659484	Be99	Belize-TC	1P'/24A–B	–	MK477989	MK477878	This study
I. macroparentheses	USNM 1659485	Be107	Belize-CBC	24C–D	–	MK477990	MK477879	This study
I. macroparentheses	ICMIL-UNAM 12000	MeUNAMYUC76	Mexico-Yuc		PP093693	–	–	Florida Museum-ICMIL-UNAM, unpubl
I. macroparentheses	UF20352	BCUR-0532	Curaçao-CMRS	24E	PP093694			Florida Museum, unpubl.
I. badionotus		UF4703	USA-Florida-GM, Off St. Petersburg		(KX874354)			Miller *et al*. (2017)
I. maculatus phoenius * (*I. badionotus*)		MHE133			(JN207564)		(JN207495)	Honey-Escandon *et al*. (2012)
I. maculatus phoenius * (*Isostichopus* sp.)		Isolate IF-2009			(FJ971400)		(FJ794474)	Wen *et al*. (2011)
I. maculatus phoenius * (*Isostichopus* sp.)		Isolate 1			(KX384008)		(KX383967)	Vergara *et al*. (2018)
I. maculatus phoenius * (*Isostichopus* sp.)		Isolate A5			(KX384001)		(KX383978)	Vergara *et al*. (2018)
I. maculatus phoenius * (*Isostichopus* sp.)		Isolate R3			(KX383999)		(KX383985)	Vergara *et al*. (2018)
I. maculatus phoenius * (*Isostichopus* sp.)		Isolate SPA2			(KX383995)		(KX383988)	Vergara *et al*. (2018)
I. badionotus		FAO 044			(EU848276)		(EU822435)	Uticke *et al*. (2010)
I. badionotus		Isolate 1H			(KX384010)		(KX383968)	Vergara *et al*. (2018)
I. badionotus		Isolate 3H			(KX384016)		(KX383972)	Vergara *et al*. (2018)
I. badionotus		Isolate Br2			(KX384011)		(KX393982)	Vergara *et al*. (2018)

Table 1 (continued). Specimens of *Isostichopus* Deichmann, 1958 analyzed for the partial regions of cytochrome oxidase subunit 1 (COI-Fr1-Barcoding region, COI-Fr2) and 16S genes. Catalog number column includes voucher specimens or tissues from where the sequences were obtained. Field numbers used in phylogenetic trees correspond to the initial letter of the locality, the code and the color patterns in Fig. 1.

Species	Museum Catalog number	Field Number	Locality	Photo	GeneBank Acc. No. COI-Fr1	GeneBank Acc. No. COI-Fr2	GeneBank Acc. No. 16S	Reference
I. fuscus		Isolate If1			(AF486424)			Uticke *et al.* (2010)
I. fuscus		Isolate If15			(AF486425)			Uticke *et al.* (2010)
Astichopus multifidus		AmuBT18	Panama-BT				MK477880	This study
A. multifidus		FAO 042			(EU848293)			Uticke *et al.* (2010)
*A. multifidus** (*I. macroparentheses*)		AMNH A113281					(AY338415)	Kerr *et al.* (2005)
Stichopus horrens		y11			(NC014454)	(NC014454)	(NC014454)	Fan *et al.* (2011)
Apostichopus japonicus		clone 1			(NC012616)	(NC012616)		Sun *et al.* (2010)
A. japonicus		clone 1					(AY852278)	Sun *et al.* (2010)

Fig. 1 (continued on next page). Color patterns of species and subspecies of *Isostichopus* Deichmann, 1958. **A–J**. ***Isostichopus badionotus*** (Selenka, 1867). **A**. Pink background and dark brown spots (Chips pattern – CH) (BT99, Panamá). **B**. Close-up of A, note large dark brown spots and small dots. **C**. Light brown background and darker ocellar spots (CH pattern) (INV TEJ1125-Ma10, Colombia). **D**. Close-up of C, note large ocellar spots and small black dots. **E**. Uniform black background (Uniform pattern – U) (BT59, Panamá). **F**. Beige background color with a reticulum of darker brown and yellow papillae (Reticulated pattern – R) (USNM 1659460-BT20, Panamá). **G**. Close-up of F, reticulated pattern in detail. **H**. Reticulated pattern with brown papillae (R pattern) (INV TEJ1167-SM4R, Colombia). **I**. Close-up of H, reticulated pattern in detail. **J**. Black background and yellow papillae (Black and yellow pattern-BY) (INV TEJ1176-SM13, Colombia). **K–Y**. ***Isostichopus maculatus phoenius*** (Clark,

(BI), Maximum Likelihood (ML), and Neighbour-Joining (NJ). BI and ML were performed , using the GTR evolutionary model and NJ using K2P distances. BI was performed with MrBayes ver. 3.2.6 (Ronquist & Huelsenbeck 2003); the data set was run twice, using four Markov chains for ten million generations; trees were sampled every 500th generation, the first 2.5 million generations were discarded, and a 50% majority tree was obtained. ML analysis was performed in MEGA X (Kumar *et al.* 2018); support was assessed with 1000 bootstrap reiterations.

1922). **K**. Red uniform background (Uniform pattern – U) (TpGa0008, Panama). **L**. Green uniform background (U pattern) (INV TEJ1336, BA319, Colombia). **M**. Dark orange background and white irregular and pointed blotches (Dark and White pattern – DW) (BT27, Panama). **N**. Close-up of M, note the black line surrounding the white blotches and the small black spots surrounded by a dark thin line. **O**. Close-up of M, note the spiral lines on the papilla collar around the mouth. **P**. DW pattern with dark brown background (BT8, Panama). **Q**. Close-up of P, note the white blotches with the small black spots surrounded by a dark thin line and the spiral lines on the papillae collar around the mouth. **R**. DW pattern with dark brown background, note the spiral lines on the papillae collar around the mouth (BT21, Panama). **S**. DW pattern with dark orange background (USNM 1659477-BT43, Panama). **T**. Close-up of S, note the black line surrounding the white blotches without the small black spots, but with the surrounding dark thin line. **U**. Light brown background and sharp darker brown irregular blotches (Light and sharp dark pattern – LSD) (BT29, Panama). **V**. Close-up of U, note the small dark brown spots surrounded by a dark thin line and the spiral lines on the large papilla in the top. **W**. Close-up of U, note the spiral lines in the largest papillae. **X**. Light brown background and blurry darker brown and orange irregular blotches (Light and blurry dark pattern – LBD) (Ga12, Panamá). **Y**. Close-up of X, note the blurry small dark brown spots and the spiral lines on the lateral and dorsal papillae. **Z–H'**. ***Isostichopus maculatus maculatus*** (Greeff, 1882). **Z**. Dark red uniform background (Uniform pattern – U) (Cape Verde). **A'**. With dark orange background and white irregular and pointed blotches (Dark and White color pattern – DW) (Cape Verde). **B'**. Close-up of A', note the black line surrounding the white blotches and the white spots on the blotches. **C'**. Dark chocolate brown background and white-cream irregular and pointed blotches (DW pattern) (Cape Verde). **D'**. Close-up of C', note the white-cream blotches with the small white spots. **E'**. Light gray background and sharp darker brown and orange irregular blotches (Light and sharp dark color pattern – LSD) (Sao Tomé). **F'**. Close-up of E', note the small white spots and spiral lines on the lateral papillae. **G'**. Dark green in the background and darker green blotches, small white dots and light papillae (Dark green and light papillae pattern – DGL) (Nigeria). **H'**. Close-up of G', note the darker blotches, small white spots and yellow papillae. **I'–O'**. ***Isostichopus fuscus*** (Ludwig, 1875). **I'**. Chocolate brown background with clearer stains and yellow papillae (Chocolate brown and stains pattern – BS) (Mexico). **J'**. Chocolate brown uniform background and yellow papillae (Chocolate brown uniform pattern – BU) (Mexico). **K'**. Chocolate brown in the dorsal background that gradually change to reddish in the lateral and ventral side (Chocolate brown and reddish pattern – BR) (Colombia). **L'**. Beige background with a reticulum of chocolate brown color and yellow papillae (Reticulated pattern – R) (USNM 1659483-Ta211, Panamá). **M'**. Close-up L', reticulated pattern in detail. **N'**. R pattern with a reticulum of green color (Colombia). **O'**. Close-up N', reticulated pattern in detail. **P'–Q'**. ***Isostichopus macroparentheses*** (Clark, 1922). **P'**. Juvenile light yellow-brown background and irregularly arranged blurred darker brown spots of different sizes (USNM 1659484-Be99, Belize). **Q'**. Preserved adult specimen, in the same color pattern as O' with larger darker brown spots (USNM E47624, British Virgin Islands). Photos: A–B, E–G, K, M–Y, L´–M´, P´–Q´by G. Borrero; L by N. Ardila; Z, A´–D´ by P. Wirtz; H–J by J. Gómez; C–D by C. Díaz; E´–F´by N. Vasco-Rodrigues; G´–H´ by fishermen NN; K´ by L. Chasqui; N´–O´ J. Vanegas; I´–J´by C. Sánchez.

Table 2. Average Kimura (1980) 2 parameter distances (%) between and within species and subespecies of *Isostichopus* Deichmann, 1958. COI-Fr1 and COI-Fr2 (in parentheses) distances are below diagonal and 16S distances above. Within-species distances along the diagonal are shown as COI-Fr1 (COI-Fr2) / 16S. "nc": not calculated because only one sequence was available.

	Species	1	2	3	4	5	6	7
1	*Isostichopus badionotus*	**0.2(0.2)/0.2**	8.9	8.6	5.2	11.9	16.6	20.6
2	*I. maculatus maculatus*	10.6(12.0)	**0.1(0.1)/0.2**	0.4	8.2	9.9	18.0	19.6
3	*I. maculatus phoenius*	9.6(11.0)	1.4(1.9)	**0.1(0.1)/0.2**	7.9	9.5	17.8	19.7
4	*I. fuscus*	6.1(10.8)	8.2(9.5)	7.7(10.1)	**0.3(0.2)/0.3**	12.3	18.2	19.4
5	*I. macroparentheses*	16.5(18.2)	17.3(16.7)	16.6(16.3)	16.2(16.7)	**0.0(0.3)/0.3**	17.3	22.2
6	*Stichopus horrens*	19.3(21.1)	19.4(23.5)	19.1(23.8)	18.4(20.4)	21.2(20.9)	**nc(nc)/nc**	24.3
7	*Apostichopus japonicus*	23.4(22.1)	24.8(19.6)	23.7(18.7)	23.2(23.7)	25.0(26.4)	25.7(22.5)	**nc(nc)/nc**

Results

Molecular analyses and species delineation

All phylogenetic analyses recovered *Isostichopus* as monophyletic, and four deeply divergent, reciprocally monophyletic, and highly supported clades corresponding to *Isostichopus macroparentheses*, *I. badionotus*, *I. fuscus*, and a fourth species, here identified as *I. maculatus* (Fig. 3A–D). *Isostichopus macroparentheses* is most divergent, while *I. maculatus* is sister to *I. badionotus* and *I. fuscus*. East Atlantic specimens form a well-supported subclade within the West Atlantic *I. maculatus* and these are here recognized as the subspecies *I. maculatus maculatus* and *I. maculatus phoenius*, respectively. Color patterns cluster in *I. badionotus*, with chips (CH) – uniform (U) and reticulated (R) – black and yellow (BY) largely clustering into two separate subclades (Fig. 3A–D). No relationship was found between color patterns and locality. A Brazilian subclade with modest support is also evident in *I. badionotus* (Fig. 3C).

Inter-specific K2P distances ranged from 6.1 to 17.3% for COI-Fr1, 9.5 to 18.2% for COI-Fr2 and 5.2 to 12.3% for 16S. Intra-specific diversity was < 0.3% for all species and markers (Table 2). Distances between the subspecies of *I. maculatus* are 1.4% for COI-Fr1, 1.9% for COI-Fr2, and 0.4% for 16S. Distances within these subspecies are 0–0.2%.The values in *Isostichopus* are comparable to distances among recognized species of *Stichopus* (COI: between species 1.1 to 16.2%, within species < 1.2%; 16S: between species 1.4% to 15.3%, within species < 1.5%) (Byrne *et al.* 2010).

The species delineated with sequence data are morphologically differentiable in the field by their color pattern, and some by their habitat preference and behavior, as well as by their ossicles. Geographic distribution and detailed examination of ossicles also allow identifying individuals that belong to each species (Table 3). Our conclusion, therefore, is that there are four species of *Isostichopus*: we confirm *I. macroparentheses* and *I. fuscus* as valid species, and in addition to *I. badionotus*, we recognize *I. maculatus*, including the subspecies *I. maculatus maculatus* and *I. maculatus phoenius*.

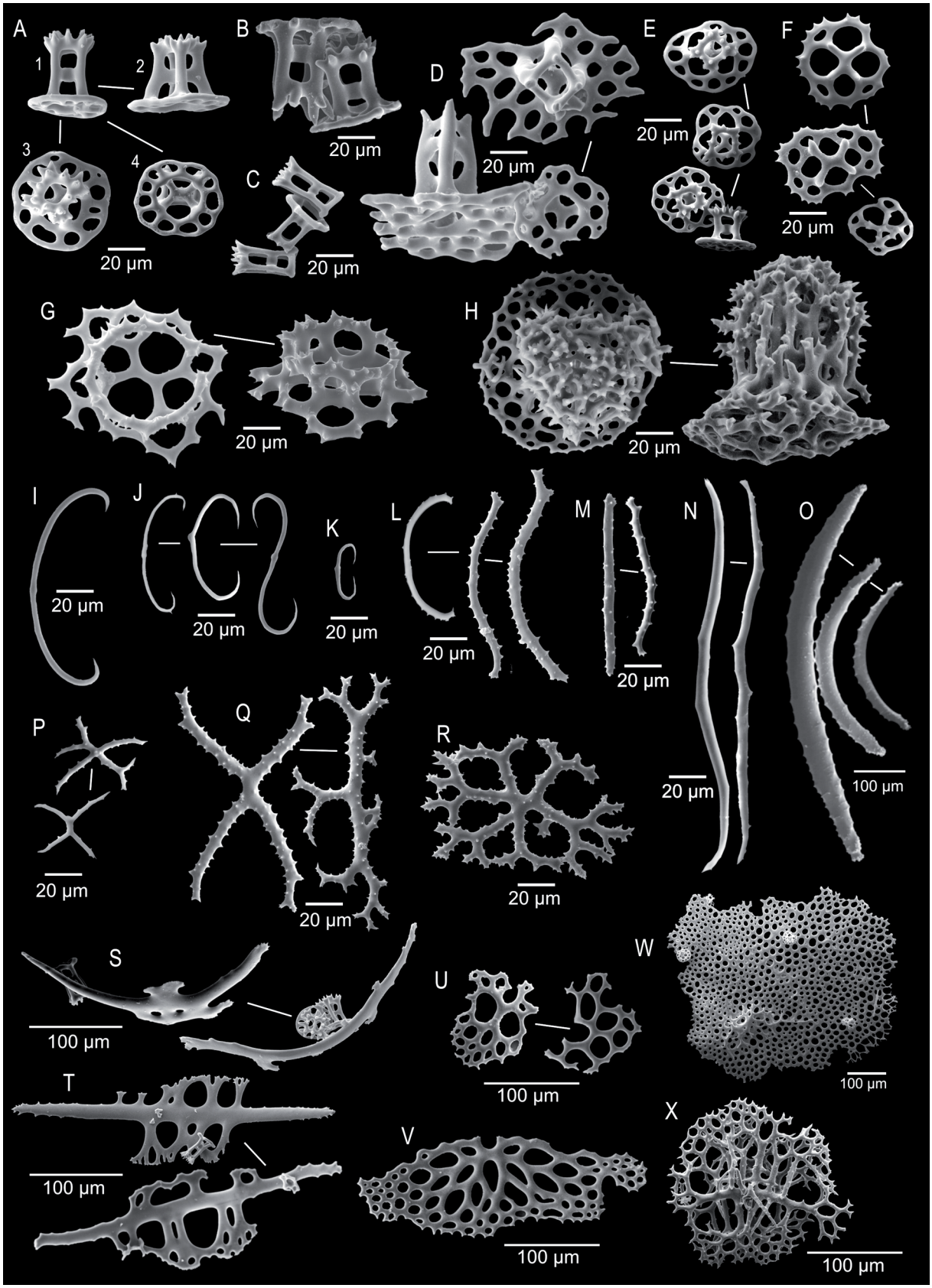
A
1
2
3
4
20 µm
B
20 µm
C
20 µm
D
20 µm
E
20 µm
F
20 µm
G
20 µm
H
20 µm
I
20 µm
J
20 µm
K
20 µm
L
20 µm
M
20 µm
N
20 µm
O
100 µm
P
20 µm
Q
20 µm
R
20 µm
S
100 µm
T
100 µm
U
100 µm
V
100 µm
W
100 µm
X
100 µm

Systematic account

Class Holothuroidea Blainville, 1834
Order Synallactida Miller, Kerr, Paulay, Reich, Wilson, Carvajal & Rouse, 2017
Family Stichopodidae Haeckel, 1896

Genus ***Isostichopus*** Deichmann, 1958

Type species

Stichopus badionotus Selenka, 1867

Description (after Deichmann 1958)

Medium to large species, length to 50 cm, body wall firm and thick. Highly variable coloration (Fig. 1). Body convex to quadrangular in cross-section. Large lateral papillae, usually sharply defining dorsum and ventrum (or bivium and trivium). Dorsal papillae irregularly arranged and in different sizes and shapes: wart-like, spiky, or with small points. Sole well developed, with three bands of cylindrical podia. Single stone canal attached to the mesentery; calcareous ring with massive radial pieces with posterior projections of different sizes, and narrow interradial pieces with projections pointed anteriorly and concave posterior margins (Fig. 4). Ossicles: dorsal papillae with tables; thin C- or S-shaped rods in varying numbers and sizes; large, curved rods with quadrangular projections, sometimes perforated in the middle (Fig. 2S); few perforated plates in the tip (Fig. 2U). Tables in a dense layer, low, squat, with a circular disc with 8 to 12 small holes, four pillars, single crossbeam, and a wreath of small spines at the crown (Fig. 2A–B); tables with reduced disc (Fig. 2C), additional holes in more than one ring (Fig. 20A), or larger and modified discs also present (Fig. 2D), mainly at the top of papillae. Dorsal body wall with tables and a few thin C- or S-shaped rods only. Ossicles in dorsal papillae and body wall change during growth, though drastic ontogenetic changes occurring only in *I. macroparentheses*. Pedicels with low tables with large and not rounded central perforation (Fig. 2E); thin C-shaped rods less frequent than in the dorsal papillae; large endplates (Fig. 2W); numerous perforated or supporting

---

Fig. 2 (see previous page). Ossicles of species and subspecies of *Isostichopus* Deichmann, 1958. **A–H**. **Tables**. **A**. Regular tables present in several parts of the body in the five species (1–2 = lateral view; 3 = top or dorsal view; 4 = ventral view). **B**. Large, regular tables, only present in *I. maculatus maculatus* (Greeff, 1882) (lateral view). **C**. Table with reduced disc, only present in the dorsal body wall of *I. macroparentheses* (Clark, 1922) adults (lateral view). **D**. Large tables with disc and spire modified, only present in the top of the dorsal papillae of *I. maculatus maculatus* – "modified *maculatus* tables" (lateral view, top view). **E**. Regular tables present in the ventral body wall and tube feet (top and lateral view). **F**. Tables with low and incomplete spires, present in the tentacles (top view). **G**. Tables with circular spire, several pillars, observed in the cloaca of *I. fuscus* (top and lateral view). **H**. Large tables with well-developed spires, several pillars forming a very dense and thick crown of spines, present in the mouth membrane and other internal organs (top and lateral view). **I–T**. **Rods**. **I**. Large thin C-shaped rods present in *I. macroparentheses*. **J–K**. Thin C, S-shaped rods present in the body wall, papillae and tube feet, and some internal organs. **L**. Thick C rods and worm-shaped rods present in the dorsal papillae of *I. maculatus maculatus* and *I. maculatus phoenius* (Clark, 1922). **M**. Simple rods present in several internal organs. **N**. Simple rods present in gonads. **O**. Simple rods present in the tentacles. **P**. Cross-shaped rods present in the intestine. **Q**. Branched rods present in several internal organs. **R**. Irregular plate-like branched rods present mostly in the anterior cloaca. **S**. Large, curved rods with quadrangular projections in the middle, present in the papillae. **T**. Large slightly or strongly curved rods with wide perforated expansions in the middle, present in the tube feet. **U–X**. **Perforated plates**. **U**. Perforated plates from papillae. **V**. Perforated plate from tube feet. **W**. End-plate. **X**. Tridimensional spheres only observed in the respiratory trees of *I. macroparentheses.* Photos by G. Borrero.

Table 3 (continued on next page). Characters distinguishing species and subspecies of *Isostichopus* Deichmann, 1958.

Characters	*I. badionotus*	*I. maculatus maculatus*	*I. maculatus phoenius*	*I. fuscus*	*I. macroparentheses*
Body color	Highly variable, four main patterns (Figs 1A–J, 8): 1) Chips (CH); 2) Uniform (U); 3) Reticulated (R); 4) Black and yellow (BY).	Highly variable, four main patterns (Figs 1Z–H', 14): 1) Uniform (U); 2) Dark and white (DW); 3) Light and sharp dark (LSD); 4) Dark green and light papillae (DGL).	Highly variable, four main patterns (Figs 1K–Y, 17–18): 1) Uniform (U); 2) Dark and white (DW); 3) Light and sharp dark (LSD); 4) Light and blurry dark (LBD).	Highly variable, four main patterns (Figs 1I'–O', 21): 1) Chocolate brown uniform (BU); 2) Chocolate brown and stains (BS); 3) Chocolate brown and reddish (BR); 4) Reticulated pattern (R).	Not variable, dorsal side light yellow-brown in the background, with irregularly arranged blurred big and small spots in a darker brown color (Figs 1P'–Q', 22, 24).
Small dark spots surrounded by a clear halo and a dark thin line on white blotches or on the background	Absent	Absent	Present	Absent	Absent
Whitish spot-like granules	Absent	Present	Absent	Absent	Absent
Spiral lines on dorsal and lateral papillae	Absent	Sometimes present	Present	Absent	Absent
Body wall appearance in live specimens	Opaque/Smooth	Opaque/Smooth	Semi translucent/Rugose	Opaque/Smooth	Semi translucent/Smooth
C–shaped ossicles	52–130 ($\bar{x}$ = 80) µm	54–90 µm ($\bar{x}$ = 69) µm	45–98 ($\bar{x}$ = 71) µm	60–109 ($\bar{x}$ = 81) µm	91–155 ($\bar{x}$ = 113) µm
Tables in dorsal papillae	Regular *Isostichopus* tables, discs fully developed (Figs 2A, 7A)	1) Regular *Isostichopus* tables, discs fully developed (Figs 2A–B, 13A) 2) Modified *maculatus* tables (Figs 2D, 13A)	Regular *Isostichopus* tables, discs fully developed (Figs 2A, 16A)	Regular *Isostichopus* tables, discs fully developed (Figs 2A, 20A)	Regular *Isostichopus* tables, discs fully developed in small and medium size specimens; discs completely reduced in large specimens (Figs 2C, 23A)
Table height in dorsal papillae	1) 33–70 ($\bar{x}$ = 52) µm Juveniles: 33–41 ($\bar{x}$ = 37) µm	1) 58–86 ($\bar{x}$ = 71) µm 2) 60–108 ($\bar{x}$ = 86) µm	1) 31–78 ($\bar{x}$ = 52) µm Juveniles: 31–46 ($\bar{x}$ = 38) µm	1) 34–65 ($\bar{x}$ =50) µm Juveniles: 34–46 ($\bar{x}$ = 41) µm	1) 29–38 ($\bar{x}$ =34) µm Juveniles: 31–48 µm ($\bar{x}$ = 40) µm
Table disc diameter in dorsal papillae	1) 39–81 ($\bar{x}$ = 58) µm	1) 62–95 ($\bar{x}$ = 80) µm 2) 66–141 ($\bar{x}$ = 106) µm	1) 39–84 ($\bar{x}$ = 64) µm	1) 42–95 ($\bar{x}$ = 63) µm	1) 17–27 ($\bar{x}$ = 23) µm Juveniles: 24–77 ($\bar{x}$ = 48) µm
Worm–like rods in dorsal papillae	Absent	Sometimes present	Present	Absent	Absent
Tables in mouth membrane (Fig. 11)	Large tables, usually tall spire	Large tables, low spire usually incomplete	Large tables, usually flat spire	Large tables, some specimens without tables	Large tables, tall spire, sometimes incomplete
Tridimensional spheres and straight/spiky rods in the Respiratory tree (Fig. 23F)	Absent	Absent	Absent	Absent	Present
Large tables with a circular spire well developed in the cloaca (Figs 11D, 19C, 20F).	Absent	Absent	Absent	Present	Absent

Table 3 (continued). Characters distinguishing species and subspecies of *Isostichopus* Deichmann, 1958.

Characters	*I. badionotus*	*I. maculatus maculatus*	*I. maculatus phoenius*	*I. fuscus*	*I. macroparentheses*
Habitat (Individuals >13 cm long)	Muddy, sandy, rocky, or mixed bottoms and seagrass beds	Rocky, sandy and mixed bottom.	Rocky bottoms associated with live corals, sponges, rubble, or rocks	Rocky or mixed bottoms.	Rocky bottom, in the back reef, reef crest, and fore reef.
Behavior (during day)	Exposed	Exposed?	Hidden, although exposed for short times	Semi–exposed or exposed	Hidden? under or among rocks
Abundance	Abundant at some localities	Abundant at some localities	Abundant at some localities	Abundant at some localities	Not common
Distribution (Fig. 5)	West Atlantic, from North Carolina to Brazil, including Bermuda and the Antilles	East and Mid Atlantic: Senegal, Sierra Leone, Liberia, Gabon, Nigeria, Cape Verde, Sao Tome and Principe, and Ascension island	West Atlantic: Gulf of Mexico and the Caribbean Sea	East Pacific, from the Gulf of California to Peru, including Isla del Coco, Malpelo, Galapagos, Lobos de Afuera Islands.	West Atlantic: Gulf of Mexico and the Caribbean Sea, confirmed in only a few localities

plates with numerous holes (Fig. 2V); slightly or strongly curved rods with broad perforated expansions in the middle (Fig. 2T); both plates and rods larger than those of dorsal papillae. Ventral body wall with only tables and a few C-shaped ossicles. Tentacles with strongly or slightly curved spiny rods in varying sizes (Fig. 2O) and small tables as those of the body wall, or modified with low and incomplete spires (Fig. 2F). Mouth membrane with thin C-shaped rods, simple rods, and large tables, not documented previously for the genus, with well-developed spire, composed of at least ten pillars joining at the top, forming very dense and thick crown of spines, without crossbeams; discs of the same width as the spire, or wider with several rings of holes and several central perforations (Figs 2H, 7D, 11, 16D). Longitudinal muscles containing C-shaped rods and simple rods. Posterior part of the cloaca with C-shaped, simple or bifurcated rods (Fig. 11); anterior part with simple, branched rods, irregular plate-like branched rods (Fig. 2R) and large tables, with well-developed and very dense and thick spire, some with circular

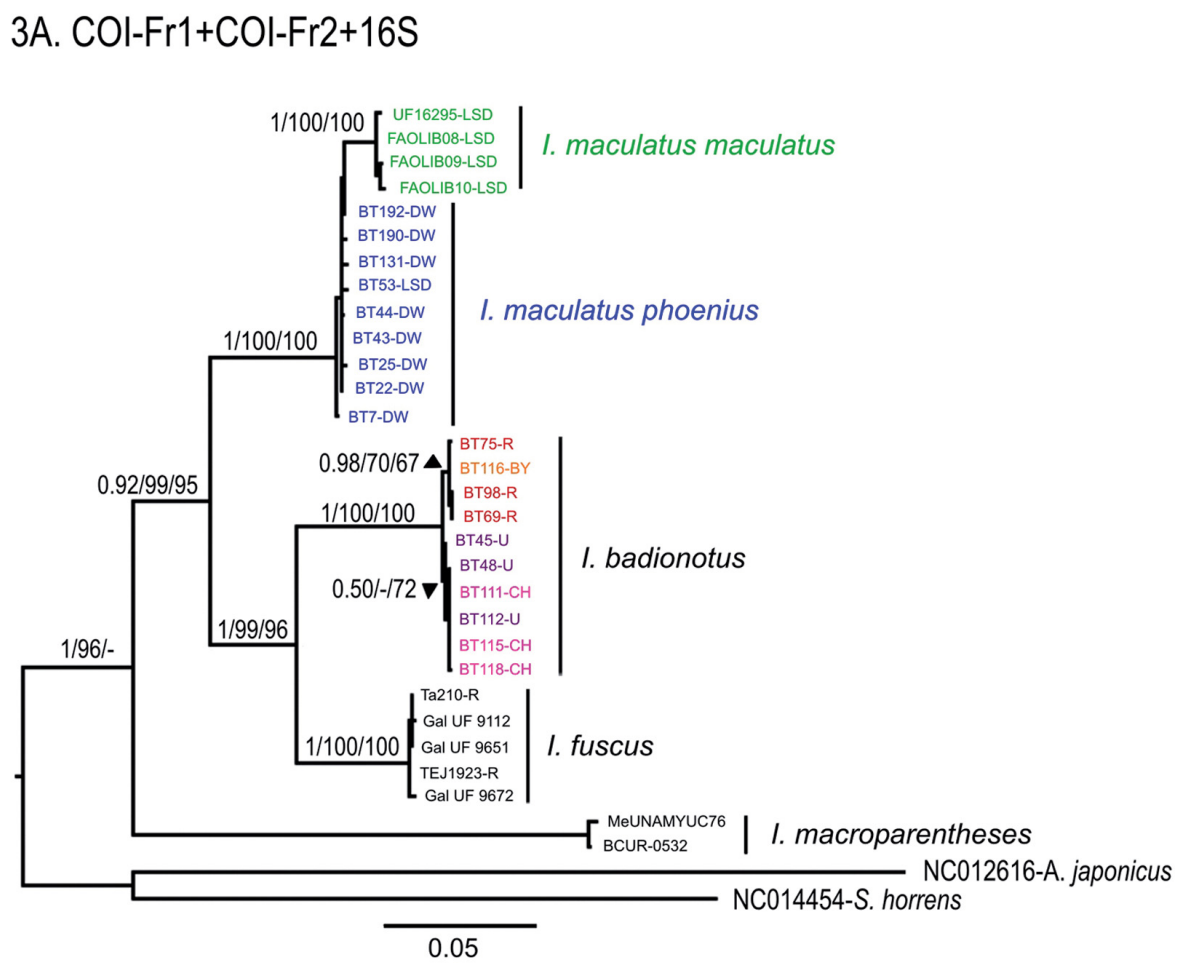

Fig. 3A. Bayesian inference tree of concatenated sequences of the mitochondrial COI-Fr1 (Barcoding region), COI-Fr2 and 16S gene fragments. The numbers on the nodes indicate Bayesian posterior probability / Maximum Likelihood (bootstrap %) / Neighbor Joining (bootstrap %). A hyphen (-) indicates that a node was absent in the tree estimated by a particular method. Individuals are indicated by the field number, which includes the initial letter of the locality and the color pattern when available (see Table 1, Fig. 1). Text color meaning: green = *Isosostichopus maculatus maculatus* (Greeff, 1882); blue = *I. maculatus phoenius* (Clark, 1922); pink = *I. badionotus* (Selenka, 1867) Chips (CH) pattern; purple = Uniform (U) pattern; red = reticulated (R) pattern; orange = Black and Yellow (BY) pattern. Sequences from GenBank are indicated with their accession number and species ID as included in GenBank (see Table 1). Outgroup species: *Apostichopus japonicus* (Selenka, 1867) and *Stichopus horrens* Selenka, 1867.

spire, without clear crossbeams, wide discs with several rings of holes and several central perforations (Fig. 11). Respiratory trees with small tables as those of the body wall or strongly spinose straight or cross-shaped rods and large tridimensional spheres (Fig. 2X), not documented previously for the genus. Intestine with spinose or smooth ossicles in a cross shape (Fig. 2P). Gonads with delicate and long rods (Figs 2N, 11). Rosettes not present in *Isostichopus*.

Distribution

Tropical and subtropical shores of America and the west coast of Africa (Fig. 5).

Isostichopus badionotus (Selenka, 1867)
Figs 1A–J, 3A–D, 4A, 5A, 6–9, 10A, 11A; Tables 1–3

Stichopus badionotus Selenka, 1867: 316, pl. 18 fig. 20.
Stichopus haytiensis Semper, 1868: 75, pl. 30 fig. 5.
Stichopus möbii Semper, 1868: 246, pl. 40 fig. 11.
Stichopus errans Ludwig, 1875: 97.

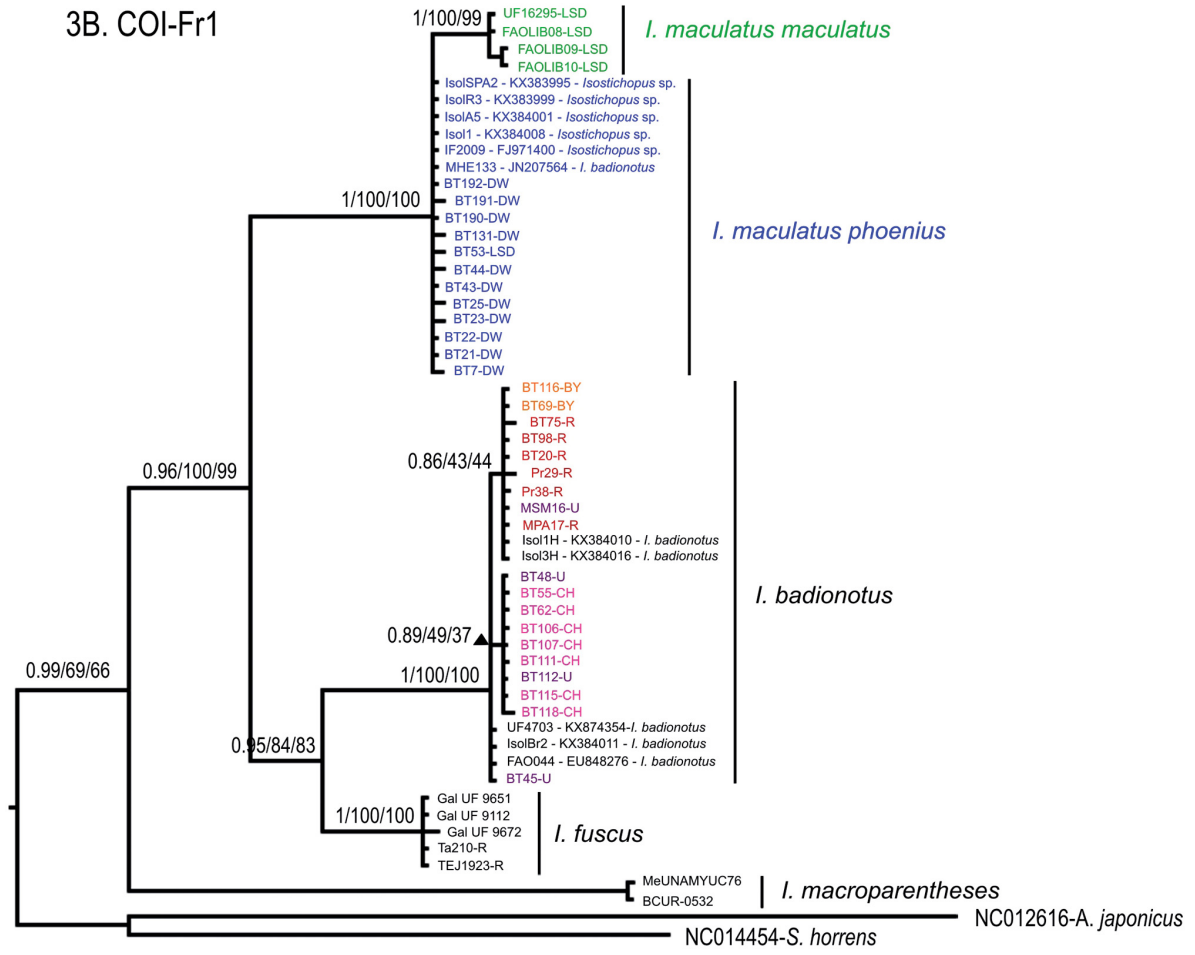

Fig. 3B. Bayesian inference tree of mitochondrial COI-Fr1 gene fragment. The numbers on the nodes indicate Bayesian posterior probability/Maximum Likelihood (bootstrap %)/Neighbor Joining (bootstrap %). A hyphen (-) indicates that the node was not recovered by a particular method. Specimen ID and color pattern designation as in Fig. 3A. Specimens of *I. badionotus* (Selenka, 1867) with unknown color pattern are indicated in black color.

Stichopus diaboli Heilprin, 1888: 312.
Stichopus xanthomela Heilprin, 1888: 313.

Stichopus acanthomella – H.L Clark in Lloyd 1900: 885. Typographic error.
Stichopus badionotus – Clark 1922: 55, pl. 2 figs 11–18; 1933: 109; 1942: 386. — Deichmann 1930: 80, pl. 5 figs 30–36; 1940: 195; 1954: 388, fig. 66, 1–8; 1957: 4, figs 1–4.
Stichopus moebii – Clark 1922: 55. — Cutress 1996: 105. Article 32.5.2.1 ICZN Code (1999).
Isostichopus badionotus – Deichmann 1958: 280; 1963: 106. — Tikasingh 1963: 84, figs 23–25. — Pawson 1976: 373. — Caycedo 1978: 159, pl. 1 figs 1–4. — Miller & Pawson 1984: 54, figs 44–45. — Hendler *et al.* 1995: 280, figs 156, 187g–i. — Cutress 1996: 105, figs 33B–D, 37–40, table 13. — Pawson *et al.* 2010: 34, figs 6f, 27. — Borrero-Pérez *et al.* 2012: 174, 175, figs b, c, e–o; 2022: 180–186. — Prata *et al.* 2014: 143, fig. 7a–h, table 5. — Vergara & Rodríguez 2015: 1022, fig. 1a.

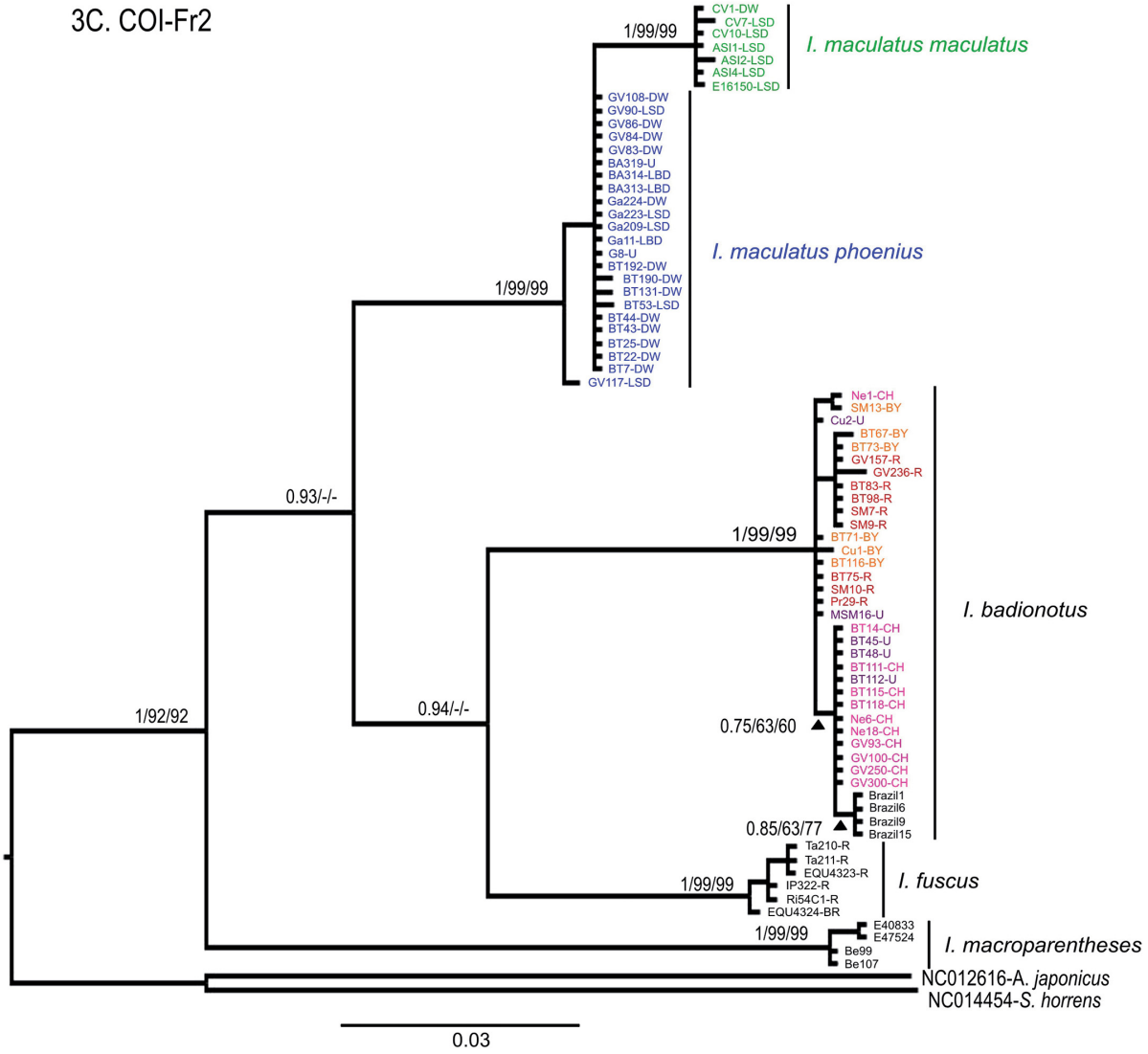

Fig. 3C. Bayesian inference tree of mitochondrial COI-Fr2 gene fragment. The numbers on the nodes indicate Bayesian posterior probability / Maximum Likelihood (bootstrap %) / Neighbor Joining (bootstrap %). A hyphen (-) indicates that the node was not recovered by a particular method. Specimen ID and color pattern designation as in Fig. 3A. Specimens of *I. badionotus* (Selenka, 1867) from Brazil with unknown color pattern are indicated in black color.

— Martínez *et al.* 2016: 19–20, figs 2, 4. — Vergara *et al.* 2018: 36–39, figs 2–3. — Acosta *et al.* 2021: 1–17. — Purcell *et al.* 2023: 142–143.

Stichopus herrmanni – Rodríguez-Forero *et al.* 2013: 12, fig. 5.

Stichopus hermanni – Vergara & Rodríguez 2015: 1022, fig. 1c. Typographic error.

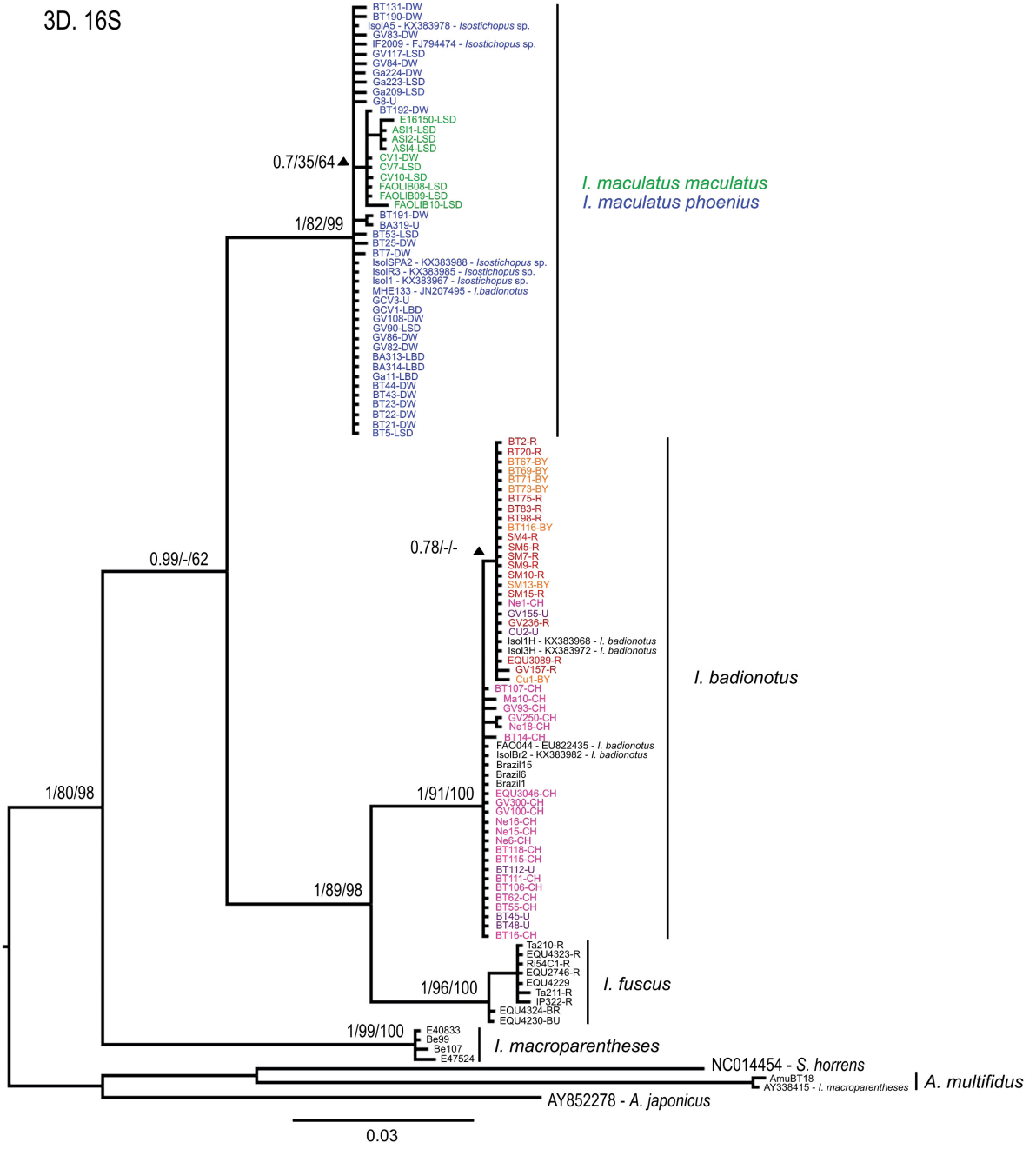

Fig. 3D. Bayesian inference tree of mitochondrial 16S gene fragment. The numbers on the nodes indicate Bayesian posterior probability / Maximum Likelihood (bootstrap %) / Neighbor Joining (bootstrap %). A hyphen (-) indicates that the node was not recovered by a particular method. Specimen ID and color pattern designation as in Fig. 3A. Specimens of *I. badionotus* (Selenka, 1867) with unknown color pattern are indicated in black color.

Original name

Stichopus badionotus Selenka, 1867.

Current status

Isostichopus badionotus (Selenka, 1867).

Name-bearing type

Lectotype MCZ HOL-509.

Type locality

Florida, USA.

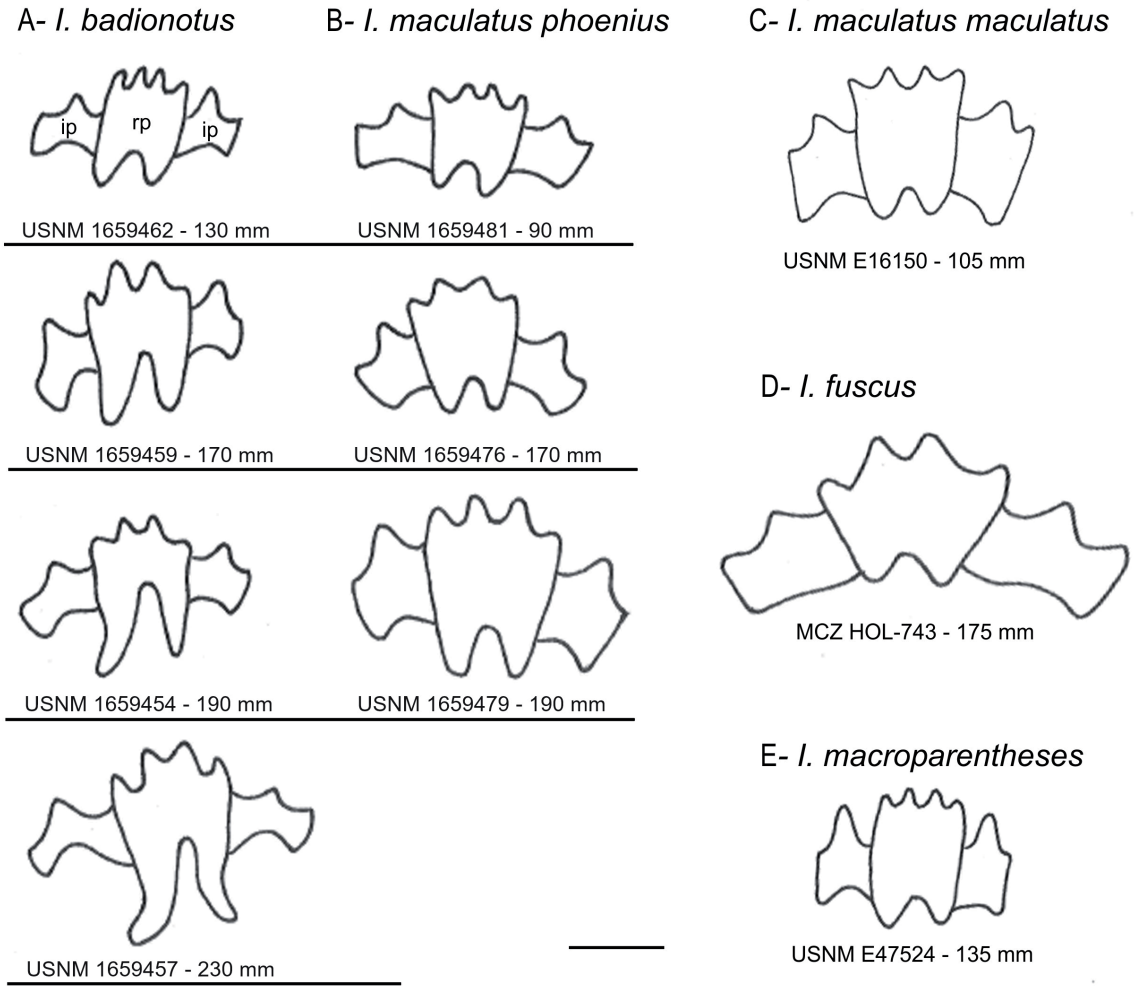

Fig. 4. Comparison of the calcareous rings of species and subspecies of *Isostichopus* Deichmann, 1958. **A**. *I. badionotus* (Selenka, 1867). **B**. *I. maculatus phoenius* (Clark, 1922) (A–B showing calcareous rings from specimens of different sizes). **C**. *I. maculatus maculatus* (Greeff, 1882). **D**. *I. fuscus* (Ludwig, 1875). **E**. *I. macroparentheses* (Clark, 1922). Dimensions of the individuals from which each ring was obtained are shown next to their museum catalog number. Abbreviations: ip = interradial plate; rp = radial plate. Scale bar = 4 mm.

Diagnosis

No spiral lines in dorsal and lateral papillae; four color patterns (Figs 1A–J, 8); no worm-like rod ossicles in dorsal papillae (Fig. 7A); mtDNA divergence from other species of the genus > 6.1% in COI-Fr1 (barcoding region), > 10.8% in COI-Fr2 and > 5.2% in 16S (Table 2).

Material examined

Lectotype (here designated)

USA • 1 reticulated color pattern (L = 190 mm); Florida; collector number 395 leg.; MCZ HOL-509.

Other material

NORTH ATLANTIC – **Bermuda** • 2 specs uniform pattern (L = 170–230 mm); Harrington Sound; 32.330556° N, 64.721944° W; 11 Jul. 1911; E.M. Grosse leg.; MCZ HOL-1082 • 1 spec. chips pattern

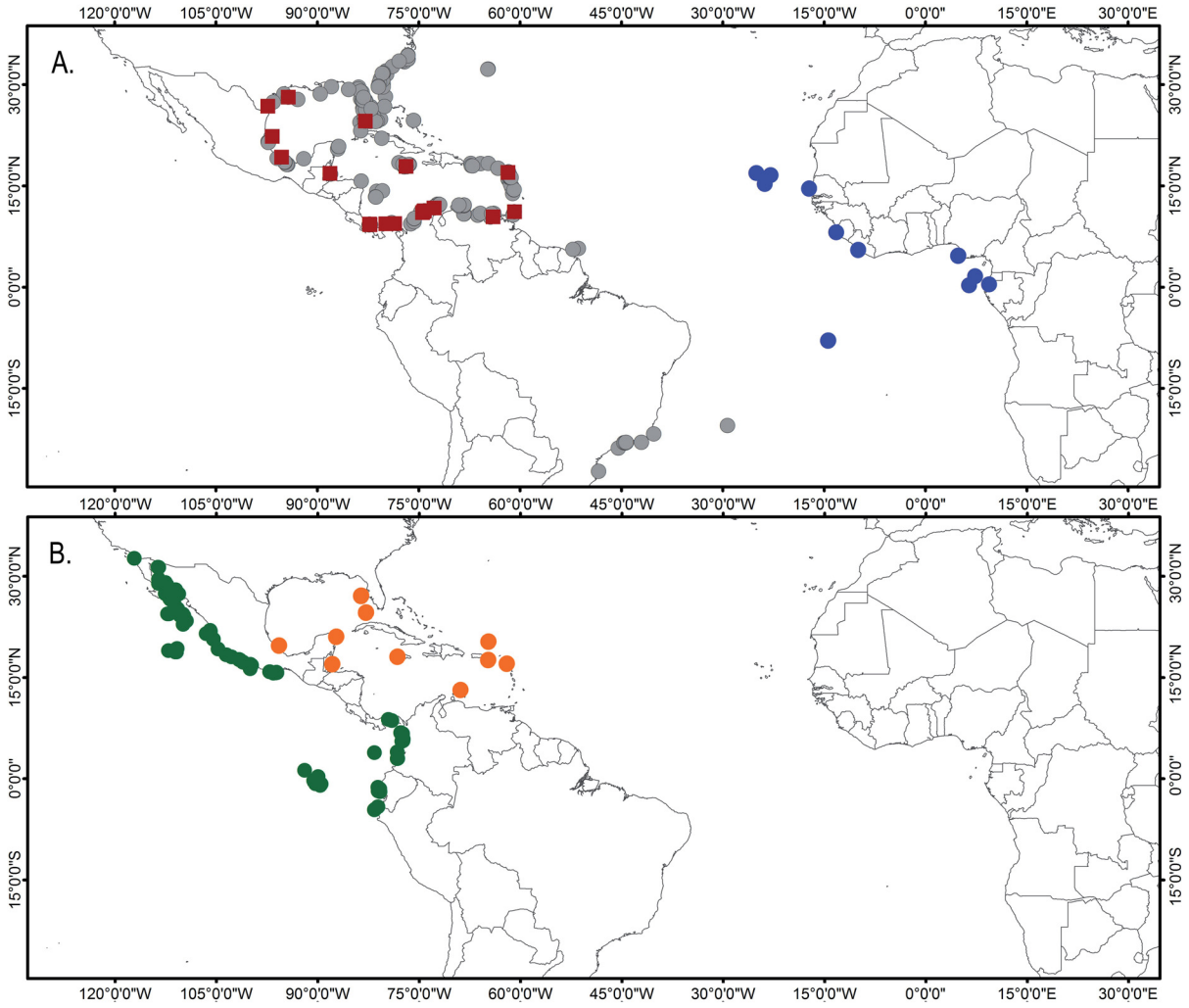

Fig. 5. Geographic distribution of species and subspecies of *Isostichopus* Deichmann, 1958. **A**. *I. badionotus* (Selenka, 1867) (gray circles), *I. maculatus phoenius* (Clark, 1922) (red squares) and *I. maculatus maculatus* (Greeff, 1882) (blue circles). **B**. *I. fuscus* (Ludwig, 1875) (green circles) and *I. macroparentheses* (Clark, 1922) (orange circles). Locations for *I. badionotus* and *I. fuscus* were constructed based on observation records in Global Biodiversity Information Facility data and from museum specimens. Locations for *I. maculatus phoenius*, *I. maculatus maculatus* and *I. macroparentheses* were constructed based only on confirmed localities of collected or preserved museum specimens.

(L = 205 mm); Harrington Sound; 32.330556° N, 64.721944° W; 1911; E.M. Grosse leg.; MCZ HOL-1083 • 1 spec. juvenile (L = 40 mm); Bailey's Bay; 11 Oct. 1972; depth 2–3 m; D.L. Pawson leg.; USNM E11783. – **Bahamas** • 1 spec. uniform pattern? (L = 145 mm); North Bimini, Lerner Marine Lab; 3 Jun. 1959; R.U. Gooding and A.G. Humes leg.; MCZ HOL-4301. – **USA** • 1 spec. chips pattern (L = 166 mm); South Carolina, Racoon Key; 3 Jul. 1963; depth 46 m; A.S. Merril leg.; USNM E9808 • 1 spec. chips pattern (L = 130 mm); Georgia; 30.8967° N, 80.6067° W; 20 Aug. 1980; depth 33 m; Georgia Marine Resources for Minerals Management Service leg.; USNM E27835 • 1 spec. chips pattern (L = 250 mm); Florida, 56.5 nautical miles off NE Inlet; 30.18° N, 80.25° W; 27 Apr. 1983; depth 64 m; W.G. Lyons leg.; USNM E33178.

GULF OF MEXICO – **USA** • 1 spec. chips pattern (L = 210 mm); Florida, Sanibel Island; 26.440359° N, 82.113705° W; Mar. 1938; A.C. Fenner Jr leg.; MCZ HOL-1876 • 1 spec. reticulated pattern (L = 230 mm); Florida, Florida Keys, Dry Tortugas, Bird Key; 24.6185° N, 82.8854° W; Jun. 1917; H.L. Clark leg.; MCZ HOL-1212 • 1 spec. uniform pattern (L = 130 mm); Florida, Florida Keys, Dry Tortugas, Garden Key; 28 Sept. 1982; depth 2 m; J.E. Miller leg.; USNM E27982 • 1 spec. chips pattern (L = 257 mm); NW of Florida Keys; 24.7853° N, 83.2181° W; 20 Nov. 1980; depth 58.6 m; Mote Marine Lab for BLM/MMS leg.; USNM E40637 • 1 spec. uniform pattern (L = 255 mm); Florida, West of Naples; 25.7656° N, 82.1558° W; 12 Feb. 1982; depth 19.6 m; Continental Shelf Associes for BLM/MMS leg.; USNM E39240 • 1 spec. uniform pattern (L = 250 mm); Florida, West of Fort Myers; 26.2803° N, 82.7336° W; 3 May 1981; depth 30.4 m; Continental Shelf Associes for BLM/MMS leg.; USNM E40334. – **Mexico** • 2 specs; Veracruz, Isla Sacrificios; 26 Jan. 1957; M.E. Caso leg.; ICML-UNAM 5.14.10 • 2 specs; Veracruz, Isla de En medio, Anton Lizardo; 19.1088889° N, 95.934445° W; 11 Jun. 2004; depth 1.5 m; P. Rodríguez leg.; on sandy bottom; ICML-UNAM 5.14.45 • 1 spec.; Veracruz, Isla Sacrificios; 19.2916667° N, 96.158056° W; 6 Apr. 2005; depth 1–2 m; J. Díaz leg.; on sandy bottom; ICML-UNAM 5.14.46 • 1 spec.; Veracruz, Bajos de Tuxpan; 21.0271667° N, 97.199° W; 15 Mar. 2011; depth 4–5 m; F. Solís-Marín leg.; coral reef; ICML-UNAM 5.14.58 • 1 spec.; Veracruz, off Isla Lobos; 21.4726667° N, 97.231167° W; 17 Mar. 2011; depth 12 m; F. Solís-Marín leg.; coral reef; ICML-UNAM 5.14.59 • 1 spec.; Veracruz, off Isla Lobos, Capirotes; 21.484° N, 97.228667° W; 17 Mar. 2011; depth 6–14 m; F. Solís-Marín leg.; coral reef; ICML-UNAM 5.14.60 • 1 spec.; Veracruz, El Morro de Punta Delgada; 19.8568333° N, 97.4565° W; 19 Mar. 2011; depth 1 m; F. Solís-Marín leg.; rocky bottom; ICML-UNAM 5.14.61 • 1 spec.; Tabasco, Paraíso Beach, Escollera Oeste; 29 Mar. 1998; M. Dominguez leg.; ICML-UNAM 5.14.41 • 1 spec.; Campeche, Sound of Campeche; Jun. 1972; ICML-UNAM 5.14.36 • 1 spec.; Campeche, Sound of Campeche; Jun. 1978; ICML-UNAM 5.14.37 • 3 specs; Campeche; 19.1716667° N, 91.648333° W; 13 Feb. 1995; ICML-UNAM 5.14.38 • 1 spec.; Campeche, Ciudad del Carmen, Bahamita Beach; 1 Aug. 1972; M.E. Caso leg.; ICML-UNAM 5.14.39 • 1 spec.; Campeche, Ciudad del Carmen, Las Playuelas Mou; 27 Nov. 1973; M.E. Caso leg.; ICML-UNAM 5.14.40 • 1 spec.; Yucatán, Arrecife Alacranes; 22.3871389° N, 89.6843612° W; 1 Aug. 2009; depth 2 m; Q. Hernandez leg.; ICML-UNAM 10736 • 1 spec.; Yucatán, Dzilan de Bravo, Yalkulub lighouse; 22.3980556° N, 88.8875° W; 21 May 2015; depth 14–18 m; A. Poot. leg.; sandy bottom; ICML-UNAM 11094 • 1 spec.; Yucatán, Celestun; 20.8597222° N, 90.4391667° W; 23 Apr. 2010; depth 3 m; S. Rodríguez leg.; sandy bottom; ICML-UNAM 18301.

CARIBBEAN SEA – **Mexico** • 3 specs; Yucatán, Yucalpeten; 21.3522222° N, 89.711111° W; 14 Dec. 2000; depth 5 m; Z. Moguel leg.; ICML-UNAM 5.14.16 • 11 specs; Yucatán, San Felipe; 21.55° N, 89.6° W; 22 Oct. 2000; depth 1.5 m; Z. Moguel leg.; ICML-UNAM 5.14.26 • 2 specs; Quintana Roo, North of Cabo Coche; 22.6566667° N, 87.2083333° W; 28 Apr. 1985; depth 54.5 m; M.E. Caso leg.; ICML-UNAM 5.14.7 • 1 spec.; Quintana Roo, Puerto Morelos; 20.8745833° N, 86.8506944° W; 17 Aug. 1999; depth 6 m; S. Frontana leg.; ICML-UNAM 5.14.42 • 1 spec.; Quintana Roo, Puerto Morelos, Bocana Chica; 20.8804083° N, 86.8509611° W; 3 Aug. 2009; depth 5.3 m; F. Solís-Marín leg.; ICML-UNAM 5.14.57. – **Belize** • 1 spec. reticulated pattern (L = 185 mm); Southwater Cay, West Side; 4 May 1974; K. Sandved leg.; USNM E18633. – **Honduras** • 1 spec. chips pattern (L = 180 mm); West of

Vivario Cays; 15.7233° N, 83.4833° W; 1 Feb. 1971; depth 29 m; leg.; USNM 1014372 • 1 spec.; Cayos Cochinos; Apr. 1998; depth 6 m; C.R. Hasbun leg.; on muddy bottom; ICML-UNAM 5.14.48. – **Panama** • 1 spec. reticulated pattern; Bocas del Toro, Cayo Adriana; 9.240528° N, 82.173417° W; 30 May 2013; depth 15 m; G. Borrero and A. Castillo leg.; mixed bottom sand, sponges, rubble coral, coral, algae and isolated seagrass, exposed, IbBT2R; Tiss-IbBT2 • 1 spec. chips pattern (L = 166 mm); same data as for preceding; IbBT14CH; USNM 1659459 • 1 spec. chips pattern; same data as for preceding; IbBT16CH; Tiss-IbBT16 • 1 spec. reticulated pattern (L = 200 mm); same data as for preceding; IbBT20R; USNM 1659460 • 1 spec. uniform pattern (L = 240 mm); same data as for preceding; depth 5 m; IbBT45U; USNM 1659461 • 1 spec. uniform pattern (L = 130 mm); same data as for preceding; depth 5 m; IbBT48U; USNM 1659462 • 1 spec. chips pattern (L = 185 mm); same data as for preceding; depth 10 m; IbBT55CH; USNM 1659463 • 1 spec. chips pattern (L = 240 mm); Bocas del Toro, Punta STRI; 9.3488889° N, 82.2616667° W; 30 May 2013; depth 6 m; G. Borrero and A. Castillo leg.; sandy bottom, exposed, IbBT62CH; USNM 1659464 • 1 spec. black and yellow pattern; same data as for preceding; IbBT67BY; Tiss-IbBT67 • 1 spec. reticulated pattern (L = 226 mm); same data as for preceding; IbBT69R; USNM 1659464 • 1 spec. black and yellow pattern; same data as for preceding; IbBT71BY; Tiss-IbBT71 • 1 spec. black and yellow pattern; same data as for preceding; IbBT73BY; Tiss-IbBT73 • 1 spec. black and yellow pattern (L = 180 mm); same data as for preceding; IbBT75R; MBMLP IbBT75 • 1 spec. reticulated pattern; same data as for preceding; IbBT83R; Tiss-IbBT83 • 1 spec. chips pattern (L = 135 mm); Bocas del Toro, STRI research station 1; 9.3502778° N, 82.25722222° W; 28 May 2013; depth 4 m; G. Borrero and I. Pedroarena-Leal leg.; seagrass bed, exposed, IBT106CH; MBMLP-IBT106 • 1 spec. chips pattern (L = 202 mm); same data as for preceding; IBT107CH; USNM 1659467 • 1 spec. chips pattern (L = 195 mm); same data as for preceding; IbBT111CH; USNM 1659454 • 1 spec. chips pattern (L = 210 mm); same data as for preceding; IbBT115CH; USNM 1659456 • 1 spec. chips pattern (L = 205 mm); same data as for preceding; IbBT118CH; USNM 1659458 • 1 spec. reticulated pattern (L = 130 mm); Bocas del Toro, STRI research station 2; 9.3488611° N, 82.2585° W; 28 May 2013; depth 5 m; G. Borrero and I. Pedroarena-Leal leg.; mixed bottom of sand, corals, sponges, and isolated seagrass, exposed, IbBT98R; USNM 1659466 • 1 spec. uniform pattern (L = 230 mm); same data as for preceding; IbBT112U; USNM 1659455 • 1 spec. black and yellow pattern (L = 235 mm); same data as for preceding; IbBT116BY; USNM 1659457. – **Colombia** • 1 spec. reticulated pattern; Magdalena, Santa Marta, Punta Betín; 11.250582° N, 74.220133° W; 23 May 2012; depth 3 m; G. Borrero and J. Gómez leg.; sandy, rocky bottom, exposed, IbSM4R; INV-TEJ1167 • 1 spec. reticulated pattern; same data as for preceding; IbSM5R; INV-TEJ1168 • 1 spec. reticulated pattern; same data as for preceding; IbSM7R; INV TEJ1170 • 1 spec. reticulated pattern; same data as for preceding; IbSM9R; INV TEJ1172 • 1 spec. reticulated pattern; same data as for preceding; IbSM10R; INV TEJ1173 • 1 spec. black and yellow pattern; same data as for preceding; IbSM13BY; INV TEJ1176 • 1 spec. reticulated pattern; same data as for preceding; IbSM15R; INV TEJ1178 • 1 spec. chips pattern; Magdalena, Parque Nacional Natural Tayrona, Nenguanje; 11.2500542° N, 74.1633922° W; 24 May 2012; depth 6 m; G. Borrero and E. Acosta leg.; IbNe1CH; INV TEJ1179 • 1 spec. chips pattern; same data as for preceding; IbNe6CH; INV TEJ1184 • 1 spec. chips pattern; same data as for preceding; IbNe15CH; INV TEJ1193 • 1 spec. chips pattern; same data as for preceding; IbNe16CH; INV TEJ1194 • 1 spec. chips pattern; same data as for preceding; IbNe18CH; INV TEJ1196 • 1 spec. chips pattern (L = 140 mm); La Guajira, El Pajaro, Tawaya; 11.7308333° N, 72.7099167° W; 9 Sep. 2013; depth 4.1 m; E. Ortíz and J. López leg.; IbGV93CH; INV TEJ1267 • 1 spec. chips pattern (L = 130 mm); same data as for preceding; IbGV100CH; INV TEJ1268 • 1 spec. uniform pattern (L = 210 mm); La Guajira, El Pajaro, Tawaya; 11.7547778° N, 72.7045833° W; 10 Sep. 2013; depth 4.5 m; E. Ortíz and J. López leg.; IbGV155U; INV TEJ1292 • 1 spec. reticulated pattern (L = 135 mm); same data as for preceding; IbGV157R; INV TEJ1294 • 1 spec. reticulated pattern (L = 180 mm); same data as for preceding; depth 6.8 m; IbGV236R; INV TEJ1301 • 1 spec. chips pattern (L = 220 mm); La Guajira, Manaure, Piedras Blancas; 11.8251389° N, 72.4600833° W; 28 Sep. 2013; depth 9.2 m; E. Ortíz and J. López leg.; IbGV250CH; INV TEJ1306 • 1 spec. chips pattern (L = 115 mm); same data as for preceding; IbGV300CH; INV TEJ1310 • 1 spec. chips pattern (L = 190 mm);

La Guajira, Manaure; 11.96030556° N, 72.57925° W; 5 Apr. 2005; depth 50 m; N. Cruz-Macrofauna-Corpoguajira Project leg.; sandy bottom, IbEQU3046CH; INV EQU3046 • 1 spec. chips pattern (L = 200 mm); La Guajira, Manaure; 11.8778333° N, 72.790361° W; 4 Apr. 2005; depth 54 m; N. Cruz-Macrofauna-Corpoguajira Project leg.; sandy bottom, INV EQU3047; GenBank: INV EQU3047 • 1 spec. chips pattern; La Guajira, Manaure; 11.327184° N, 74.081037° W; 29 Oct. 2011; depth 7 m; G. Borrero and C. Díaz leg.; sandy bottom, IbMa10CH; INV TEJ1125 – **Venezuela** • 1 spec. chips pattern (L = 160 mm); USNM E11411. – **Curaçao** • 1 spec. black and yellow pattern; 12.170247° N, 69.039721° W; IbCu1BY; Tiss-IbCu1 • 1 spec. uniform pattern; 12.170247° N, 69.039721° W; leg.; IbCu2U; Tiss-IbCu2. – **Cuba** • 1 spec. chips pattern (L = 210 mm); 1914; J.B. Henderson and P. Bartsch leg.; USNM 34802. – **Jamaica** • 1 spec. chips pattern (L = 150 mm); Portland Bight; 17.8367° N, 77.11° W; 5 Jul. 1970; depth 13 m; leg.; USNM 1014365. – **Puerto Rico** • 1 spec. uniform pattern (L = 50 mm); La Parguera, Enrique reef; 26 Apr. 1986; C.E. Cutress leg.; USNM E43381 • 1 spec. reticulated pattern (L = 160 mm); La Parguera, Enrique reef; Nov. 1986; C.E. Cutress leg.; USNM E43382. – **British Virgin Islands** • 1 spec. uniform pattern (L = 160 mm); Guana Island; Jul. 1999; A.M. Kerr leg.; USNM E51775 • 1 spec. juvenile (L = 55 mm); Guana Island; depth 2 m; A.M. Kerr leg.; USNM E47522. – **Antigua and Barbuda** • 1 spec. uniform pattern (L = 280 mm); Antigua Island, English Harbor; 17° N, 61.7667° W; Jul. 1918; C.C. Nutting, State University of Iowa leg.; USNM E41459.

SOUTH ATLANTIC – **Brazil** • 1 spec.; Santa Catalina, Island of Arvoredo; 27.273601° S, 48.366889° W; IbBr1; Tiss-IbBr1, only tissue • 1 spec.; same data as for preceding; IbBr9; Tiss-IbBr9, only tissue • 1 spec.; Santa Catalina, Desert Island; 27.273601° S, 48.366889° W; IbBr6; Tiss-IbBr6, only tissue • 1 spec.; same data as for preceding; IbBr15; Tiss-IbBr15, only tissue.

Description

External appearance. Preserved and live ex situ specimens, up to 300 mm long, range of examined specimens 40–240 mm (n = 39, lectotype: 190 mm long). Body loaf-like, length/width ratio 4 ± 0.7 (n = 18, 2.5–5.9, lectotype 2.5). Rounded posteriorly and anteriorly (Fig. 6), convex or somewhat quadrangular in cross-section (Fig. 8); largest specimens usually quadrangular. Body wall firm and thick (2–6 mm thick in the lectotype). Anus supra-terminal, circular and surrounded by large papillae. Mouth directed ventrally, encircled by collar of large papillae (3–4 mm high in the lectotype). Large peltate tentacles 20, up to 10–12 mm long, with shields 7–10 mm wide. Dorsal and lateral papillae variable in size, shape, and organization. Dorsal papillae wart-like, rounded, and low or flat with only one pointed tip, scattered irregularly in convex specimens or in two irregular rows along each flank defining the quadrangular shape (Fig. 8). Lateral papillae large and stout, conical, pointed or rounded, or forming a continuous fringe (Fig. 8), sharply defining the ventral surface. Dorsal body wall of the lectotype deteriorated, but with some medium size papillae (up to 1–2 mm high and 3–6 mm wide at the base), not conspicuous; most of the papillae in the lectotype in the two dorso-lateral rows (Fig. 6A). Ventral surface covered with numerous cylindrical and large pedicels arranged in three longitudinal rows (Fig. 6B).

Color and body wall appearance. The body wall in living specimens is smooth and opaque in adults longer than 130 mm (Figs 1A–J, 8). Dorsal coloration extremely variable; four main color patterns (Figs 1, 8): (1) Chips color pattern (CH) (Fig. 1A–D): the most common, light or dark brown, pink, orange background, with scattered darker spots of variable size, rounded or irregular, and separated or joined. in blotches; the species owes one of its common names “chocolate chip sea cucumber” to this coloration. (2) Uniform color pattern (U) (Fig. 1E): uniformly brown, orange, pink, yellowish, or black; some with darker papilla tips. (3) Reticulated color pattern (R) (Fig. 1F–I): beige background with a darker brown reticulum, which may also appear as small beige irregular spots on a darker brown background; papillae inside the reticulum, darker with yellow or beige sharply pointed tips, and dark brown rings at the base. (4) Black and yellow color pattern (BY) (Fig. 1J): black background with large yellow rounded or low and pointed papillae. Ventral coloration also highly variable, uniformly

of the same color as the dorsal side, or spotted, or blotched. Specimens in alcohol always lighter, but color pattern retained. Lectotype brown with a clear "Reticulated" color pattern in the best preserved areas; papillae, shield of tentacles, ventral surface, and pedicels same color as the background; stalk of tentacles lighter (Fig. 6A–B). Juveniles (40–50 mm) with semi-translucent body wall, and of similar color as the adults (Fig. 8R–U, F').

Internal anatomy (based on MCZ HOL-509, lectotype; USNM 1659462; USNM 1659459; USNM 1659454 and USNM 1659457, specimens 130–230 mm long). Calcareous ring of lectotype 14 mm in diameter, radial elements roughly quadrangular, 7 mm wide and 7 mm long, with four small anterior lobes; two dorsal radial plates with long posterior projections (3–4 mm long) turned inwards; the three ventral radial plates with shorter posterior projections than the two dorsal plates; interradial elements, 5 mm wide and 2 mm long, less wide than radial elements, shorter than half the length of radial elements, pointed anteriorly with a concave posterior margin (3.5 mm long) (Fig. 4A). Posterior projection in the dorsal radial plates lengthens during growth and turnes inwards in the largest specimens, as described in the lectotype (Fig. 4A). Stone canal in the lectotype irregularly helical, about 22 mm long, including a flat leaf-like madreporite 6 mm at its longest diameter, attached to the mesentery, partially calcified, and ending in a point. Single stone canal similar to lectotype in shape in other examined specimens (L(body length) = 130 mm: 5 mm long; L = 230 mm: 21 mm). Tentacle ampullae in the lectotype about 20–25 mm long and 1 to 2.5 mm wide, with small branches at the tips and the bases, increasing with size in other specimens (L = 130 mm: ampullae = 2 mm; L = 230 mm: ampullae = 21 mm). Single Polian vesicle about 24 mm long by 5 mm wide in the lectotype; similar in other examined specimens (L = 130 mm: 11 mm long by 3 mm wide; L = 230 mm: 19 mm by 5 mm). Gonad in two tufts, one on either side of dorsal mesentery, branched in numerous cylindrical tubes about 0.5–1.5 mm wide, extending 85 mm from the anterior to the posterior body and filled with eggs 72–99 µm diameter in the lectotype (Fig. 11A). Gonads present in specimens from 130 mm long. Longitudinal muscles divided, about 10 to

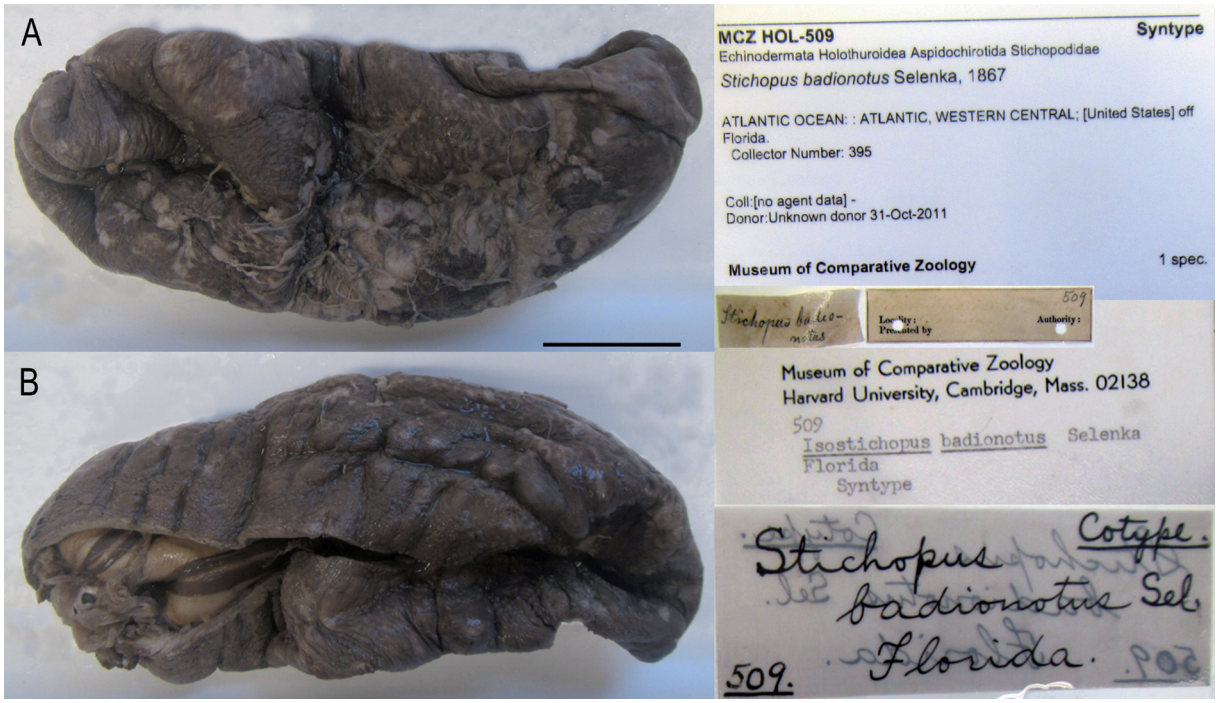

Fig. 6. Preserved lectotype of *Isostichopus badionotus* (Selenka, 1867) from Florida, USA (MCZ HOL-509, 190 mm long). **A**. Dorsal view. **B**. Ventral view with original labels. Scale bar = 35 mm. Photos by G. Borrero.

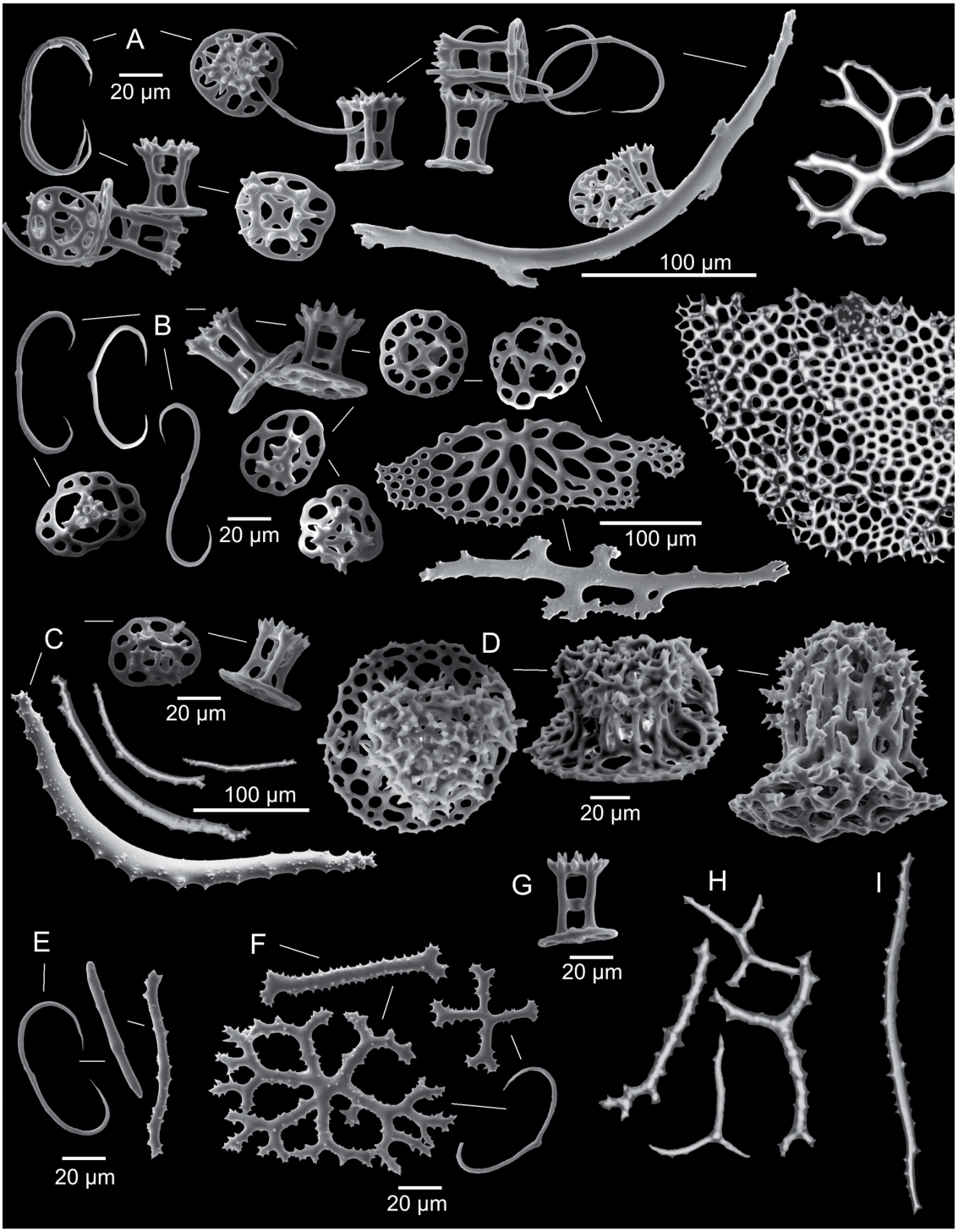

Fig. 7. *Isostichopus badionotus* (Selenka, 1867) ossicles (specimen USNM 1659454-BT111, 190 mm long). **A**. Thin C-shaped rods, tables, perforated plates and large, curved rods from dorsal body wall and papillae. **B**. Thin C- and S-shaped rods, tables, perforated plates, large, curved rods and end plate (not complete, ¼ of the plate) from ventral body wall and tube feet. **C**. Rods and tables from tentacles. **D**. Large tables from mouth membrane. **E**. Thin C-shaped rods and simple rods from longitudinal muscles. **F**. Thin C-shaped rods, simple, cross-shaped and irregular plate-like branched rods in the cloaca. **G**. Table from respiratory trees. **H**. Cross-shaped ossicles from intestine. **I**. Simple rod from gonads. Photos by G. Borrero.

12 mm wide in the lectotype, attached to body wall medially and unattached laterally. Respiratory trees inserted near the anterior part of the cloaca, arising from a 16 mm long common stem in the lectotype. Right tree about 100 mm long, left tree about 110 mm, extending along the intestine. Similar respiratory trees in other specimens, with the right branch shorter than the left.

Ossicles (based on MCZ HOL-509, lectotype, for mouth membrane and gonads, other ossicles deteriorated; USNM 1659462; USNM 1659454 (SEM images); USNM 1659457 and USNM E11783 (juvenile, only for dorsal papillae), specimens 40–230 mm long).

Dorsal papillae with tables, thin C-shaped rods, perforated plates, and large, curved rods (Figs 7A, 10A). Numerous C-shaped deposits, fewer S-shaped, 52–130 ($\bar{x}$ = 80) µm, usually present in the papillae, especially towards the tip, variable in abundance in different papillae of the same specimen. Length of C-shaped deposits increasing with body length (Fig. 9A). Numerous table ossicles 33–70 ($\bar{x}$ = 52) µm high and 39–81 ($\bar{x}$ = 58) µm across the disc; spires composed of four pillars, usually parallel or slightly constricted proximally to the disc, ending in triplets of blunt spines forming a wide crown, one crossbeam connecting adjacent pillars. Table spire of 40 mm long juvenile with many minute spines. Disc margins smooth and wide; discs with one rounded central perforation and 8 to 12 peripheral holes, usually arranged in one simple ring (Figs 7A, 10A). Tables close to the tip of the papillae larger, taller, and with wider discs, with several extra perforations arranged in more than one ring, becoming smaller and with fewer perforations toward the base of the papillae where they are similar to those from the body wall (Fig. 10A). Small changes of tables in size and shape during growth; but tables with shorter spire in the 40 mm specimen (33–41 µm high; $\bar{x}$ = 37) than in other examined sizes (42–70 µm high; $\bar{x}$ = 58) (Figs 9B, 10A); disc tables in smaller specimens wider than in larger ones (Figs 9C, 10A), usually with more than 8–10 holes arranged in more than one ring; in larger specimens disc tables typically with 8–12 holes set in one ring (Fig. 10A). Few perforated plates (112–179 µm), located at the tip of the papillae, with a few large perforations, larger at the center of the plate (Fig. 7A); not found in the 40 mm specimen. Large, curved rods (240–493 µm) with quadrangular occasionally perforated projections in the middle (Fig. 7A).

Dorsal body wall with only tables and a few C-shaped ossicles (63–83 µm), less frequent than in papillae, rarely S-shaped (Fig. 7A). Tables similar in shape as in papillae but smaller 47–62 ($\bar{x}$ = 54) µm high, 39–69 ($\bar{x}$ = 49) µm across the disc, the discs with one ring of 8–12 holes (Fig. 10A).

Pedicels with tables, thin C-shaped rods, perforated plates, large, slightly or strongly curved rods, and end plates (Fig. 7B). A few specimens also with a few C-shaped, rarely S-shaped, deposits 70–95 ($\bar{x}$ = 85) µm. Numerous table ossicles 24–42 ($\bar{x}$ = 34) µm high and 25–72 ($\bar{x}$ = 53) µm across the disc, less high than those from dorsal papillae and the dorsal body wall, similar in shape to the ones from the dorsal papillae, but with the central perforation usually larger and not rounded, with four points that sometimes interrupt the simple ring of holes in the disc, usually one ring of holes, with no extra perforations (Fig. 7B). Numerous elongated perforated plates (174–432 µm), with numerous perforations larger and elongated in the center of the plate; large slightly or strongly curved rods (316–483 µm) with broad perforated expansions in the middle; end plates 687 µm across, increasing in size during growth.

Ventral body wall with only tables and a few C-shaped ossicles.

Tentacles with rods and tables (Fig. 7C). A few table ossicles similar to those from the dorsal body wall 40–56 µm high and 40–73 µm across the disc; numerous strongly or slightly curved spiny rods (37–804 µm), sometimes with perforations at the ends.

Mouth membrane with C-shaped ossicles, large tables, and rods in some specimens (Figs 7D, 11A). Thin 43–102 µm C-shaped rods and numerous large tables 89–160 µm high and 100–159 µm across

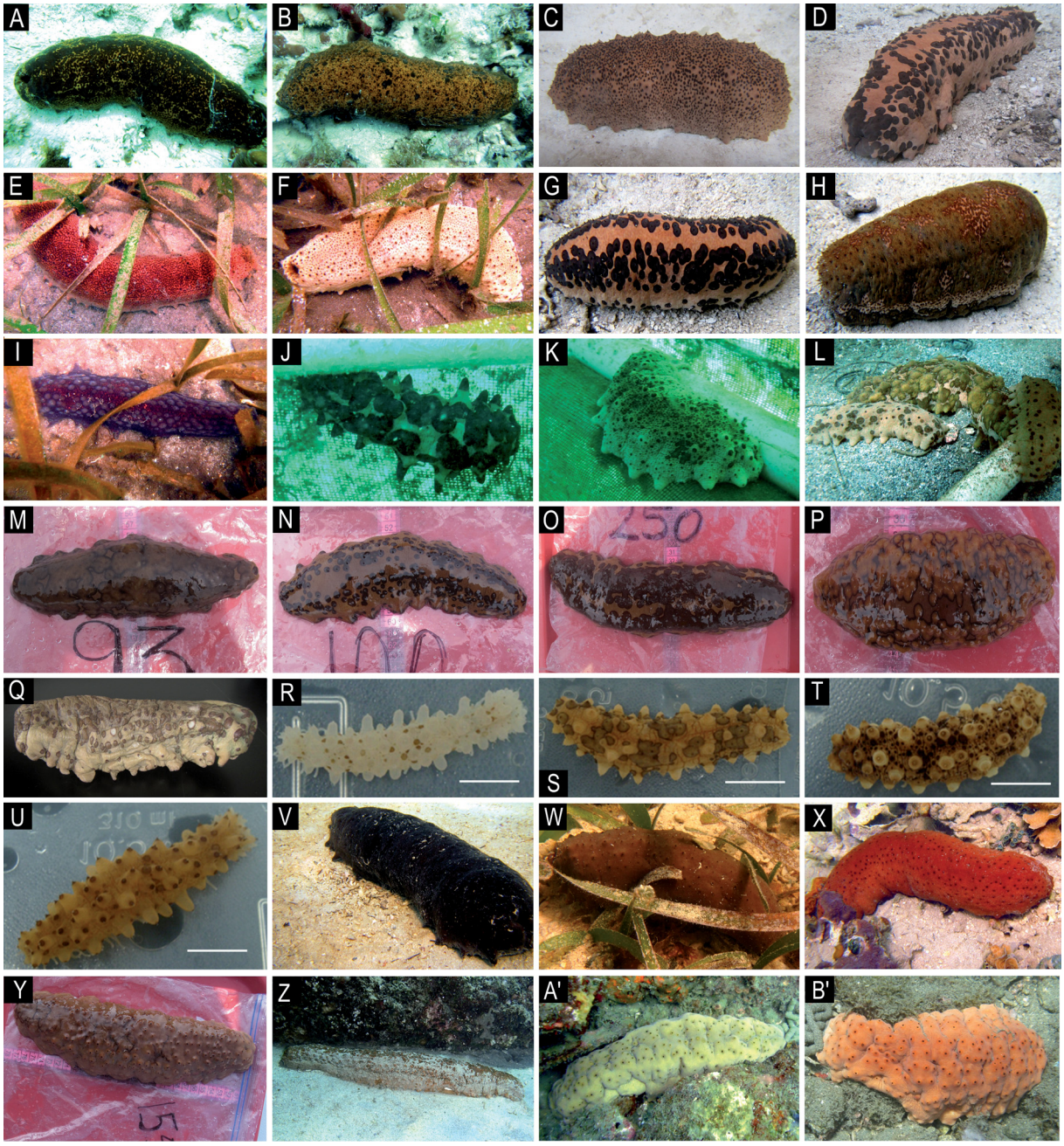

Fig. 8 (continued on next page). Color patterns and morphological variation of *Isostichopus badionotus* (Selenka, 1867) (DNA sequences and detailed information of some specimens are indicated in Table 1, see Photo ID column for correspondence). **A–U, I'**. Specimens with "Chips" color pattern from Bocas del Toro, Panamá (A–I), Neguanje, Colombia (J–L), La Guajira, Colombia (M–Q); juveniles from Neguanje, Colombia (R–U). **V–B'**. Specimens with "Uniform" pattern from Bocas del Toro (Panama) (V–X), La Guajira, Colombia (Y), Curaçao (Z), Magdalena, Colombia (A'–B'). **C'–K'**. Specimens with "Reticulated" pattern from Bocas del Toro, Panama (C'–E'), Juvenile from Neguanje, Colombia (F'), Punta Betin, Magdalena, Colombia (G'–I'), La Guajira, Colombia (J'–K'). **L'–O'**. Specimens with "Black and yellow" pattern from Bocas del Toro, Panamá (L'), Magdalena, Colombia (M'–O'). Photos: A–I, Q, V–X, C'–E', L', O' by G. Borrero; R–U by G. Ospina; J–L by E. Acosta; M–P, Y, J'–K' by E. Ortiz; Z, M' by M. González-Wangüemert; G'–I' by J. Gómez; and A'–B', N' by S. Zea. Scale bars = 10 mm.

the disc. Large tables with the spire well developed, composed of at least ten pillars that are joining at the top, forming a very dense and thick crown of spines, without crossbeams connecting adjacent pillars, lateral edges of the external pillars usually with pointed projections. Table discs generally wide with several rings of holes; sometimes reduced, same width as the spire in 130 mm specimen (Figs 7D, 11A); large tables taller and more slender in the 130 mm long specimen, 166–271 µm heigh, whereas 125–188 µm high in specimens 195 and 230 mm long.

Longitudinal muscles with thin C-shaped rods 40 to 85 ($\bar{x}$ = 58) µm long and small, simple 59–145 ($\bar{x}$ = 112) µm rods (Fig. 7E). Posterior cloaca with numerous C-shaped rods (48–73 µm), simple rods (74–131 µm), and spinous irregular plate-like branched rods (Figs 7F, 11A); anterior cloaca with large and complex tables 105–140 µm high and 139–180 µm across the disc (Fig. 11A). Respiratory trees with few tables 46–55 µm high and 45–56 µm across the disc in the 130 and 195 mm long specimens, but not in the 230 mm long one (Fig. 7G). Intestine with spinose or smooth 43–110 µm rods in a cross shape, sometimes with bifurcated ends (Fig. 7H). Gonads with delicate, long rods 449–775 µm (Fig. 7I). Rods in the gonads present even in the 130 mm long specimen. Gonads of the lectotype with rods 301–452 µm long (Fig. 11A).

Distribution

Western Atlantic, from Bermuda and North Carolina, USA to Santa Catarina, South Brazil, including the Gulf of México and the Caribbean Sea (Fig. 5A). The geographic range of *I. badionotus* as defined here is restricted to the Western Atlantic, where it is sympatric with *I. maculatus phoenius* currently confirmed in the Gulf of Mexico and the Caribbean Sea, and with *I. macroparentheses* reported from some locations in the Gulf of Mexico and the Caribbean Sea. The southernmost record of *I. badionotus* in Santa Catarina, Brazil, was confirmed by mitochondrial DNA (Fig. 3C–D). It has been reported from

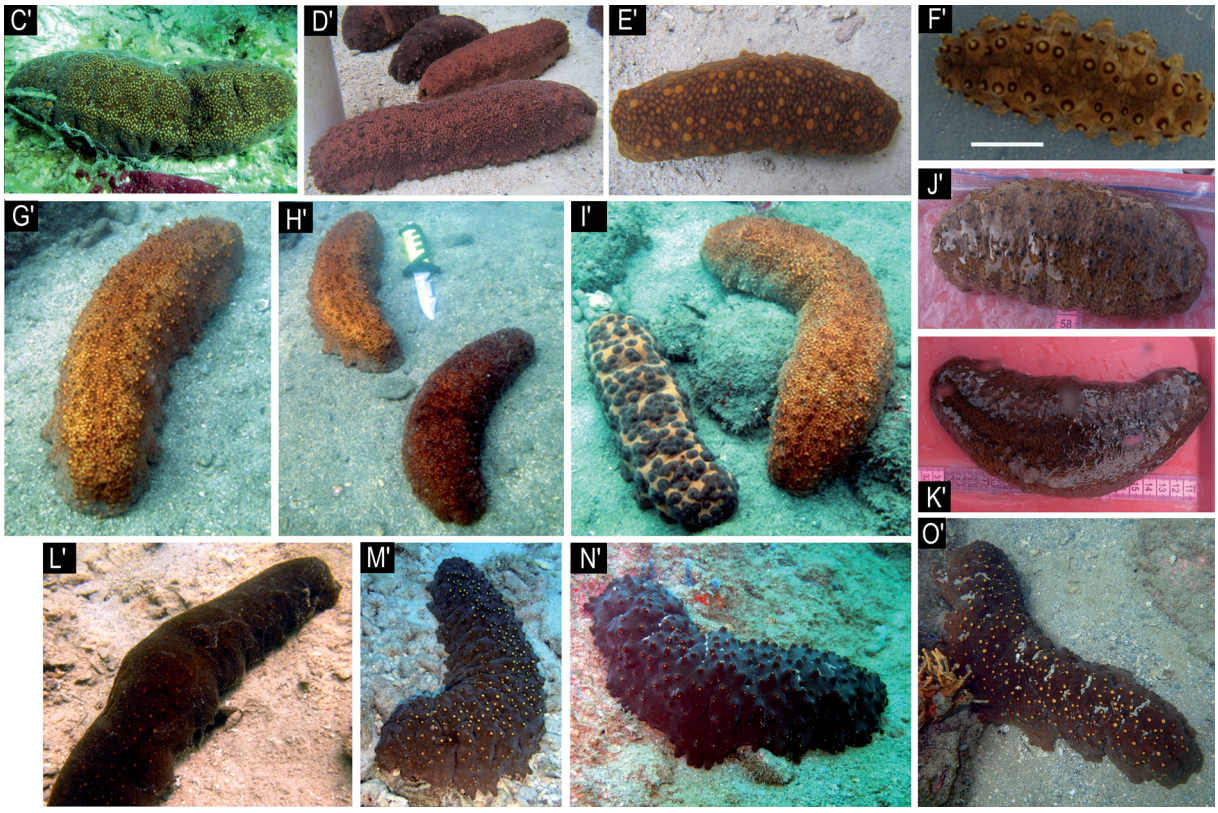

Fig. 8 (continued).

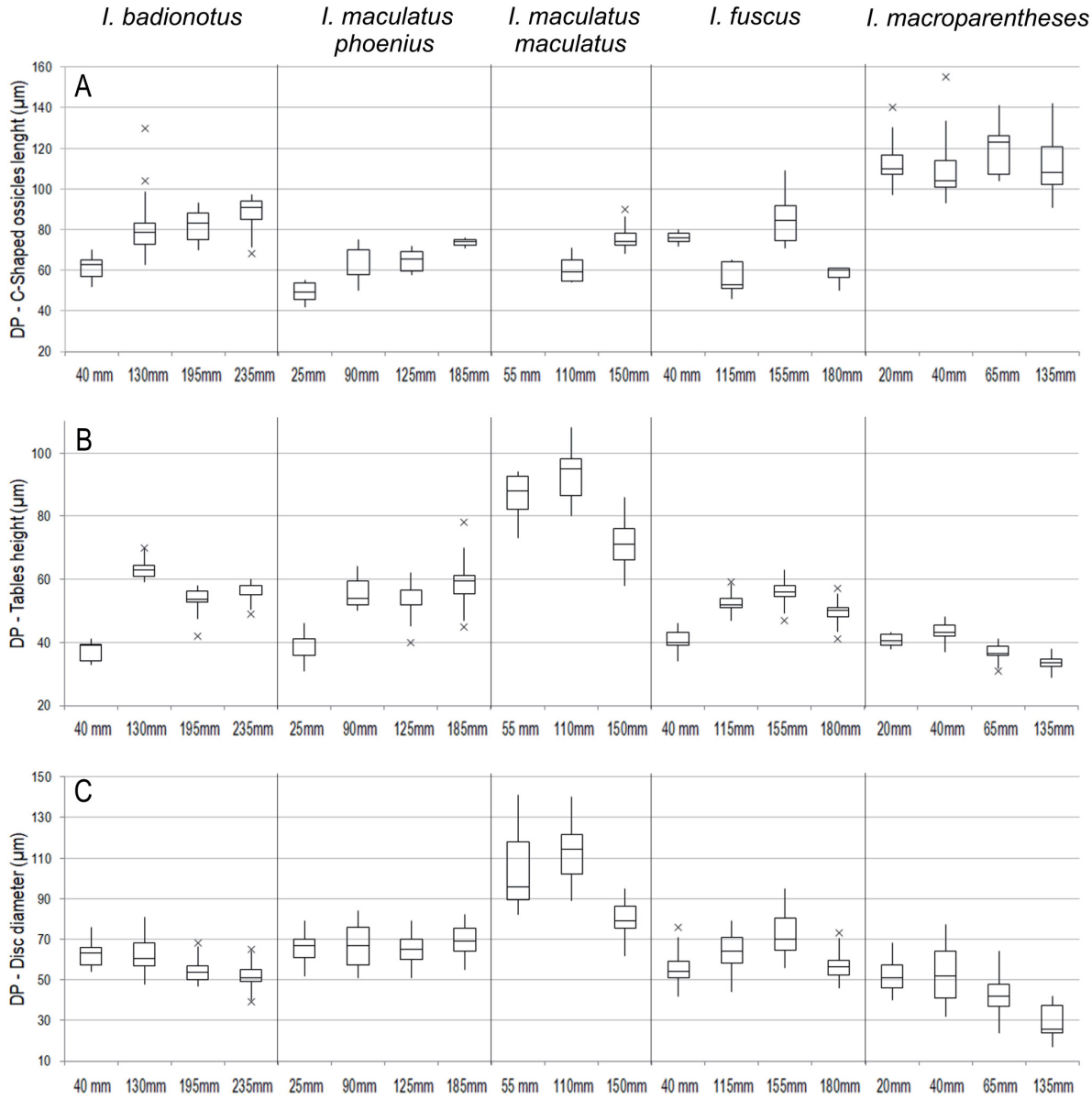

Fig. 9. Box-plots comparing ossicle size from dorsal papillae from small to large specimens(along x axis) from each of the species and subspecies of *Isostichopus* Deichmann, 1958. **A**. Dorsal papillae: C-shaped ossicle length. **B**. Dorsal papillae: table height. **C**. Dorsal papillae: table disc diameter. Photos of the ossicles of the same specimens are presented in Fig. 10. Specimens IDs: *I. badionotus* (Selenka, 1867) L = 40 mm, USNM E11783; L = 130 mm, USNM 1659462-BT48; L = 195 mm, USNM 1659454-BT111; L = 230 mm, USNM 1659447–BT116; *I. maculatus phoenius* (Clark, 1922) L = 25 mm, INV EQU4565; L = 90 mm, USNM 1659481-Ga224; L = 125, USNM 1659472-BT192; L = 185, USNM 1659479-BT53; *I. maculatus maculatus* (Greeff, 1882) L = 55 mm, ASI1; L = 110 mm, ASI4; L = 150 mm, CV1; *I. fuscus* (Ludwig, 1875) L = 40 mm, INV EQU4229; L = 115 mm, INV EQU4324; L = 55 mm, MBMLP-If212; L = 180 mm, INV EQU4323; *I. macroparentheses* (Clark, 1922) L = 20 mm, USNM 1659484-Be99; L = 40 mm, USNM 1659485-Be107; L = 65 mm, MCZ HOL-1214; L = 135 mm, USNM E47524.

the Brazilian coast and nearby islands, in São Sebastião, the northeast coast of Brazil, and the Trindade and Martin Vaz Archipelago by Netto *et al.* (2005), Netto (2006), Prata *et al.* (2014) and Martins *et al.* (2016), whose photographs depict *I. badionotus*. Bathymetric distribution 0–183 m (USNM E39041). The species is common between 0–30 m.

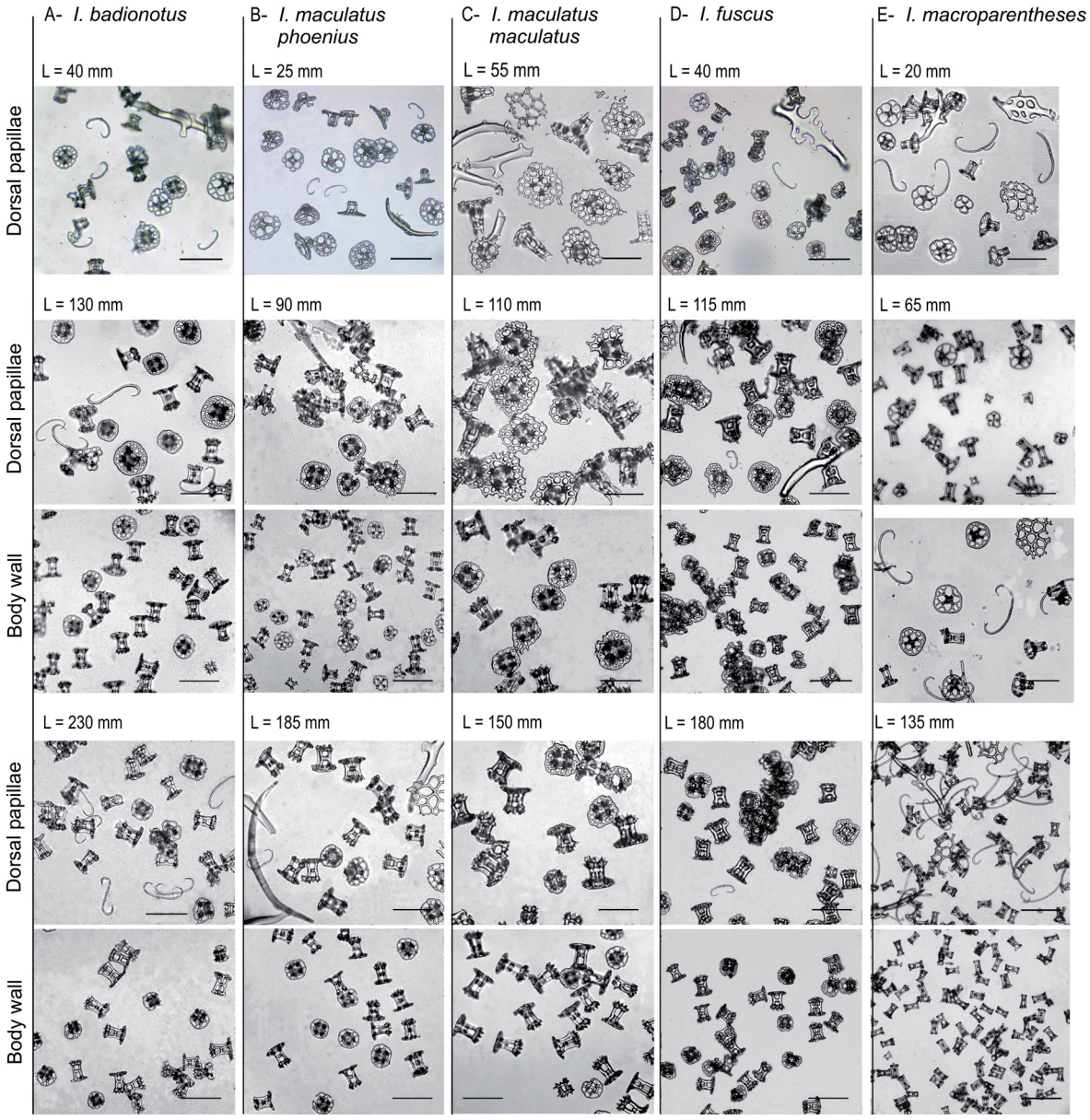

Fig. 10. Light microscope photographs of the same specimens as in Fig. 9 (see the length (L) for correspondence), comparing ossicle size and shape from dorsal papillae and dorsal body wall from small to large specimens from each of the species and subspecies of *Isostichopus* Deichmann, 1958. **A**. *I. badionotus* (Selenka, 1867). **B**. *I. maculatus phoenius* (Clark, 1922). **C**. *I. maculatus maculatus* (Greeff, 1882). **D**. *I. fuscus* (Ludwig, 1875). **E**. *I. macroparentheses* (Clark, 1922). Photos by G. Borrero. Scale bars = 100 µm.

Habitat

Isostichopus badionotus is common and abundant. Field observations have recorded juveniles of *I. badionotus* on seagrass (Shiell 2004) and attached to the underside of rubble or coral slabs (Clark 1933; Hendler *et al.* 1995; Conand 2006), although some of these reports may include juveniles of *I. maculatus phoenius*. The species is found on muddy, sandy, sandy-muddy, rocky substrates, seagrass beds, mostly *Thalassia testudinum* K.D. Koenig, and mixed bottoms (sand, corals, algae, sponges, and scattered seagrass). As a distinctive characteristic of *I. maculatus phoenius*, individuals larger than 130 mm in length are exposed, as also reported by Acosta *et al.* (2021). An indication of a relationship between habitat preferences and color patterns was observed. Individuals with a "Reticulated" and "Black and yellow" pattern were never found in dense seagrass beds; they were associated with mixed bottoms of corals and sand. In some places, it is possible to find several color patterns, whereas in others

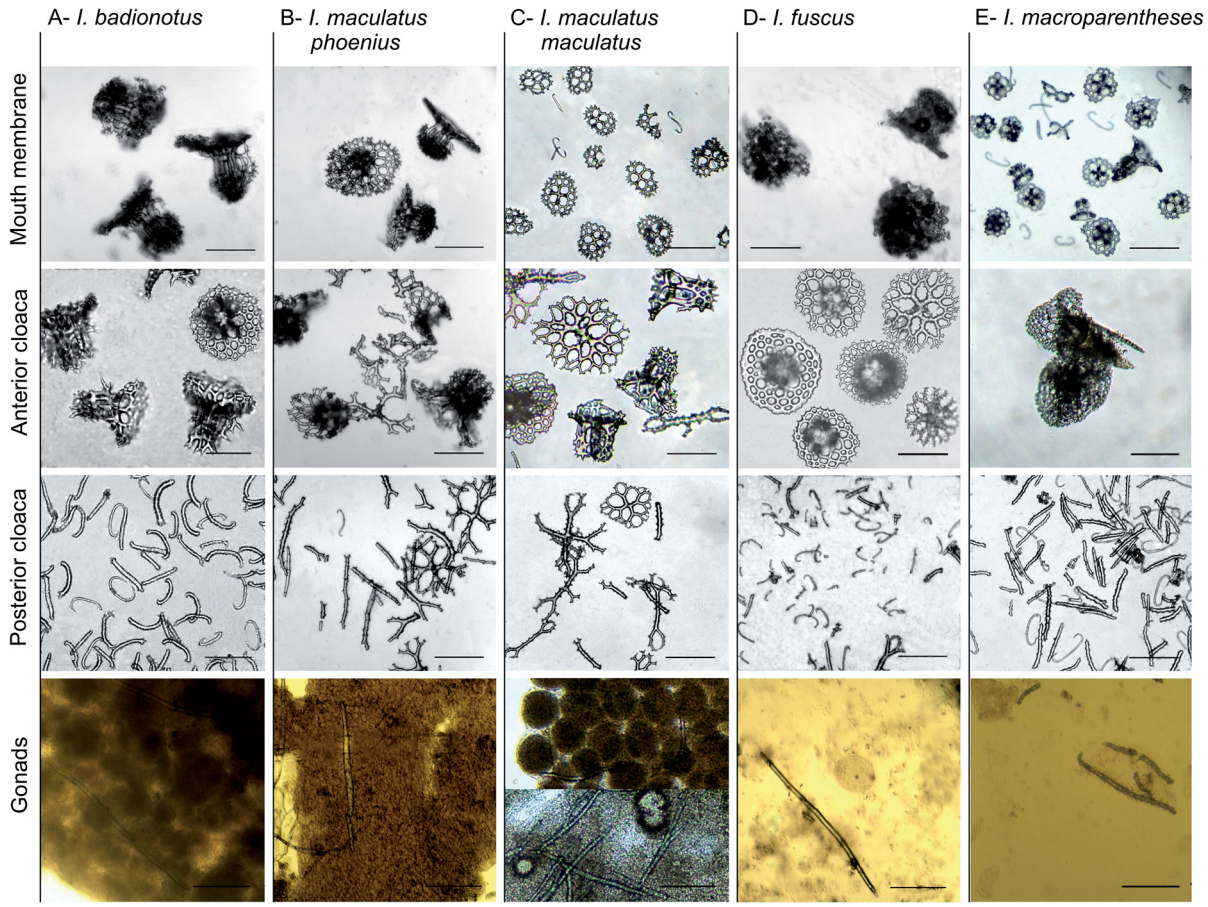

Fig. 11. Light microscope photographs showing ossicles from the mouth membrane, anterior cloaca, posterior cloaca, and gonads of the species and subspecies of *Isostichopus* Deichmann, 1958. **A**. *I. badionotus* (Selenka, 1867) (mouth membrane and gonads from the lectotype MCZ HOL-509; anterior and posterior cloaca from USNM 1659457-IbBT116). **B**. *I. maculatus phoenius* (Clark, 1922) (all ossicles from the holotype MCZ HOL-1182). **C**. *I. maculatus maculatus* (Greeff, 1882) (all ossicles from the neotype USNM E16150; male gonads at the bottom from the neoparatype USNM E16151). **D**. *I. fuscus* (Ludwig, 1875) (mouth membrane from MCZ HOL-742; anterior cloaca from MBMLP-If212; posterior cloaca and gonads from MCZ HOL-743). **E**. *I. macroparentheses* (Clark, 1922) (mouth membrane, anterior and posterior cloaca from USNM E47524; gonads from the holotype MCZ HOL-921). Photos by G. Borrero. Scale bars = 100 µm.

only one color is present or is the most abundant. This was also noted by Clark (1942), who compared coloration variation in the populations in Bermuda and Jamaica.

Remarks

The taxonomic status of *Isostichopus badionotus* (Selenka, 1867) is considered stable since Clark's 1922 revision of the genus *Stichopus*, which included a detailed study of *Stichopus badionotus* (currently *Isostichopus badionotus*) based on museum and living specimens. Six species of *Stichopus* had been described from the tropical West Atlantic region (*Stichopus badionotus* Selenka, 1867; *S. haytiensis* Semper, 1868; *S. moebii* Semper, 1868; *S. errans* Ludwig, 1875; *S. diaboli* Heilprin, 1888 and *S. xanthomela* Heilprin, 1888), and two species from West African regions (*Stichopus maculatus* and *S. assimilis*). After a detailed study of the diagnostic characters, Clark (1922) united all eight species under *S. badionotus*. He concluded that "color is absolutely unreliable as a distinguishing character, and body-texture, form, and tuberculation seem to be equally hopeless. The calcareous particles too undergo growth changes which lead into difficulties".

Our extensive sampling and revision, including mtDNA sequences of each color pattern, revealed that Clark (1922) was correct in synonymizing as *S. badionotus* the other five species of *Stichopus* that had been described at that time in the West Atlantic. However, he was not right in synonymizing the two species from the East Atlantic as *S. badionotus*. mtDNA sequences, coloration and ossicles distinguish *I. badionotus* from *I. maculatus* as a different species. This species includes two subspecies, the nominal *I. maculatus maculatus* from the East Atlantic and *I. maculatus phoenius* from the West Atlantic, sympatric with *I. badionotus*. This means that Clark (1922) was also correct in distinguishing one specimen with the entire back and sides bright carmine-red as *Stichopus badionotus* var. *phoenius*, which we here elevate to sub-specific rank and transfer to *I. maculatus*. The East Atlantic species, *S. assimilis*, proved to belong to the genus *Holothuria* Linnaeus, 1767 (see *I. maculatus maculatus* remarks). Our comparative examination of ossicle differences in the species and subspecies of *Isostichopus* showed that Clark (1922) was also right in describing *I. macroparentheses* as a distinct species based on the longest C-shaped ossicles.

Although the types of the previously accepted West Atlantic species (*S. haytiensis*, *S. moebii*, *S. errans*, *S. diaboli* and *S. xanthomela*) were not available for examination, their original description, online pictures and the revision in the present paper strongly suggest they are synonymous to *I. badionotus*, concurring with the decision by Clark (1922, 1933, 1942). These species were not thoroughly described by the original authors, and the illustrations of their ossicles were not informative, because they are so similar to each other. Heilprin (1888) presented the most extensive discussion of these five species. He noted the presence of wart-like tubercles, number of pedicels, and color as characters that would clarify confusion between *S. diaboli* and *S. haytiensis*, and among *S. xanthomela*, *S. moebii* and *S. errans*. Regarding color, *S. diaboli* was described as black, *S. haytiensis* as dark chocolate-brown, blotched with yellow spots, which form five longitudinal bands in the interradii, *S. xanthomela* as reddish-yellow with irregular blotches of black or very dark brown, *S. moebii* as reddish gray, slightly lighter on the abdomen with numerous large round brown-black, sometimes confluent spots on the back, and *S. errans* as of similar color to *S. moebii*. These original descriptions of color patterns from these previously accepted species fit the color patterns of specimens examined and assigned to *I. badionotus* in the present paper. They do not, however, fit the color patterns of *I. maculatus phoenius*, because there was no mention of the white blotches and small black dots characteristic of this subspecies. Some *I. maculatus phoenius* are uniform red or green, again colors not reported in any of these nominal species (Figs 1K–L, 15A).

The three West Atlantic species and subspecies of *Isostichopus* accepted in this paper can be most easily differentiated by coloration, in addition to molecular differences. Ossicles are not the best character for distinguishing *I. badionotus* from *I. maculatus phoenius*, although they are very useful for differentiating

them from *I. macroparentheses.* The only internal morphology character to distinguish between large specimens of *I. badionotus* and *I. maculatus phoenius* is the size and shape of the calcareous ring. The dorsal radial plates in *I. badionotus* are longer with two dorsal radial plates having long posterior projections (3–4 mm long) turned inwards in larger individuals (L = 160-235 mm); large specimens of *I. maculatus phoenius* (L = 185 mm), on the other hand, have dorsal radial plates that are shorter and thicker (Fig. 4A–B). Habitat is also useful for distinguishing *I. badionotus* from *I. maculatus phoenius* (see *I. maculatus phoenius* remarks).

The four color forms of *I. badionotus* raises the question of whether these are genetically differentiated. A slight phylogenetic structure related to the color pattern was found ("Reticulated" and "Black and yellow" vs "Chips" and "Uniform" patterns) (Fig. 3A–D). These slight variations in mtDNA, correlated with color variation of the individuals in which they occur and their habitat, suggest that there may be some form of non-random mating. However, these differences are certainly not sufficient to indicate the existence of different species. Data from more populations and other molecular markers are needed to assess these results.

Examination of dorsal papillae in four specimens (and several that were not measured) of *I. badionotus*, from 40 mm to 230 mm long, showed that C-shaped ossicle length and table height increases during growth (Fig. 9A–B), that spines at the crown spires are thick and strong in largest specimens, and that table disc diameter and number of holes decreases in size and in number. Ossicles become more abundant in the middle-sized specimens. Ontogenetic changes in ossicle shape and size in *I. badionotus* have been described by Cutress (1996). Differences between our results and those presented by Cutress were in the table height of the juveniles and the number of C-shaped ossicles in the ventral body wall. We found lower tables in juveniles than in the adults. This pattern was common in all the species and subspecies of *Isostichopus* for which juveniles were examined. Perhaps the very small size of Cutress's specimens (16 mm and 25 mm) could explain these differences. Cutress found the C-shaped ossicles to be more abundant in the ventral than dorsal body wall of most of the specimens she examined, while we found the opposite pattern.

The identification of specimens of *I. badionotus* ("Reticulated" color pattern) as belonging to the Indo-Pacific species *Stichopus herrmanni* in the Caribbean Sea (Rodríguez-Forero *et al.* 2013: 12, fig. 5), Agudelo & Rodríguez 2015: 1022, fig. 1c) is clearly erroneous. This is supported by the morphology of the ossicles. *Stichopus* possesses rosettes, while *Isostichopus* does not (Deichmann 1958). Martínez *et al.* (2016: 21, fig. 4) reported rosettes (Martínez *et al.* 2016: 21, fig. 5a) in specimens with the "Reticulated" color pattern as *I. badionotus* Morphotype II; however, in reality these ossicles were rods. More details about the morphology of the rosettes can be found in Samyn *et al.* (2005: 105, fig. 2; 2006: 31, fig. 41) and in Purcell *et al.* (2012, 2023).

Biology

Perhaps because of the growing interest in commercial exploitation of *Isostichopus badionotus* in the Caribbean Sea, there is extensive literature on the population density, distribution, fishery, and reproductive characteristics of this species. Toral-Granda (2008a) extensively reviewed the biology, ecology, and population status of sea cucumbers in Latin America and the Caribbean, including *I. badionotus*. Reproductive biology information was reported from Panama, Venezuela, Brazil, Bonaire, Cuba, Yucatán (Mexico) and Colombia. The smallest size at sexual maturity has been reported from Panama (13–15 cm) (Guzmán *et al.* 2003) and the largest from Venezuela (30 cm) (Purcell *et al.* 2023); in Yucatán, Cuba and Colombia the size of first maturity has been documented at 18.5, 21.5 and 22 cm, respectively (Zetina *et al.* 2002; Alfonso *et al.* 2008; Acosta *et al.* 2021). The sex ratio has been reported to be 1:1 in Cuba (Aleaga 2003 in Ortega 2015), Panama (Guzmán *et al.* 2003), Brazil (Pires-Nogueira *et al.* 2001; Lima *et al.* 2003) and La Guajira and Santa Marta, Colombia (Invemar

2015: Acosta *et al.* 2021). Guzmán *et al.* (2003), Foglietta *et al.* (2004), Zacarías-Soto *et al.* (2013), Invemar (2015), and Acosta *et al.* (2021) reported that *I. badionotus* reproduces throughout the year, with a peak of reproductive activity between July and November, with some differences according to the location in the Caribbean Sea. In Brazil, the reproductive season has been reported in January and February and in October and November (Pires-Nogueira *et al.* 2001). Zacarías-Soto *et al.* (2013) have established that larval development from early auricularia to pentactula occurs between 19 and 22 days after fertilization. Juveniles of 654.3 μm in length were obtained on average 25 days after fertilization at 25 ± 1°C (Zacarías-Soto *et al.* 2013). After three months, juveniles reach lengths of 1–2 cm; in one year they have average sizes of 8 cm (Zetina *et al.* 2002).

Individuals of *I. badionotus* move approximately 0.5 m per day (Hammond 1983). Crozier (1918) calculated that in this species in Bermuda each individual fills its intestine twice a day and that the population can ingest between 500 and 1000 tons of sediment per year. Hammond (1983), on the other hand, calculated that each individual fills its intestine three or four times during daily movements.

Vergara *et al.* (2016) have described the relationship of *I. badionotus* with the pearlfish *Carapus bermudensis* (Jones, 1874) in Taganga Bay, Colombia. Luna-Fontalvo *et al.* (2014) listed the bacterial and fungal communities associated with the skin and the gut of this species. Gut histology of *I. badionotus* has been described by Vergara & Rodríguez (2015), including specimens of the "Chips" (Vergara & Rodríguez 2015: 1022, fig. 1a) and "Reticulated" color patterns (Vergara & Rodríguez 2015: 1022, fig. 1c, as *Stichopus hermanni*). They also described the histology of individuals of *I. maculatus phoenius* (Vergara & Rodríguez 2015: 1022, fig. 1b, as *Isostichopus* sp.). These authors found a similar histology of the digestive tract between the two species, but they observed differences in the thickness of the intestinal submucosal tissue, which can be related to specific feeding habits. Albinism in *I. badionotus* has been recorded by Wakida-Kusunoki *et al.* (2016) in one specimen collected in Yucatán, Mexico.

The highest population densities of *I. badionotus*, ranging from 5600 to 8800 ind/ha, were reported in the southeastern region of Cuba (Alfonso *et al.* 2004; Alfonso 2006). Ortega (2015) reported densities ranging between 900 and 3300 ind/ha in a survey conducted from 2008 and 2013 in the north part of Isla de la Juventud, Cuba, with no significant differences between years and localities. Jesús-Navarrete *et al.* (2018) reported a mean density of *I. badionotus* of 5570 ind/ha in 2011–2012 in Sisal, Yucatán, Mexico, but other surveys in this region found much lower densities. Lopez-Rocha (2011), also for Sisal, reported 217 ind/ha and compared this value with previous densities ranging between 267 to 437 ind/ha in 2007 in Progreso, Yucatan, and between 5 to 25 ind/ha at the central and east coast of Yucatan in 2000–2001. Poot-Salazar *et al.* (2015) and Hernández-Flores *et al.* (2015) estimated a density of 720 ind/ha in fishing areas near Progreso. In the Mexican Caribbean coast (Banco Chinchorro, Quintana Roo), *I. badionotus* is not among the most abundant species (Fuente-Betancourt *et al.* 2001). In Belize, significant differences in density were found in three habitats, with 10 ind/ha on the sand and sparse seagrass beds, 50 ind/ha in seagrass and rubble, and 17.7 ind/ha in sparse seagrass near shore (Rogers 2013). Guzmán & Guevara (2002) reported a density of 117.4 ind/ha in Bocas del Toro (Panama). Invemar (2015) has reported the highest mass density of *I. badionotus* in two regions of the Colombian Caribbean coast, 12 640 kg/km² (126.4 kg/ha) in La Guajira and 11 ind/km² (0.11 ind/ha) in Magdalena; the species, however, is scarce in other regions (Cordoba and Bolivar). In Venezuela, Tagliafico *et al.* (2011) reported that *I. badionotus* was most abundant on the East coast of Cubagua Island. At this location, it is found over *Thalassia testudinum* beds or mollusk shell aggregations, with an average density of 117 ind/ha.

Conservation status

Isostichopus badionotus is recognized as one of the most highly exploited and commercially valuable species in the Caribbean region, along with *Holothuria* (*Halodeima*) *mexicana* Ludwig, 1875 and *Isostichopus maculatus phoenius* (Purcell *et al.* 2023, as *Isostichopus* sp. '*phoenius*'). The prices of

dried *I. badionotus* in Guangzhou and Hong Kong, China SAR retail markets ranged from US$ 203 to 402 kg^{-1} (Purcell *et al.* 2012, 2023). Currently, *I. badionotus* is listed as a species of Least Concern by the IUCN Red List of Threatened Species (Toral-Granda *et al.* 2013). However, this category could change in the future, considering, among other reasons, that the distribution of the species is now restricted to the West Atlantic. The incessant growth of Asian market demands has led the opening of new fisheries and the depletion of some populations. Furthermore, preoccupation about the conservation of this species is justified because of the differences in population densities in different areas. López-Rocha (2011) suggested that differences in density may be due to different sampling methods applied to the patchy distribution of sea cucumbers. Differences in densities of populations require differences in their management. Hernández-Flores *et al.* (2018) proposed a technique of improving stock assessment by considering the distribution pattern of *I. badionotus*.

Purcell *et al.* (2012, 2023) included Cuba, Nicaragua, and Venezuela as the countries where *I. badionotus* is fished commercially; they also reported on the illegal, unregulated, and non-quantified fishery in Colombia and Florida (USA), Puerto Rico, and the United States Virgin Islands, where the species is of potential commercial interest. Currently, in addition to those countries, reported commercial fisheries include Mexico and Belize (Rogers 2013; Rogers *et al.* 2017; Jesús-Navarrete *et al.* 2018). Characteristics and current state of the fishery in each country are different. In Yucatán, Mexico, where perhaps one of the better regulated sea cucumber fisheries in the Caribbean occurs, the resource has decreased (Rodríguez-Gil *et al.* 2015). In Belize, *H. mexicana* and *I. badionotus* have been legally fished since 2009 (Perez & Garcia 2012 in McNab & Rogers 2017). In Cuba, the most recent fishery analysis in Isla de la Juventud, a well studied fishery since 2004 (Alfonso *et al.* 2008; Ortega & Alfonso 2011; Ortega 2015), showed that the population of *I. badionotus* is healthy, and its fishery remains stable (Ortega 2015). In Colombia, illegal and unregulated fishery of *I. badionotus* has been reported and quantification is being developed (Borrero-Pérez *et al.* 2006; Reyes-Sánchez *et al.* 2011; Invemar 2013, 2015; Rodríguez-Forero *et al.* 2013). Currently, *I. badionotus* is included in the Red Book of Marine Invertebrates of Colombia (Borrero-Pérez *et al.* 2022); data from La Guajira fishery showed a 32% reduction in catches per unit of effort between 2006–2017, despite some cessations of the fishery during these years (Reyes-Sánchez *et al.* 2011; Borrero-Pérez *et al.* 2022). In Panamá, the fishing of sea cucumbers is banned by Executive Decrees (157-2003, 217-2009), but an illegal fishery occurs in areas such as Bocas del Toro (Vergara-Chen *et al.* 2015). In Florida, there has been, since 2014, a regulation about a vessel limit of 200 sea cucumbers per trip in state and federal waters (FWC 2014). Nicaragua fishery is the subject of the most alarming report, because it involves not only the overexploitation of *I. badionotus* and *H. mexicana*, including immature sea cucumbers as an increasing proportion of the catches, but also human injustice, abuse and even death (Rogers *et al.* 2017). This fishery also involves Honduras, from where its operating financiers (Chinese and Koreans) originate.

Rogers *et al.* (2017) highlight another reality of the sea cucumber fishery, which is the price at which artisanal fishers in the Caribbean having been selling their catches. In Nicaragua, this price is only US$ 6.00 kg^{-1} (Rogers *et al.* 2017) and in Colombia it is less than US$ 0.29–1.89 kg^{-1} (Invemar 2013), prices that are far from the US$ 22 kg^{-1} value reported by Purcell *et al.* (2012, 2023) and those in Hong Kong China SAR retail markets.

Aquaculture is a strategy for species conservation. In the most complete review about sea cucumber aquaculture (Lovatelli *et al.* 2004), *I. badionotus* is not mentioned, possibly because interest in this species as a resource for aquaculture started only after 2004. Currently, there is some research on this subject (Zacarías-Soto *et al.* 2013), but most studies are still in progress (Pelegrín-Morales *et al.* 2009; Sarkis 2015; Felaco & Olvera-Novoa 2017; Rogers 2018). Martínez *et al.* (2016) present a manual for the cultivation and processing of sea cucumbers including specimens of the "Chips" (as *I. badionotus* Morfotipo I) and "Reticulated" color patterns (as *I. badionotus* Morfotipo II). In Panama, the use,

exclusively for mariculture, of *I. badionotus* and *H. mexicana*, is permitted (Executive Decree 20-2019) and farming projects are being established. In Colombia, sea cucumbers are not considered a fishing resource, so fishing and aquaculture are not allowed (Puentes *et al.* 2014; Invemar 2015; Borrero-Pérez *et al.* 2022).

Isostichopus maculatus maculatus (Greeff, 1882)
Figs 1Z–H', 3A–D, 4C, 5A, 9, 10C, 11C, 12–14; Tables 1–3

Stichopus maculatus Greeff, 1882: 158.

Stichopus maculatus – Théel 1886: 195. — Sluiter 1910: 333. — Ancona-López 1957: 7.
Isostichopus badionotus – Clark 1922: 55. — Cherbonnier 1975: 631–637, pl. 1a–c figs 1a–g, 2h–o. — Pawson 1978: 27–28, fig. 11m. — Pérez-Ruzafa *et al.* 1999: 54. — Entrambasaguas 2008: 134–138. — Entrambasaguas *et al.* 2008: 479–481.
Isostichopus cf. *badionotus* – Wirtz *et al.* 2020: 38.
Isostichopus maculatus maculatus – Borrero-Pérez *et al.* 2022: 180.
Isostichopus sp. *'maculatus'* – Purcell *et al.* 2023: 146–147.

Original name

Stichopus maculatus Greeff, 1882.

Current status

Isostichopus maculatus maculatus (Greeff, 1882).

Name-bearing type

Neotype USNM E16150, neoparatype USNM E16151.

Type locality

English Bay, Ascension Island for the neotype, instead of Rolas Island, São Tomé for the holotype.

Diagnosis

White spots as white granules on the skin (Figs 1Z–H', 14); table ossicles from top of the dorsal papillae in two shapes, large, regular *Isostichopus* tables 58–86 ($\bar{x}$ = 71) µm high (Fig. 2B) and modified "*maculatus*" tables 60–108 ($\bar{x}$ = 86) µm high (Figs 2D, 10C, 12C, 13A); distributed in the Mid and East Atlantic (Fig. 5A); mtDNA divergence from other species of the genus >8.2% in COI-Fr1 (barcoding region), >9.5 in COI-Fr2 and >8.2% in 16S; between subspecies 1.4%, 1,9% and 0.4% respectively (Table 2).

Material examined

Neotype (here designated)
ASCENSION ISLAND • 1 spec. (L = 105 mm); Ascension Island, English Bay, Station number RBM-ASC21; 1971; R. Manning leg.; USNM E16150.

Neoparatype (here designated)
ASCENSION ISLAND • 1 spec. (L = 125 mm); Ascension Island, Southwest Bay, Station number RBM-ASC9; 1971; R. Manning leg.; USNM E16151.

Other material
EAST ATLANTIC – **Cape Verde** • 1 spec. (L = 55 mm); São Vicente Island, Mindelo; 16.889267° N, 25.000642° W; 24 Aug. 2015; P. Wirtz leg.; ImuCV1, only images and tissue (used) • 1 spec. (L =

85 mm); same data as for preceding; ImuCV2, only images • 1 spec. (L = 120 mm); same data as for preceding; ImuCV3, only images • 1 spec. (L = 110 mm); same data as for preceding; ImuCV4, only images • 1 spec. (L = 145 mm); Santiago Island, Tarrafal; 15.275056° N, 23.758656° W; 28 Oct. 2015; P. Wirtz leg.; ImuCV5, only images • 1 spec.; same data as for preceding; ImuCV6, only images • 1 spec.; same data as for preceding; ImuCV7, only images and tissue (used) • 1 spec.; same data as for preceding; ImuCV8, only images • 1 spec.; same data as for preceding; ImuCV9, only images • 1 spec. spotted dark pattern; same data as for preceding; ImuCV10, only images and tissue (used). – **São Tomé and Príncipe** • 3 specs; São Tomé; 0.273383° N, 6.476564° E; N. Vasco-Rodríguez leg.; only images • 5 specs; Ilha do Principe; 1.606606° N, 7.355° E; R. Haroun leg.; only images. – **Senegal** • 1 spec.; Dakar–Îles Madeleines; UF16295. – **Sierra Leone** • 1 spec.; 8.135025° N, 13.198139° W; P. Wirtz leg.; only images. – **Liberia** • 1 spec.; Kligba, Rivercess County; FAOLIB08 • 1 spec.; same data as for preceding; FAOLIB09 • 1 spec.; Artah Beach, Sasstow Grand Kru County; FAOLIB10. – **Nigeria** • 2 specs; 4.528551° N, 5.491359° E; fishermen leg.; only images. – **Gabon** • 1 spec.; Libreville; 0.393065° N, 9.427977° E; P. Wirtz leg.; only images.

MID ATLANTIC – **Ascension Island** • 2 specs (L = 70–90 mm); Pan Am Base; depth 12–14 m; K. Jourdan leg.; USNM E17246 • 1 spec. (L = 10 mm); English Bay, Station number ASC3A; 7.93° S, 14.4° W; 1 Jul. 1976; M. Jones leg.; USNM E16166 • 1 spec. (L = 35 mm); Porpoise Point NE Side, Station 80-28; 7.9017° S, 14.355° W; depth 10.7–12.2 m; 27 Jul. 1980; Ascension I Expedition, Grice Marine Biological Laboratory exped.; USNM E34268 • 1 spec.; English Bay, One Hook; 7.893231° S, 14.387247° W; 9 Nov. 2015; P. Wirtz leg.; ImuASI1, only images and tissue (used) • 1 spec.; same data as for preceding; ImuASI2, only images and tissue (used) • 1 spec.; same data as for preceding; ImuASI3, only images • 1 spec.; Georgetown Town Pier; 7.924708° S, 14.414214° W; 15 Nov. 2015; P. Wirtz leg.; ImuASI4, only images and tissue (used) • 1 spec.; same data as for preceding; ImuASI5, only images.

Description

External appearance. Medium species, up to 220 mm long (Greeff 1882), examined specimens 55–145 mm long (n = 7, neotype: 150 mm long (contracted); neoparatype: 125 mm long). Body loaf-like, length/width ratio 3.3 ± 0.9 (n = 5, 1.6–4.3, neotype 1.6, paratype 2.6). Specimens convex or somewhat quadrangular in cross section; rounded in the anterior and posterior parts (Figs 12B, 14). Contracted neotype tapering posteriorly and anteriorly (Fig. 12A). Body wall firm and thick (2–5 mm thick in the neotype). Anus supra-terminal, circular and surrounded by large papillae. Mouth directed ventrally, encircled by a collar of large papillae (2–3 mm high in the neotype). Large peltate tentacles 20, about 5–6 mm long, and shield 5–6 mm wide, in the neotype partially retracted. Dorsal papillae medium to large, wart-like; conical in the neotype (up to 5 mm high and 3 to 5 mm wide at the base) and neoparatype, usually scattered irregularly, in some specimens, including neotype and neoparatype, arranged in two irregular rows along each flank, defining a slightly quadrangular shape; smaller papillae irregularly arranged, usually wart-like, sometimes rounded and low with a thin tip in live specimens. Dorsal papillae less obvious than lateral ones; lateral papillae conical and large, sharply defining the dorsal and ventral surface (Fig. 14). Papillae in preserved specimens conspicuous (Fig. 12A–B). Ventral surface densely covered with large cylindrical pedicels, arranged in three longitudinal rows barely visible, most retracted in the neotype, but most relaxed in the neoparatype (2–3 mm long, 1 mm wide) (Fig. 12A–B).

Color and body wall appearance. Body wall opaque and smooth, not translucent, nor rugose. Color extremely variable, four main color patterns (Figs 1, 14): (1) Uniform pattern (U) (Fig. 1Z): uniform dark red, specimens of this color are rare. (2) Dark and white color pattern (DW) (Fig. 1A'–D'): red, orange, or brown background with white irregular blotches of different shapes and sizes, arranged in longitudinal or transversal orientations; a dark line occasionally surrounding white blotches. The white irregular blotches with off-white spots as white granules, not rugose. (3) Light and sharp dark color pattern (LSD)

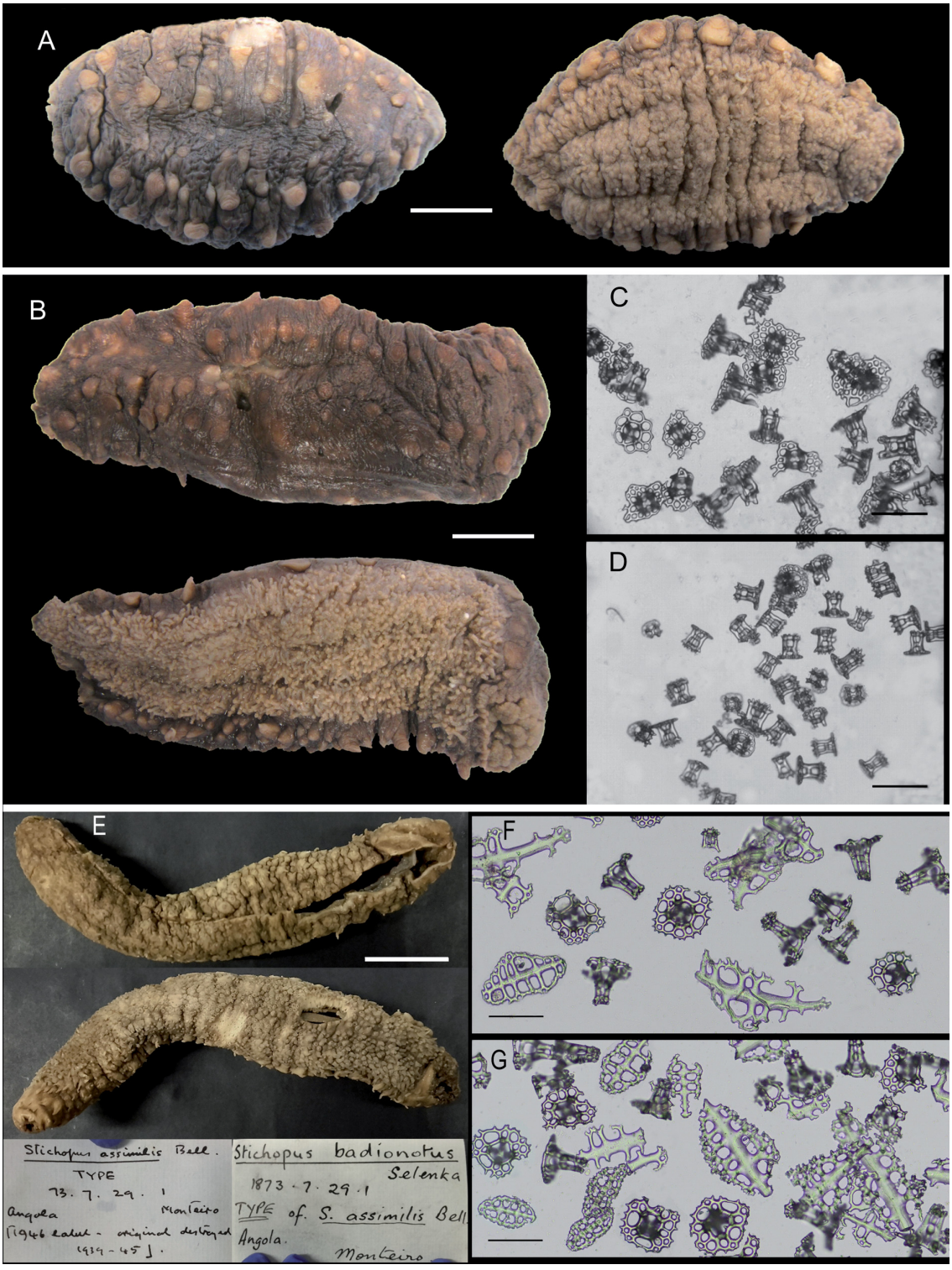

Fig. 12. A. Neotype of *Isostichopus maculatus maculatus* (Greeff, 1882) from English Bay, Ascension Island (USNM E16150, 105 mm long, contracted). **B**. Neoparatype of *I. maculatus maculatus* from Southwest Bay, Ascension Island (USNM E16151, 125 mm). **C–D**. Neoparatype ossicles showing tables from dorsal papillae (C) and dorsal body wall (D). **E**. Holotype of *Stichopus assimilis* Bell, 1882 (ZOO 1873.7.29.1). **F–G**. Ossicles of *S. assimilis* holotype from dorsal papillae (F) and dorsal body wall (G). Photos by G. Borrero. Scale bars: A–B, E = 20 mm; C–D, F–G = 100 µm.

(Fig. 1E'–F'): lighter background in brown, beige, white, pink colors, and sharp darker irregular blotches in brown or brown-orange of different size and irregularly arranged. The lighter background area with white spots as white granules, not rugose; most lateral papillae with spiral lines from the base to the tip, which are darker than the background. (4) Dark green and light papilla pattern (DGL) (Fig. 1G'–H'): dark green color with white spots as white granules in the background and light-yellow papillae, with darker green blotches in some specimens. DGL color pattern resembling the reticulated pattern color of *I. fuscus*, in live and preserved specimens. Preserved, neotype and neoparatype (Fig. 12A–B) with dark brown background with the biggest dorsal and lateral papillae conspicuous and lighter in a yellow-brown color; white granules present in the dorsal side; some papillae with a spiral line from the base to the tip; tentacles, ventral surface and pedicels of the same color as the dorsal and lateral papillae.

Internal anatomy (based on USNM E16150, Neotype, and USNM E16151, neoparatype, specimens 105–125 mm long). Calcareous ring 14 mm in diameter, radial elements roughly quadrangular, 5 mm wide and 6 mm long, with four anterior small lobes, dorsal radial plates with posterior projections longer (1.5 mm long) than those of the ventral plates (0.5 mm long); interradial elements about half as wide as radial elements (3 mm wide), pointed anteriorly with concave posterior margin (Fig. 4C). Neotype and neoparatype stone canal irregularly helical, about 10 and 12 mm long respectively, including the ending flat, leaf-like 4 and 6 mm long madreporite, broken free in the neotype; stone canal in good condition, attached to the dorsal tegument in the neoparatype. Tentacle ampullae variable in size, 10 to 21 mm long in the neotype and about 8 to 16 mm in the neoparatype. One elongated Polian vesicle, about 17 mm long by 3.5 mm wide in the neotype and 21 mm by 4 mm in the neoparatype. Gonads in two tufts, one on either side of dorsal mesentery, branched in cylindrical tubes about 0.5–1 mm wide, extending 50 mm from the anterior to posterior body and filled with eggs 31–64 μm diameter in the neotype (Fig. 11C), and extending 24 mm and filled with sperm in the neoparatype (Fig. 11C). Longitudinal muscles divided, about 8 mm wide, attached to body wall medially in both neotype and neoparatype. Respiratory trees inserted near the anterior cloaca, arising from a common stem 12 and 11 mm long in the neotype and neoparatype respectively; then divided in a left tree about 67 and 72 mm long and a right tree about 50 and 60 mm long, extending along the intestine.

Ossicles (based on USNM E16150 (neotype, SEM images); USNM E16151 (neoparatype); USNM E17246 (for mouth membrane); fifteen not collected specimens (only tissue for dorsal papillae), specimens 55–145 mm long).

Dorsal papillae with regular *Isostichopus* tables (Fig. 2A–B), modified *maculatus* tables (Fig. 2D), few C-shaped ossicles, perforated plates, and large rods (Fig. 13A). All types of ossicles present in all the sizes examined. Modified *maculatus* tables not common in some specimens, in which only large and stout regular *Isostichopus* tables are present. C-shaped deposits 54–90 ($\bar{x}$ = 69) μm long, not abundant even on the top of the papillae, but more common in the neoparatype; S-shaped ossicles not observed. Tables varying in shape from the top to the base of the papillae; at the top numerous modified *maculatus* tables 60–79 ($\bar{x}$ = 70) μm high and 66–116 ($\bar{x}$ = 96) μm across disc; spire very high, slightly or strongly constricted at the crown, composed of four pillars ending in only one large and blunt spine; two to three crossbeams connecting adjacent pillars; disc margins irregular and wide, having one rounded central perforation and a variable number of peripheral perforations, irregularly arranged, usually in two rings, 9 to 14 perforations in the inner ring, and 1 to 20 in the external ring; outer edge of disks with some blunt projections resulting from incomplete holes (Figs 10C, 13A). In addition to the neotype and neoparatype, four examined specimens from Ascension 55 to 145 mm long with modified "*maculatus*" tables at the top of the papillae. Presence of these tables not related to the size of the specimens, present in the smallest specimen (L = 55 mm, 73–94 ($\bar{x}$ = 86) μm high and 82–141 ($\bar{x}$ = 104) μm across the disc) and in one of the largest (L = 110 mm, 80–108 ($\bar{x}$ = 94) μm high and 89–140 ($\bar{x}$ = 114) μm across the disc) (Figs 9B–C, 10C). In one specimen from Ascension and 10 specimens from Cape Verde the most

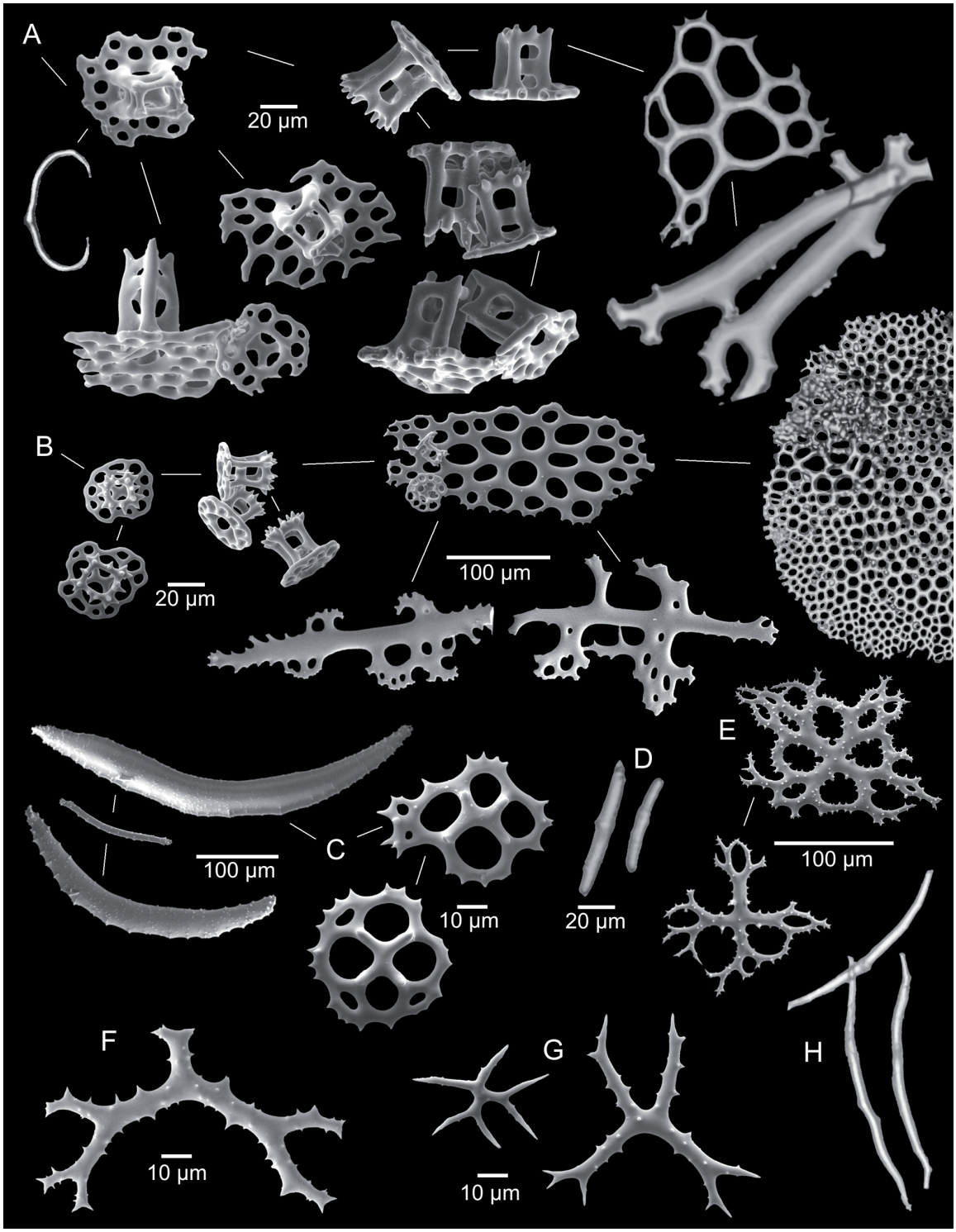

Fig. 13. *Isostichopus maculatus maculatus* (Greeff, 1882) ossicles (neotype USNM E16150, 105 mm long). **A**. Thin C-shaped rods, modified *maculatus* tables, regular *Isostichopus* tables, perforated plates, and large, curved rods from the dorsal body wall and papillae. **B**. Tables, perforated plates, large, curved rods and end plate (not complete, ½ of the round plate) from the ventral body wall and tube feet. **C**. Rods and tables from tentacles. **D**. Rods from longitudinal muscles. **E**. Spinous irregular plate-like branched rods in the cloaca. **F**. Bifurcated spinous rod in the respiratory trees. **G**. Cross-shaped ossicles from the intestine. **H**. Simple rods from the gonads. Photos by G. Borrero.

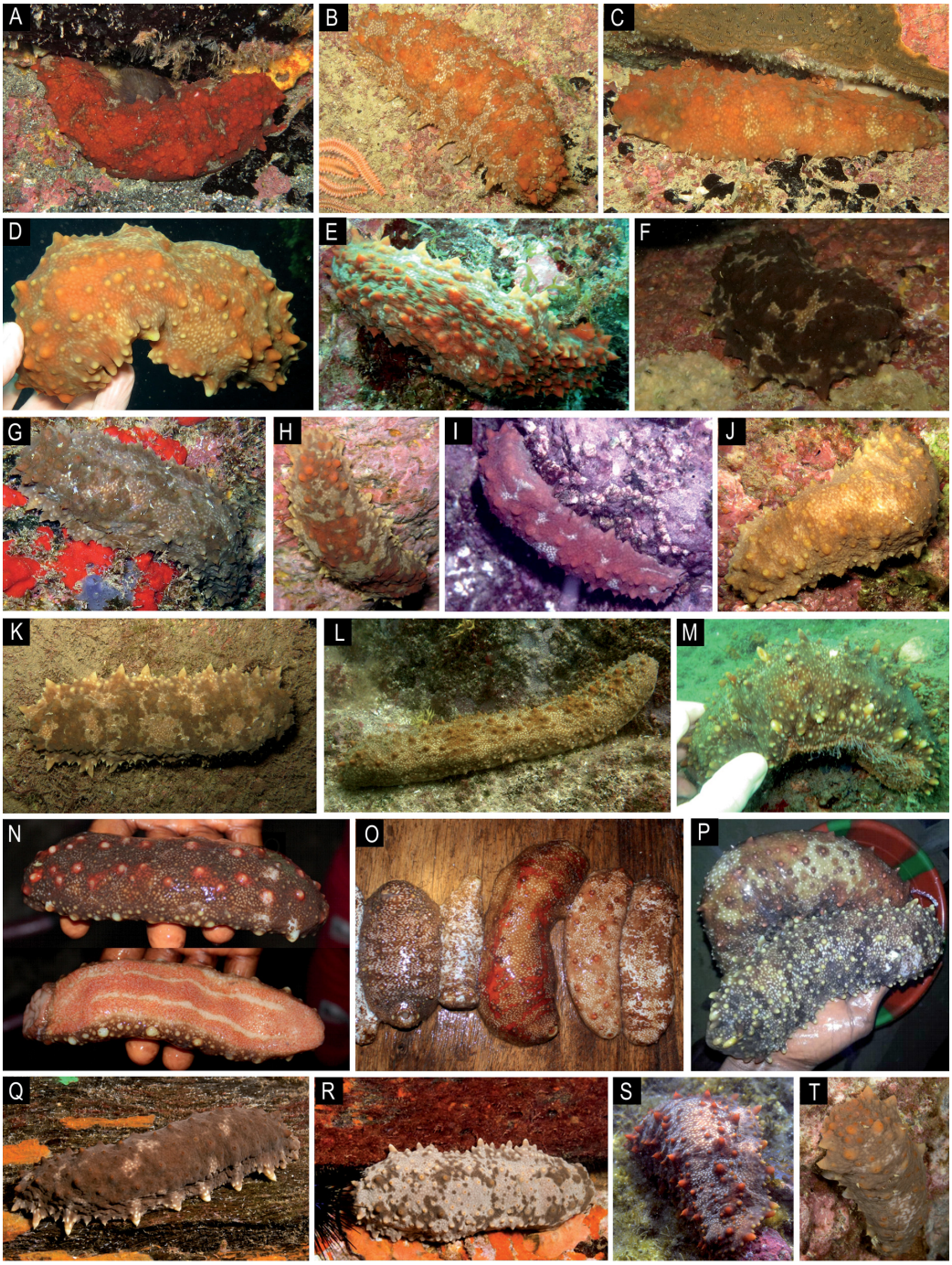

Fig. 14. Color patterns and morphological variation of *Isostichopus maculatus maculatus* (Greeff, 1882). (DNA sequences and detailed information of some specimens are indicated in Table 1, see Photo ID column for correspondence). A**–C, F, I, Q, T**. Specimens with "Dark and White" pattern from Cape Verde (A, B–C, F, I), São Tomé (Q) and Ascension Island (T). **D–E, G–H, J–L, O–P (top), R–S**. Specimens with "Light and sharp dark" pattern from Cape Verde (D–E, G, H, J–K), Dakar, Senegal (UF 16295) (L), Liberia (N dorsal and ventral view, O except left specimen), Nigeria (P top specimens), São Tomé (R), Libreville, Gabon (S). **M, O (left), P (bottom)**. Specimens with "Dark green and light papillae" pattern from Sierra Leone (M), Liberia (O-left specimen) and Nigeria (P bottom specimen). Photos: A–K, M, S–T by P. Wirtz; L by Florida Museum of Natural History Data Collection; N–O by T. Collison; P by fishermen NN; Q-R by N. Vasco Rodrigues.

common tables at the top of the papillae regular *Isostichopus* tables, but larger and stouter, more square profile than those of the middle and the base of the papillae (top papillae: 58–86 μm high ($\bar{x}$ = 71 μm) and 62–95 ($\bar{x}$ = 80) μm across the disc) (Figs 9B–C, 10C). Toward the papilla base modified *maculatus* tables absent, regular *Isostichopus* tables present, more numerous and decreasing in size toward the base, the latter with sizes similar to tables from the body wall. Large, regular *Isostichopus* tables at the middle of the papillae (50–78 ($\bar{x}$ = 60) μm high and 51–67 ($\bar{x}$ = 59) μm across disc) composed of four pillars slightly constricted proximally to the disc; one crossbeam connecting adjacent pillars; pillars ending in triplets of spines forming a crown with a middle hole; disc margins smooth and wide, having one rounded central perforation and 8 to 12 peripheral holes, usually arranged in one simple ring; tables nearest to the top of the papillae with 4 to 7 extra perforations. Few perforated plates, located in the top of the papillae, with few large perforations, larger in the center, 104–121 μm across. Slightly curved rods 228–317 μm long, usually with quadrangular extentions distributed mostly in the central part, occasionally perforated (Fig. 13A).

Dorsal body wall with numerous tables and a few C-shaped ossicles (Figs 10C, 13A). Regular *Isostichopus* tables similar to those in the middle and the base of the papillae, but smaller, 38–51 ($\bar{x}$ = 43) μm high and 43–60 ($\bar{x}$ = 48) μm across the disc, usually with perforations arranged in one simple ring. Few C-shaped ossicles (49–58 μm), scarce in the neotype, more common in the neoparatype; S-shaped ossicles not observed.

Pedicels with tables, thin C-shaped rods, perforated plates, large, curved rods and end plates (Fig. 13B). Few C-shaped deposits 79–81 μm long in the neotype, but more common 47–78 μm long in the neoparatype. Numerous small, regular *Isostichopus* tables 24–35 ($\bar{x}$ = 29) μm high and 36–54 ($\bar{x}$ = 49) μm across the disc; shape of the tables similar to those from median dorsal papillae and body wall. Numerous elongated perforated plates (195–282 μm), with numerous perforations larger and elongated in the center of the plate; slightly curved rods (300–389 μm), usually with perforated central expansions; end plates 638 μm across.

Ventral body wall only with tables similar to those from pedicels, 32–41 ($\bar{x}$ = 37) μm high and 36–49 ($\bar{x}$ = 43) μm across disc; no C-shaped ossicles.

Tentacles with tables and rods (Fig. 13C). Few table ossicles 38–42 μm across disc; spire low, composed of four incomplete pillars that usually are not joined at the top, without crossbeams connecting adjacent pillars, discs having a big and not rounded central perforation, usually with four peripheral perforations, margins spinous and thin; some tables in the neoparatype (36–51 μm long) with complete single ring of holes when situated at the base of the tentacles. Numerous strongly curved spiny rods 50–284 μm long.

Mouth membrane with tables, C-shaped rods, and simple rods (Fig. 11C). Numerous large tables 71–97 μm across disc; spire low, composed of four incomplete pillars that usually are not joined at the top and end in some small spines, without crossbeams connecting adjacent pillars; discs having a large and not rounded central perforation, appearing as four perforations from dorsal view, usually with one or two rings of holes irregularly arranged, margins spinous and thin; numerous C-shaped deposits (38–55 μm); numerous small rods (48–81 μm).

Longitudinal muscle with small rods (46–68 μm) (Fig. 13D). Thin C-shaped rods in the neoparatype (26–38 μm), absent in the neotype. Posterior cloaca with spinous rods simple or bifurcated (110–192 μm); spinous, irregular plate-like branched rods, 84–203 μm across; no C-shaped deposits (Figs 11C, 13E). Anterior cloaca with large tables 83–137 μm high and 109–208 μm across the disc (Fig. 11C). Respiratory trees with spinous rods, simple or bifurcated (91–157 μm); no table ossicles (Fig. 13F). Intestine with cross-shaped rods, sometimes with bifurcated ends (48–91 μm long), spinose or smooth (Fig. 13G).

Gonads, with delicate and long spiny rods (169–256 μm) (Figs 11C, 13H); a few table ossicles in the neotype, one table ossicle 50 μm across the disc, spire low and incomplete.

Distribution

Isostichopus maculatus maculatus was only known from Rolas Island, São Tomé and Príncipe, Gulf of Guinea in the East Atlantic. We extend its geographical distribution to the tropical and subtropical East and Mid Atlantic, as there are confirmed specimens from Ascension Island, Cape Verde Archipelago, São Tomé and Príncipe, Senegal, Sierra Leone, Liberia, Nigeria, and Gabon (Fig. 5A) (Cherbonnier 1975; Pawson 1978; Pérez-Ruzafa *et al.* 1999, 2003; Entrambasaguas 2008; Entrambasaguas *et al.* 2008, as *I. badionotus*; Wirtz *et al.* 2020, as *Isostichopus* cf. *badionotus*). Specimens recorded by Pawson (1978) from Ascension Island as *I. badionotus* are designated here as neotype and neoparatype of *I. maculatus maculatus*. Bathymetric distribution: intertidal to 40 m (Purcell *et al.* 2023).

Habitat

Isostichopus maculatus maculatus is common in shallow habitats in the Mid and East Atlantic as reported by Pawson (1978), Pérez-Ruzafa *et al.* (1999, 2003), Entrambasaguas (2008), Entrambasaguas *et al.* (2008), Wirtz *et al.* (2020) and Purcell *et al.* (2023). In Ascension, *I. maculatus* lives exposed on sand or rock but is not common intertidally (Pawson 1978). In the Cape Verde Archipelago it is reported that adults (L = 150–200 mm) live completely exposed on mud, sand or rock bottoms, although they can also be found in cracks or under rocks (Entrambasaguas 2008). The species was recorded at most islands in the Cape Verde Archipelago, but not at São Antao and Santa Luzia. Where present, *I. maculatus maculatus* was very abundant and was one of the species that "were well correlated with some variables indicating heterogeneous (with an important proportion of algal cover and sand) and/or complex habitats (determined by small and medium-sized boulders)" (Entrambasaguas *et al.* 2008). Feeding activity begins in the afternoon and peaks before midnight. Juveniles are usually located under gravel or slabs of coral, in isolation or aggregated (Perez-Ruzafa *et al.* 1999; Entrambasaguas 2008). Purcell *et al*. (2023) found this this species on sandy or rocky substrates and refuging under rocks and in crevices in Cape Verde. Observations made in Ilha do Principe, São Tomé and Príncipe in April–June 2016, found it to be common in shallow marine habitats, composed of volcanic rocks; the individuals were in crevices during the day and moved to nearby soft bottoms during the night (R. Haroun pers. com.). In subsequent sampling efforts in October–November 2016, the species was rarer than in April–June. At one locality where specimens were common at 1–3 m depth during April–June, they were only encountered at 15–25 m in October–November. The probable reason was excessive fishing for sale to the Chinese market (R. Haroun pers. com.). In Liberia, this species occurs mostly on reefs with large boulders (Purcell *et al.* 2023).

Remarks

Even though specimens of the African coasts and its neighboring islands were not examined by Clark (1922), he synonymized *Stichopus assimilis* from Angola and *Stichopus maculatus* from São Tomé under *S. badionotus*. He considered that there was nothing in the original descriptions that would justify their status as separate species. We examined the holotype of *S. assimilis* at the Natural History Museum of London (ZOO 1873.7.29.1) and determined that it belongs to the genus *Holothuria*, subgenus *Holothuria*, considering external morphology and ossicles (Fig. 12E–G). Although the types of *S. maculatus* were not found, several elements of evidence allowed us to resurrect *I. maculatus* and to designate the specimen USNM E16150 as the neotype and USNM E16151 as neoparatype. English Bay, Ascension Island is the new type locality, according to article 76.3 of the ICZN Code (1999). Attempts to obtain specimens of *I. maculatus maculatus* from São Tomé, were not successful, and neither was the attempt to examine at the Muséum national d'Histoire naturelle, Paris, the specimen described by Cherbonnier (1975). Greeff's (1882) original description of this species is short and not accompanied by

drawings of ossicles. However, coloration was considered by Greeff as an important diagnostic character. He described it as chocolate-brown in the background with numerous larger irregular yellow spots, and whitish round spots as white granules. Although the coloration was highly variable in the specimens we examined, the "whitish round spots as white granules" were a common pattern (Fig. 14). Cherbonnier (1975) examined one specimen of *Isostichopus* collected near São Tomé, the original type locality of *I. maculatus*, and concluded that it corresponds with the description of Greeff, but he also agreed with Clark (1922) in accepting *S. maculatus* as a synonym of *S. badionotus*. Cherbonnier (1975) observed a perfect match of ossicles of the São Tomé specimen and the ossicles of *S. badionotus*, except for some large tables from its dorsal papillae, which were twice as large as tables of *S. badionotus.* This is the kind of tables considered here as modified "*maculatus*" tables. These tables had a slenderer spire or pillars with some rough edges and ended with some blunt spines instead of a regular crown (Cherbonnier 1975: 632, fig. 1a–c, e). mtDNA sequences from our specimens and their ossicles, including the specimens reported by Pawson (1978) from Ascension (designated here as neotype and neoparatype), indicated that the table differences reported by Cherbonnier (1975) are not due to intraspecific variability in *I. badionotus*, but to interspecific differences. Tables of dorsal papillae in *I. maculatus maculatus* are of two shapes, the regular *Isostichopus* tables and the modified "*maculatus*" tables (Figs 2A–B, D, 13A). The regular *Isostichopus* tables in this species are the largest in the genus (in height and disc diameter) (Figs 9B–C, 10C, 13A); they are similar in size to those of *I. badionotus* only in the body wall. The coexistence in the dorsal body wall of two kinds of tables can lead to confusion in identification. The regular *Isostichopus* tables are located in the middle and the base of the papillae and in the body wall, whereas the modified "*maculatus*" tables, when present, are located at the top of the papillae. Perhaps because of their location, and of their absence in some specimens, neither Pawson (1978), Pérez-Ruzafa *et al.* (1999), or Entrambasaguas (2008) have recorded them.

Examination of three specimens (and several without measurements) of *I. maculatus maculatus*, from 55 mm to 150 mm long, showed that ossicles become more abundant in the largest specimens. No dramatic changes in size and shape were observed in the modified "*maculatus*" tables during ontogeny, but fewer regular *Isostichopus* tables with smallest discs were observed in the 55 mm long specimens in comparison to those from 110 mm. Entrambasaguas (2008) described a higher and slightly tapered spire in a 19 mm juvenile (HO 1028), a very small size not examined by us. C-shaped rods in this subspecies are less abundant than in the other species of *Isostichopus*. C-shaped rods are fewer in the neotype and more frequent in the neoparatype.

Biology

Purcell *et al.* (2023) reported that this species is mostly nocturnal, hiding during the day and foraging at night. These authors also report a reproductive season in late summer, when seawater is warmest.

Conservation status

As a species previously synonymized with *I. badionotus*, and currently recognized as a subspecies of a different species, it has not been included in the IUCN Red List of Threatened Species. Nuno *et al.* (2015) recorded an increasing harvest of sea cucumbers in the eastern Atlantic for the international trade, but presented no details as to the species, locality, and removed quantities. It has been reported that *I. maculatus maculatus* is being illegally fished in Ilha do Principe, São Tomé, even though the government issued a law in November 2016 to completely ban the fishing of this species (R. Haroun pers. com.). Recently, the species was included in the FAO catalog of commercially important sea cucumbers of the world (Purcell *et al.* 2023, as *Isostichopus* sp. '*maculatus*') as a high-value species in Asian dried seafood markets. Trading is reported in Liberia and Sierra Leone, where it is sold by fishermen for US$ 1.75 kg^{-1} for fresh sea cucumbers, and US$ 50–150 kg^{-1} for dried animals. Average price of dried *I. maculatus maculatus* in Hong Kong, China SAR markets ranged from US$ 930 to 1237 kg^{-1} (Purcell *et al.* 2023). In Liberia there has been a legal fishery by holders of government-issued fishing

licenses since 2021. The sea cucumbers are harvested by hookah divers from inshore reefs, catching 130–150 kg per diver per night in 2016, declining to 50–60 kg per diver per night by 2021 (Purcell *et al.* 2023). In Cape Verde there has also been a legal fishery since 2021 when fishing and trading was permitted by government regulations. Records from December 2020 to April 2021 (when the fishery was illegal), reported harvests of 2.7 tons (average catch rate of 37 kg per diver per night). The species is now found at depths of 30 to 40 m, perhaps due to fishing pressure in shallow waters (Purcell *et al.* 2023). Potential fishery interest in the species has been reported in Nigeria (Fig. 14P) (Solís-Marín pers. com.). Conservation status of this subspecies is unknown. The current geographic distribution could be considered as restricted, which is a new criterion for its inclusion in the IUCN Red List.

Isostichopus maculatus phoenius (Clark, 1922)
Figs 1K–Y, 3A–D, 4B, 5A, 9, 10B, 11B, 15–18; Tables 1–3

Stichopus badionotus var. *phoenius* Clark, 1922: 60.

Stichopus badionotus var. *phoenius* – Clark 1933: 109. — Deichmann 1930: 82.
Isostichopus badionotus – Gómez-Maduro & Hernández-Ávila 2011: 223, figs k–l (at least one specimen). — Borrero-Pérez *et al.* 2012: 175, figs a, d.
Stichopus sp. – Agudelo & Rodríguez 2015: 51–52, figs 1–3. — Vergara & Rodríguez 2015: 1022, fig. 1b.
Isostichopus sp. – Invemar 2015: 115. — Vergara & Rodríguez 2015: 1022, fig. 1b; 2016: 130–137. — Martínez *et al.* 2016: 15, fig. 1, 22, fig. 6. — Vergara *et al.* 2018: 39–41, figs 4–6. — Acosta *et al.* 2020: 1–14, fig. 1; 2021: 1–17.
Isostichopus sp. nov. – Agudelo-Martínez & Rodríguez-Forero 2017: 73.
Isostichopus sp. aff. *badionotus* – Agudelo-Martínez & Rodríguez-Forero 2017: 6, figs 3–4. — Arias-Hernández *et al.* 2017: 278–289. — Fontalvo-Martínez & Rodríguez 2017: 95. — Medina-Lambrano *et al.* 2017: 175.
Isostichopus isabellae n. sp. – Vergara *et al.* 2018: 40, fig. 4. Not an available name.
Isostichopus maculatus phoenius – Borrero-Pérez *et al.* 2022: 180, 186.
Isostichopus sp. *'phoenius'* – Purcell *et al.* 2023: 148–149.

Original name

Stichopus badionotus var. *phoenius* Clark, 1922.

Current status

Isostichopus maculatus phoenius (Clark, 1922).

Name-bearing type

Holotype MCZ HOL-1182.

Type locality

Buccoo Reef, Tobago.

Diagnosis

Small dark spots surrounded by a clear halo and a dark thin line on white blotches on the background; semi-translucent and rugose body wall (Figs 1K–Y, 17–18); mtDNA divergence from other species of the genus > 7.7% in COI-Fr1 (barcoding region), > 10.1% in COI-Fr2 and > 7.9% in 16S; between subspecies 1.4%, 1,9% and 0.4%, respectively (Table 2).

Material examined

Holotype

TRINIDAD AND TOBAGO • spec. uniform color pattern (L = 135 mm); Tobago, Buccoo Reef; 11.179396° N, 60.811479° W; 5 Apr. 1916; J. Mills leg.; living under or among rocks; MCZ HOL-1182.

Other material

GULF OF MEXICO – **USA** • 1 spec. (contracted); Texas, Stetson Bank; 28.17° N, 94.28° W; 28 Jun. 2005; depth 22 m; M. Wicksten leg.; USNM 1080469 • 1 spec. (L = 120 mm); Texas, Stetson Bank; 24 Oct. 1971; J. Teerlings leg.; USNM 1096856 • 1 spec. (L = 135 mm); Texas, North Padre Island; 26.82° N, 97.32° W; T. Shirley leg.; USNM E17227 • 2 specs (L = 95–195 mm); Florida, Tortugas, Bird Key; 24.6185° N, 82.8854° W; Jun. 1917; H. Lyman Clark, Carnegie Expedition exped.; MCZ HOL-1213. – **Mexico** • 2 specs; Veracruz, Bajos de Tuxpan, off Tuxpan; 21 Apr. 1994; J.D. Aghub leg.; ICML-UNAM 5.14.11 • 2 specs; Veracruz, Isla Sacrificios; 26 Jan. 1962; E. Caballero leg.; ICML-UNAM 5.14.28 • 2 specs; same locality as for preceding; 24 Jan. 1957; M.E. Caso leg.; ICML-UNAM 5.14.30 • 1 spec.; same locality as for preceding; 26 Jan. 1957; ICML-UNAM 5.14.34 • 1 spec.; Veracruz, Isla Sacrificios; 19.1749361° N, 96.09303056° W; 14 May 1997; depth 3 m; A. Medina leg.; rocky bottom; ICML-UNAM 18302 • 1 spec.; Veracruz, Isla Lobos; 21.4541667° N, 97.22500001° W; 14 Jun. 1976; depth 3 m; *Acropora* reef; ICML-UNAM 11459 • 1 spec.; Veracruz, Isla de Enmedio, Anton Lizardo; 19.1144444° N, 95.93583333° W; 5 Apr. 2005; depth 1–2 m; F. Solís-Marín leg.; on sandy bottom; ICML-UNAM 18303.

CARIBBEAN SEA – **Belize** • 2 specs (L = 120–180 mm); Coco-Plum Key, edge of mangrove swamp; 16.877841° N, 88.120048° W; 2 May 1972; R. Larson leg.; USNM E18639. – **Panama** • 1 spec. (L = 130 mm); Bocas del Toro, Cayo Adriana; 9.2405278° N, 82.1734167° W; 30 May 2013; depth 5 m; G. Borrero-Pérez and A. Castillo leg.; mixed bottom of sand, sponges and corals, IpBT5; USNM 1659468 • 1 spec. (L = 135 mm); same data as for preceding; IpBT7; MBMLP-IpBT7 • 1 spec. (L = 170 mm); same data as for preceding; IpBT21; USNM 1659473 • 1 spec. (L = 140 mm); same data as for preceding; IpBT22; USNM 1659474 • 1 spec. (L = 138 mm); same data as for preceding; IpBT23; USNM 1659475 • 1 spec. (L = 170 mm); same data as for preceding; IpBT25; USNM 1659476 • 1 spec. (L = 160 mm); same data as for preceding; IpBT43; USNM 1659477 • 1 spec. (L = 150 mm); same data as for preceding; IpBT44; USNM 1659478 • 1 spec. (L = 185 mm); same data as for preceding; IpBT53; USNM 1659479 • 1 spec. (L = 150 mm); same data as for preceding except 31 May 2013; on mixed bottom of sand, sponges and corals, completely hidden in a crevice between sponges, IpBT26; TpBT0026 • 1 spec. (L = 160 mm); same data as for preceding; MBMLP IpBT27 • 4 specs (L = 135–180 mm); same data as for preceding; Ip8, 24, 28, 29 BT; TpBT0008, TpBT0024, TpBT0028, TpBT0029 • 1 spec. (L = 130 mm); Bocas del Toro, STRI research station; 9.3488611° N, 82.2585° W; 4 Jun. 2013; depth 5 m; G. Borrero-Pérez leg.; mixed bottom of sand, corals and isolated seagrass, exposed, between coral colonies, IpBT131; USNM 1659469 • 1 spec. (L = 130 mm); Bocas del Toro, Popa Island Cay; 9.2495° N, 82.1815279° W; 6 Jun. 2013; depth 7 m; G. Borrero-Pérez and A. Castillo leg.; mixed bottom of sand, corals and sponges at the reef fringe, completely hidden, under a loose coral head and among rubble coral, IpBT190; USNM 1659470 • 1 spec. (L = 140 mm); Bocas del Toro, near Popa Island Cay; 9.2541944° N, 82.1829444° W; 6 Jun. 2013; depth 2 m; G. Borrero-Pérez and A. Castillo leg.; mixed bottom dominated by *Porites porites*, with isolated seagrasses, octocorals and sponges, exposed, IpBT191; USNM 1659471 • 1 spec. (L = 125 mm); same data as for preceding; depth 3 m; IpBT192; USNM 1659472 • 1 spec.; Galeta; 9.4018444° N, 79.86053056° W; 15 Dec. 2015; depth 2 m; G. Borrero-Pérez leg.; mixed bottom of rocky, corals and isolated seagrass, exposed, IpGa8; Tiss-IpGa8 • 1 spec.; same data as for preceding; IpGa11; Tiss-IpGa11 • 1 spec.; same data as preceding, IpGa209; Tiss-IpGa209 • 1 spec. (L = 100 mm); Galeta; 9.4018444° N, 79.86053056° W; 17 Sep. 2016; depth 3 m; G. Borrero-Pérez leg.; mixed bottom of corals and rocks, exposed but camouflaged between *Porites porites*, IpGa269; Tiss-IpGa269 • 1 spec. (L = 158 mm); same data as for preceding;

depth 1 m; A. Calderón leg.; completely hidden inside rocks, IpGa223; USNM 1659480 • 1 spec. (L = 90 mm); same data as for preceding; IpGa224; USNM 1659481. – **Colombia** • 1 spec. (L = 120 mm); Magdalena, Banco de las Ánimas; 11.0397778° N, 74.39919445° W; 1 Dec. 2013; depth 15 m; G. Borrero-Pérez and N. Ardila leg.; rocky bottom, anterior part exposed, IpBA313; INV EQU4144 • 1 spec. (L = 130 mm); same data as for preceding; IpBA314; INV EQU4146 • 1 spec. (L = 140 mm); same data as for preceding; rocky bottom, partially exposed within crevices between rocks, concealed by spines of *Diadema antillarum*, IpBA315; INV EQU4147 • 1 spec.; same data as for preceding; depth 4.5 m; IpBA319; INV TEJ1336 • 1 spec. (L = 25 mm); Magdalena, Bahía del Rodadero; 11.2070556° N, 74.2303916° W; 23 Jul. 2017; depth 1 m; G. Borrero leg.; hidden under a rock in a mixed bottom of sediment and small rocks, IpRod; INV EQU4565 • 1 spec. (L = 125 mm); La Guajira, El Pájaro-Tawaya; 11.7308333° N, 72.70436111° W; 9 Sep. 2013; depth 4.5 m; E. Ortíz and J. López leg., IpGV82; INV TEJ1257 • 1 spec. (L = 100 mm); same data as for preceding; IpGV83; INV TEJ1258 • 1 spec. (L = 125 mm); same data as for preceding; IpGV84; INV TEJ1259 • 1 spec. (L = 160 mm); same data as for preceding; IpGV86; INV TEJ1261 • 1 spec. (L = 170 mm); same data as for preceding; IpGV90; INV TEJ1265 • 1 spec. (L = 120 mm); same data as for preceding; IpGV108; INV TEJ1269 • 1 spec. (L = 180 mm); same data as for preceding; IpGV117; INV TEJ1272 • 1 spec.; La Guajira, Cabo de la Vela; 12.2086422° N, 72.1674894° W; 28 Oct. 2011; depth 2 m; G. Borrero-Pérez and C. Díaz leg., IpGV1; INV-TEJ1113 • 1 spec.; same data as for preceding; IpGV3; INV-TEJ1115. – **Trinidad and Tobago** • 4 specs (L = 90–115 mm); Tobago, Buccoo Bay; 11.177882° N, 60.811479° W; Apr. 1916; J. Mills leg.; MCZ HOL-1181. – **Jamaica** • 1 spec. (L = 120 mm); Kingston Harbor, Port Royal, Drunken Man's Cay; 17.905085° N, 76.845067° W; 3 Sep. 1959; H. Lyman Clark leg.; MCZ HOL-4282. – **Antigua and Barbuda** • 2 specs (L = 90–120 mm); Antigua Island, English Harbor; 1 Jul. 1918; C. Nutting leg.; USNM 1283367 • 1 spec. (L = 170 mm); Antigua Island, Falmouth Bay; 17° N, 61.7667° W; 1918; J. Henderson leg.; USNM E41458.

Description

External appearance. Medium sized species, preserved and live ex situ specimens examined range from 25 to 260 mm in length (n = 68, holotype: 130 mm long and 40 mm wide). Body loaf-like, length/width ratio 3.7 ± 0.8 (n = 38, 3.2–5.5, holotype 3.2). Rounded posteriorly and anteriorly (Fig. 15A), quadrangular in cross section (Figs 17–18). Live specimens also tapering slightly posteriorly and widened anteriorly when the animal is relaxed (Fig. 17E, O), or when it is coming out of its crevice, especially when only the anterior part of the body is exposed (Fig. 18O). Body wall firm and thick (0.5 to 4 mm thick in the holotype). Anus supra-terminal, circular and surrounded by large papillae. Mouth directed ventrally in live and preserved animals, encircled by a collar of large papillae (2–4 mm long in the holotype). Large peltate tentacles 20, about 7–9 mm long, 6 mm shield width, with indentations 0.5–3 mm deep. Dorsal papillae medium to large, conical, and spiky (although some of them somewhat rounded) ending in a sharply pointed tip (5 to 10 mm high; 5 to 8 mm wide); some smaller papillae rounded and scattered irregularly; most of the largest dorsal papillae arranged in two dorsal irregular rows along each edge, defining the quadrangular shape. Holotype covered with medium size conical papillae (up to 4 mm high and 5 mm wide at the base), most of them flattened and not very conspicuous. Lateral papillae large and spiky, sharply defining the dorsal and ventral surface (Figs 17–18); in the holotype they are larger than dorsal ones (up to 5 mm high and 5 mm wide at the base) (Fig. 15A). Ventral surface covered with cylindrical, large pedicels (2–4 mm long and 0.5 mm wide in the holotype) arranged in three longitudinal rows (Fig. 15A).

Color and body wall appearance. Living specimens are semi translucent and appearing slightly rugose (Figs 1K–Y, 17–18). Color extremely variable; four main color patterns (Figs 1, 17–18). The first three patterns are similar to those of *I. maculatus maculatus*, with some variations in the second (DW) and third (LDS), with regard mostly to the white spots as white granules: (1) Uniform pattern (U) (Fig. 1K–L): uniform brown, green, or red. Specimens of this uniform color are rare; in most cases at least a

very small white blotch is present. (2) Dark and white color pattern (DW) (Fig. 1M–T): red, orange, or brown background with white irregular blotches of different shapes and sizes, arranged in longitudinal or transversal orientations; usually with a dark line surrounding the white blotches, or with only a line in very small blotches. Blotches markedly or gently rugose, with small dark spots surrounded by a clear halo and a dark thin line; larger spots occasionally inside the white blotches. Ventral surface with a margin at the outer edge of the same color background as the dorsal side. Middle area sometimes of almost uniform color or sometimes off-white with small spots and scattered or abundant brown blotches, or some of the same color as the margin. (3) Light and sharp dark color pattern (LSD) (Fig. 1U–W): lighter background in brown, beige, white, pink, and sharp darker irregular blotches in brown or brown-orange, of different size and irregularly arranged. Lighter background area markedly or gently rugose, with or without small dark spots surrounded by a clear halo and a dark thin line. Ventral surface off-white with scattered or abundant small brown spots and blotches, without margin at the outer edge. (4) Light and blurry dark pattern (LBD) (Fig. 1X–Y): similar to the LSD pattern, but with lighter background in brown, white, pink colors and blurry darker irregular blotches in brown or brown-orange color of different size and irregularly arranged. Spiral lines in the papillae more conspicuous than those in *I. maculatus maculatus*. Spiral lines in dorsal and lateral papillae in the four described patterns, although more conspicuous in the patterns 3 (LSD) and 4 (LBD). Sharply pointed tips of the papillae white, light yellow, or lighter than the base. Collar papillae usually white translucent, with the spiral lines very marked in a dark color. Tentacles and pedicels white to light yellow-brown. Specimens preserved in alcohol lighter than live ones but with white blotches with the small dark spots of patterns 2 (DW), 3 (LSD) and 4 (LBD) persisting (Fig. 15C–G). According to Clark (1922), the live holotype was semi translucent with the entire back and sides bright carmine-red (Uniform pattern), the tentacles, pedicels, and median ventral surface gray. Preserved dorsal coloration of the holotype light yellow-brown. Body wall somewhat translucent and rugose. Some of the largest papillae with a spiral line from the base to the tip; tentacles, ventral surface, and pedicels of the same color as the dorsal side; some darker small stains among the pedicels on the ventral side; tips of the pedicels darker than the tube (Fig. 15A). Juveniles semi translucent and appearing slightly rugose; color pattern in juveniles (40–50 mm) the same as in adults; the spiral lines in dorsal and lateral papillae present (Fig. 17D, B'–C').

Internal anatomy (Based on MCZ HOL-1182 (holotype), USNM 1659481, USNM 1659476, USNM 1659479, specimens 90–190 mm). Calcareous ring of the holotype stout, 13 mm in diameter; radial elements almost as wide as long (5 mm wide and 6 mm long) with four anterior small lobes; posterior projections 2 mm long in the dorsal radial plates; middle ventral radial plates without posterior projections; interradial plates 3 mm wide and 3 mm long, pointed anteriorly and with a concave posterior margin. Proportion of radial plates in other examined specimens similar to the holotype (L = 90 mm: 2.9 mm wide, 3.3. mm long; L = 190 mm: 6 mm wide, 7 mm long); posterior projections proportionally equal to radial plate size during growth; interradial plates stouter in large specimens (L = 90 mm: 2 mm wide, 1.4 mm long; L = 190 mm: 3 mm wide, 4 mm long) (Fig. 4B). Holotype stone canal irregularly helical, about 10 mm long, including the flat madreporite, leaf-like 2.5 mm long, attached to the mesentery; stone canal variable in size not related to body size (L = 90 mm: 8 mm; L = 130 mm: 10 mm; L = 160 mm: 14; L = 185 mm: 12 mm). Tentacle ampullae in the holotype 16–18 mm long by 1–1.5 mm wide, and 4.5 mm long in the smallest specimen (L = 90 mm). One sac-like Polian vesicle in the holotype 14 mm long by 5.5 mm wide, and 13 mm in the other specimens (L = 160 mm and 185 mm). Gonads in two tufts, one on either side of dorsal mesentery, branched in cylindrical tubes about 0.5 mm or less wide, not very bulky, extending 16 mm left and 12 mm right along the length of the body, filled with male gametes in the holotype (Fig. 11B). Gonads present in examined specimens 130 mm and 190 mm long, but absent in the smallest (L = 90 mm). In the holotype, longitudinal muscles divided, about 4 mm wide, attached to body wall medially and laterally every 2 mm. Specimen L = 90 mm longitudinal muscles 3 mm wide; and L = 195 mm 10 mm wide. Respiratory trees in the holotype inserted near the anterior cloaca with a

Fig. 15. Preserved specimens of *Isostichopus maculatus phoenius* (Clark, 1922). **A**. Dorsal and ventral view of the holotype from Buccoo Reef, Tobago (MCZ HOL-1182, 135 mm long). **B**. Holotype ossicles from dorsal papillae showing tables, thin C-shaped rods, worm-like rods, large, curved rods and perforated plates. **C**. Specimen from Antigua (USNM 1283367), dorsal and ventral view. **D**. Specimen from Antigua (MCZ HOL-4282), dorsal and ventral view. **E**. Specimen from Coco-Plum Key, Belize (USNM E18639), dorsal view. **F**. Specimen from Texas, Stetson Bank, USA (USNM 1080469), dorsal view. **G**. Specimens from Buccoo Reef, Tobago (MCZ HOL-1181; same locality as the holotype), dorsal view. Photos by G. Borrero. Scale bars: A = 10 mm; B = 100 µm; C–E, G = 20 mm; F = 10 mm.

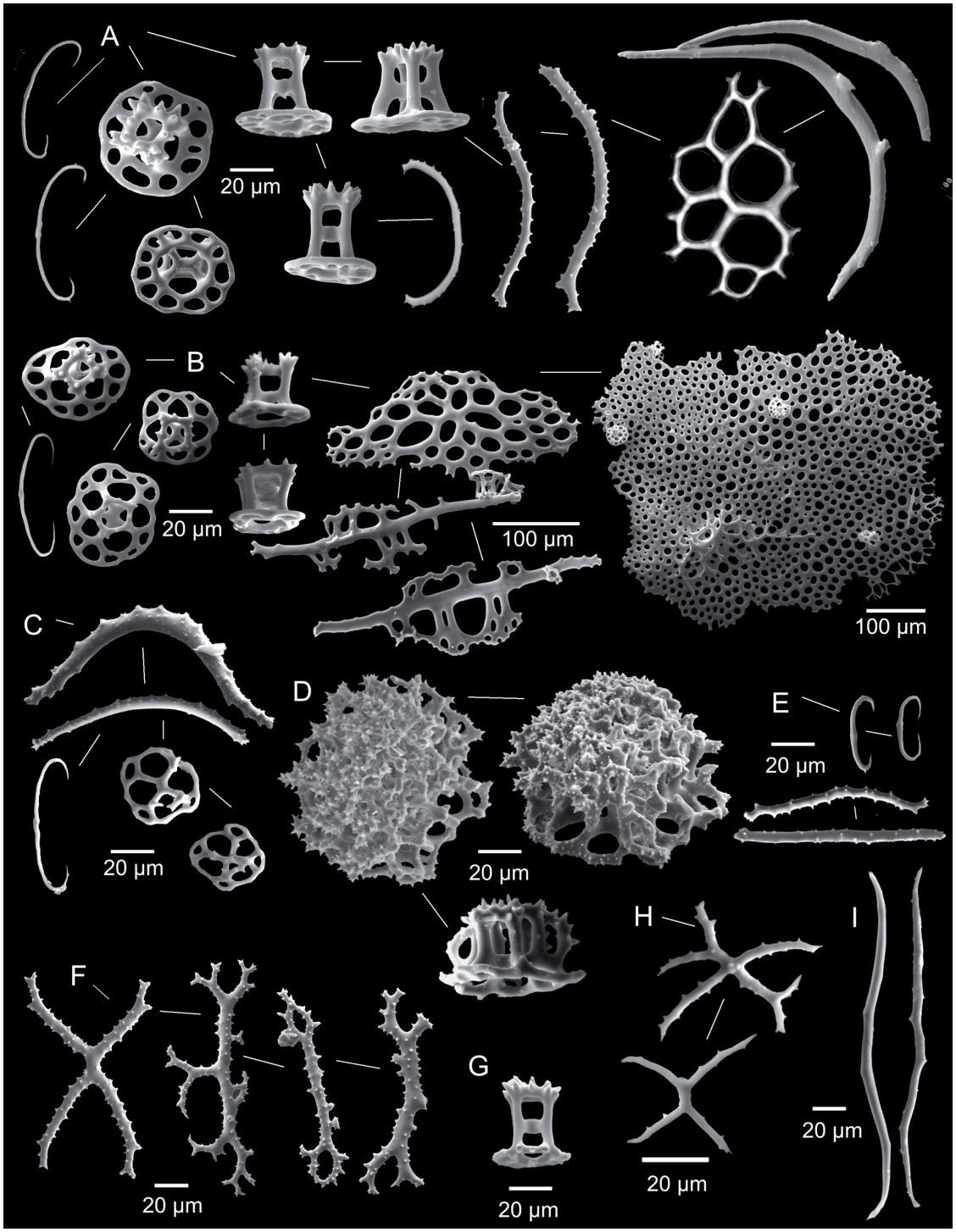

Fig. 16. *Isostichopus maculatus phoenius* (Clark, 1922) ossicles (specimen USNM 1659477-BT43, 160 mm long). **A**. Thin C-shaped rods, tables, worm-like rods, perforated plates and large, curved rods from papillae and dorsal body wall. **B**. Thin C-shaped rods, tables, perforated plates, large, curved rods and end plate (not complete, broken at the outer edge) from ventral body wall and tube feet. **C**. C-shaped rods, simple rods and tables from tentacles. **D**. Large tables from mouth membrane. **E**. Thin C-shaped rods and simple rods from longitudinal muscles. **F**. Simple and bifurcated rods in a cross shape in the cloaca. **G**. Tables from respiratory trees. **H**. Cross-shaped rods from intestine. **I**. Simple rods from gonads. Photos by G. Borrero.

common stem of 15 mm; right tree about 55 mm long and left 65 mm long, extending in association with the intestine; in other specimens, right tree also usually shorter than the left.

Ossicles (based on MCZ HOL-1182 (holotype), USNM 1659481, USNM 1659472, USNM 1659476, USNM 1659479, INV EQU4565 (juvenile, for dorsal papillae), USNM 1659477 (SEM images), specimens 25–190 mm).

Dorsal papillae with tables, thin C- and S-shaped rods, perforated plates, large, curved rods and worm-like rods (Fig. 16A). Perforated plates and worm-shaped rods not found in the 25 mm specimen. Numerous few thin C-shaped rods, and rare S-shaped rods, 45–98 μm ($\bar{x}$ = 71 μm), usually in the papillae, especially towards the tip, varying in abundance in the same specimen. The length of C-shaped rods increasing in relation to body length in specimens from 25 mm to 190 mm long (Fig. 9A). Numerous table ossicles 31–78 ($\bar{x}$ = 52) μm high and 39–84 ($\bar{x}$ = 64) μm across disc (holotype 35–53 μm high; 39–51 μm across the disc); juveniles 31–46 ($\bar{x}$ = 38) μm high. Spires composed of four usually parallel pillars, or slightly constricted medially, distally, or proximally to the disc; pillars ending in triplets of blunt spines forming a wide crown; many minute spines in the 25 mm long specimen, with one crossbeam connecting adjacent pillars. Disc margins smooth and wide; with one rounded central perforation and 8 to 12 peripheral holes, usually arranged in one simple ring; tables near the top with 4 to 10 extra perforations arranged in more than one ring. Tables at top of the papillae larger, more square, with a wider disc, and with more perforations than those in the base of the papillae; those of the base similar to those of the body wall (Fig. 10B). Changes of table shape during growth not remarkable, but size of C-shaped rods and height of tables increasing in relation to body length (Figs 9A–B, 10B); disc diameter of tables without substantial change during growth (Figs 9C, 10B). Few perforated plates, located in the papilla tip, with large and few perforations, larger in the center of the plate, 72–158 μm across, absent in 20 mm juveniles, and rare in other small specimens. Slightly or strongly curved rods usually with quadrangular projections distributed mostly in the middle, occasionally perforated, 150–377 μm long, increasing in size in relation to the body length (Fig. 16A). Numerous small slightly or strongly spinous worm-shaped rods 78–197 μm long, without substantial change in size during growth (Figs 15B, 16A).

Dorsal body wall only with tables and few C-shaped ossicles 45–68 μm long, found only in the holotype and in one of the examined specimens (L = 125 mm) (Figs 10B, 16A). Numerous tables similar to those from papillae but smaller in size 30–58 ($\bar{x}$ = 44) μm high and 31–74 ($\bar{x}$ = 49) μm across the disc, with regular discs with one ring of 8–10 holes. In the holotype tables 35–47 μm high and 31–41 μm across disc, usually with 9–12 perforations arranged in one simple ring.

Pedicels with tables, thin C-shaped rods, perforated plates, large and curved rods, and end plate (Fig. 16B). A few C-shaped rods 79–98 ($\bar{x}$ = 87) μm long. Numerous table ossicles 27–47 ($\bar{x}$ = 36) μm high and 27–71 ($\bar{x}$ = 53) μm across the disc (holotype 29–40 μm high; 39–59 μm across the disc); shape of tables similar to those from the dorsal papillae and body wall, central perforation usually bigger and not rounded, with four points that interrupt the simple ring of holes on the disc. Tables with the same pattern during growth as dorsal papillae; height of tables increasing with body length (table height L = 25 mm: 27–39 μm; L = 170 mm: 38–47 μm); disc diameter not notably changing with body size (disc diameter L = 25 mm: 47–71 μm; L = 170 mm: 52–67 μm). Numerous elongated perforated plates, with numerous perforations larger and elongated in the center of the plate, 171–392 μm long; slightly curved rods 207–467 μm long, usually with wide perforated expansions in the middle; end plates 372–602 μm across, increasing in size during growth (Fig. 16B).

Ventral body wall in holotype with numerous tables similar to those from pedicels (32–40 μm high; 35–58 μm across disc) and a few thin C-shaped rods (78–79 μm long).

Tentacles with tables and rods (Fig. 16C). A few table ossicles 36–70 μm across disc (holotype 36–46 μm); spire low, composed of four pillars, some of them incomplete, only two or three joined at the top, without crossbeams connecting adjacent pillars; discs with a large and not rounded central perforation, with four points and usually no more than four peripheral perforations with margins smooth and thin. Numerous strongly and slightly curved spiny rods 34–722 μm long (holotype 34 to 294 μm), increasing in size during growth.

Mouth membrane with tables, C-shaped ossicles, and simple rods (Figs 11B, 16D). Numerous large tables 70–102 μm high and 68–160 μm across disc (holotype 85–87 μm high; 100–160 μm across disc); spire well developed, composed of at least ten pillars, that are joined at the top, forming a very dense crown of spines, without distinguishable crossbeams connecting adjacent pillars; spire is flat. Table discs with many peripheral perforations arranged in two or three rings; margins spinous and thin, sometimes reduced to the same width as the spire. Flat table spires in all specimens from Panama, taller spires in specimens from other localities in the Caribbean. Some C-shaped rods 48–106 μm long (holotype 42–65 μm), and small rods 48–107 μm long in some specimens (holotype 58–107 μm).

Longitudinal muscles with thin C-shaped rods 28–53 μm long (holotype rods 30 μm) and small rods ranging from 37 to 93 μm in length (holotype 37–56 μm) (Fig. 16E). Posterior cloaca with numerous simple or bifurcated rods in 71–195 μm long (holotype 145–195 μm); some C-shaped ossicles 38–84 μm long (holotype 38–52 μm). Anterior cloaca with large and complex tables 106–179 μm high and 73–244 μm across disc (holotype 71–113 μm high; 113–176 μm across disc) (Fig. 11B); in the holotype irregular plate-like branched rods, 133–201 μm across (Figs 11B, 16F). Respiratory trees with a few small tables, similar in shape to those of the dorsal body wall, 43–51 μm high and across the disc (holotype 43 μm high; 44 μm across the disc); few rods 54–229 μm long in some specimens (holotype 54–111 μm) (Fig. 16G). Intestine with spinose or smooth rods in a cross shape 50–122 μm long, sometimes with bifurcated ends (holotype 75–113 μm) (Fig. 16H). Gonads with delicate and long rods 187–364 μm long (holotype 187–262 μm) (Figs 11B, 16I); rods in gonads present even in the smallest specimen examined (L = 125 mm); a few small tables 48 μm high and 43 μm across disc in the holotype.

Distribution

Isostichopus maculatus phoenius is known from the Caribbean Sea and the Gulf of Mexico (Fig. 5A). We have collected it from Mexico, Costa Rica, Panama (Bocas del Toro, Galeta, San Blas) and Colombia (Banco de las Ánimas, Santa Marta, La Guajira). We also identified it from Museum specimens from the Florida Keys (MCZ HOL-1213), North Padre Island, and Stetson Bank, Texas (USNM E17227; USNM 1080469; USNM 1096856), Belize at Coco Plum Cay (USNM E18639), Jamaica (MCZ HOL-4282), Antigua (USNM E41458, USNM 1283367) and Trinidad and Tobago (MCZ HOL-1182, MCZ HOL-1181). We also identified it from photographs of living specimens from Estado de Sucre, Venezuela (Gómez-Maduro y Hernández-Ávila 2011 unpubl. photographs). *Isostichopus maculatus phoenius* appears to be sympatric with *I. badionotus* in the Caribbean Sea and the Gulf of Mexico, but more samples are needed to confirm the presence of this subspecies at other localities of the West Atlantic. Currently, *I. maculatus phoenius* has not been recorded in South Brazil, where *I. badionotus* was confirmed by DNA (Table 1). It is not possible to assess the distribution of *I. maculatus phoenius* from the literature, because it has been confused with *I. badionotus*. It is not easy to identify this subspecies from museum specimens either due to the similarity of the ossicles to those of *I. badionotus* and the loss of color in preserved specimens. We have only designated specimens as *I. maculatus phoenius* from the USNM and MCZ collection that could be clearly identified (examples in Fig. 15C–G). Bathymetric distribution 0–22 m. Most of the specimens observed in the present study were in shallow habitats, no more than 10 m deep. Acosta *et al.* (2021) found this species (as *Isostichopus* sp.) in the upper 2.5 m. However, museum specimens (USNM 1080469) have been collected from 22 m (Fig. 15F).

Habitat

Isostichopus maculatus phoenius can be quite abundant, although, because of its cryptic habits and because its ossicles resemble those of *I. badionotus*, it has been overlooked for many years. Clark (1922) described the habitat of the holotype (MCZ HOL-1182, as *S. badionotus* var. *phoenius*) living under or among rocks, as were the four specimens from MCZ HOL-1181, collected along with the red holotype. Clark (1922) assigned these four specimens as subadults of *I. badionotus* and suggested that semi-translucent subadults of *I. badionous* (length less than 150 mm) with a distinctive coloration (often marked with a dark spiral line that runs from the base to tip of dorsal and lateral papillae) are common under rocks, or in crevices. However, in the light of the present results, the dark spiral line and the habitat indicate that they were *I. maculatus phoenius*. *Isostichopus maculatus phoenius* is smaller than *I. badionotus* and prefers a more cryptic habitat. Its activity is nocturnal. Our observations from Colombia and Panama showed that juveniles and adult individuals of *I. maculatus phoenius* remain completely hidden during the day under rocks or coral heads, or in cracks (Figs 17–18). Acosta *et al.* (2021) in Santa Marta (Colombia) found 98% of individuals of *I. maculatus phoenius* (as *Isostichopus* sp.) on rocky bottoms between cracks (upper 2.5 m depth), while 73% of individuals of *I. badionotus* were collected on sandy bottoms (3–7.8 m). Diurnal observations, between 9:00 am and 12:00 pm, at Punta Galeta (Panama) showed that *I. maculatus phoenius* can be exposed for approximately one hour, then they became completely hidden. During the observations, some individuals exposed only the anterior part of their body to feed (Fig. 18O), and only a few were found fully exposed during the day. Frequently during the time of exposure, they were partially hidden by the spines of *Diadema antillarum* (Philippi, 1845) (Fig. 18J, M–N). Some individuals, partially or completely exposed, seemed to be rubbing their mouths against the rocks and the leaves of *Thalassia testudinum*, or scraping on them. Observations made between 5:00 and 6:00 pm at some localities in the Caribbean showed that specimens of *I. maculatus phoenius*, previously unnoticed during the day, start to appear. Observation during the night showed individuals completely exposed on top of sponges (Fig. 18P). Purcell *et al.* (2023) stated that after reaching 15–20 cm in length, individuals can become less cryptic and can live on open sand flats, but this is a mistake.

Remarks

Stichopus badionotus var. *phoenius* was described as a variety of *Stichopus badionotus* on the basis of the bright-carmine red color on the dorsal side of one specimen collected in Bucco Reef, Tobago. Clark (1922) designated this specimen as the holotype (MCZ HOL-1182) (still preserved in very good condition (Fig. 15A)) and described the external morphology, ossicles, and the habitat of the type locality (Clark 1922: 59–60), and explained the etymology. Despite the distinctive color pattern of the holotype of *I. maculatus phoenius*, which is "a most unusual shade in a shallow-water holothurian" (Clark 1922), and despite the marked spiral lines in the papillae, *I maculatus phoenius* has remained unnoticed in holothurian research in the West Atlantic, perhaps because of the great color variability of both *I. maculatus phoenius* and *I. badionotus*. Since Clark (1922), *S. badionotus* var. *phoenius* was mentioned only by Deichmann (1930) and Clark (1933).

The coloration of the holotype corresponds to the first Uniform color pattern described in the present study. The semi translucent appearance, the habitat, and the worm-shaped rods in the dorsal papillae of other specimens of all color patterns are similar to the holotype. Our analyses revealed significant molecular, morphological and habitat differences from the sympatric species *I. badionotus*. The analyses also revealed significant morphological differences, such as ossicle shape and body coloration, from *I. maculatus* from the East Atlantic. However, because the molecular phylogeny shows DNA sequences of *I. maculatus maculatus* as nested in sequences of *I. maculatus phoenius* the latter is considered as a subspecies of *I. maculatus*. We propose that *I. badionotus* var. *phoenius* is elevated to the sub-specific rank, as this is an available subspecific name (Articles 10.2 and 45.6.4 ICZN Code 1999).

Fig. 17. Color patterns and morphological variation of *Isostichopus maculatus phoenius* (Clark, 1922) (DNA sequences and detailed information of some specimens are indicated in Table 1, see Photo ID column for correspondence). **A–C, M, B'**. Specimens with "Uniform" pattern from Bocas del Toro, Panamá (A–B, M); La Guajira, Colombia (C) and juvenile from Neguanje, Colombia (B'). **D–L, N–R**. Specimens with "Dark and White" pattern, juvenile from Neguanje, Colombia (D), Bocas del Toro, Panamá (E–I, N–O, R); La Guajira, Colombia (J–L, P–Q). **S–T, X–Z, A'**. Specimens with "Light and sharp dark" pattern Galeta, Panama (S), Bocas del Toro, Panamá (T, A'), La Guajira, Colombia (X–Y), Magdalena, Colombia (Z). **U, V–W, C'**. Specimens with "Light and blurry dark" pattern from Galeta, Panama (U), Banco de las Animas, Colombia (V–W), juvenile from Rodadero, Colombia (C'). Photos: A–B, E–I, M–O, R–U, A', C' by G. Borrero; C by C. Díaz; J–L, P–Q, X–Y by E. Ortiz; V–W by N. Ardila; D, B' by G. Ospina; Z by J.F. Lazarus. Scale bars = 10 mm.

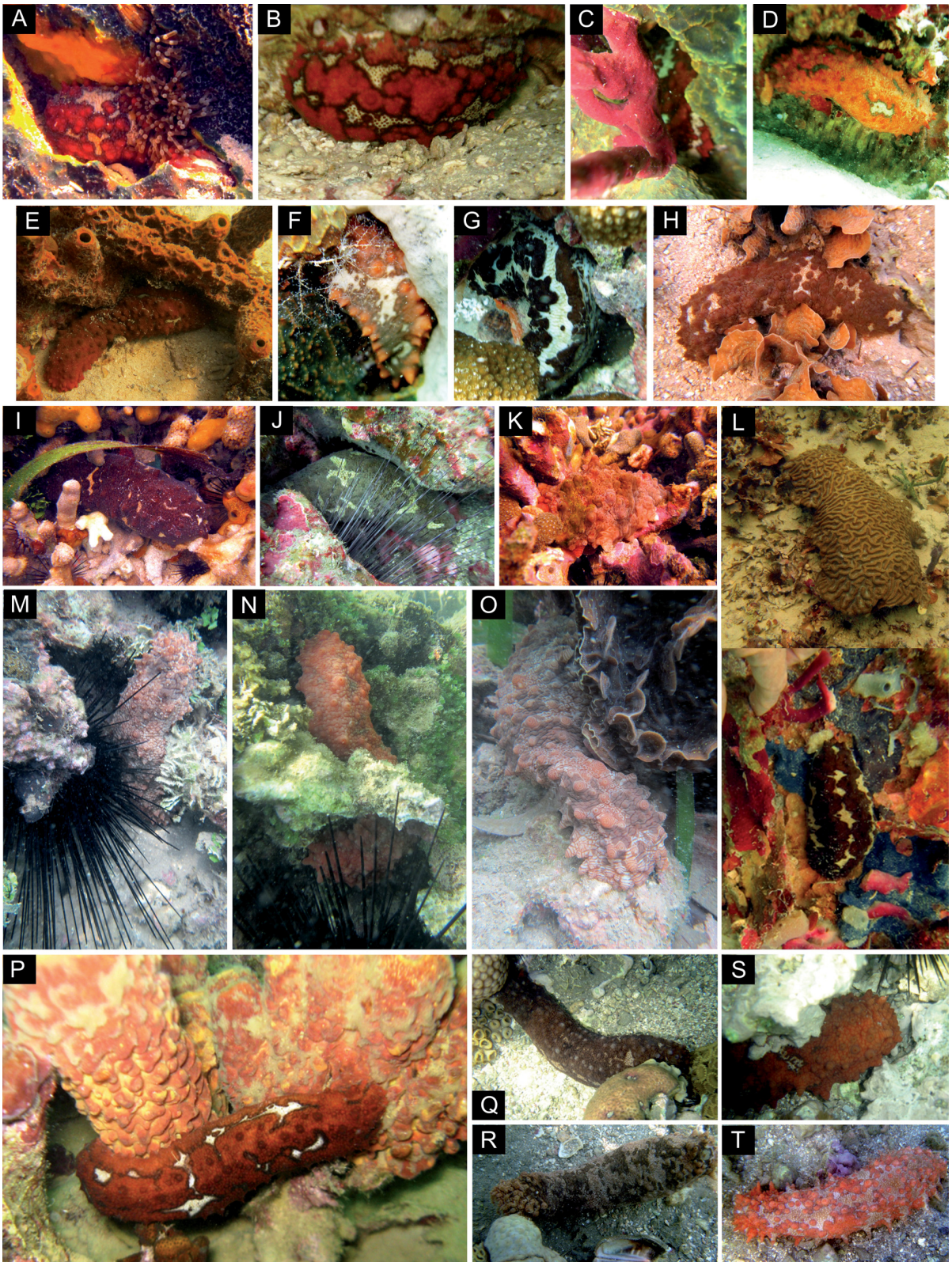

Fig. 18. In situ photographs of *Isostichopus maculatus phoenius* (Clark, 1922), showing the habitat of the species. **A–I, L, P**. Specimens from Bocas del Toro, Panama (L, the specimen was under the coral head; P, during the night). **K, M–O**. Galeta, Panama. **J**. Banco de las Ánimas, Colombia. **Q–T**. Mexico. Photos: B–D, F–G, P by A. Castillo; Q–T by F. Solís-Marín; J by N. Ardila; A, H–I, K–O by G. Borrero.

Isostichopus maculatus phoenius is extremely variable in coloration. Clark (1922) considered the individuals with the LSD color pattern described here as *I. badionotus* subadults (MCZ HOL-1181, Fig. 15G). However, spiral lines in papillae are one of the diagnostic characters of both *I. maculatus maculatus* and *I. maculatus phoenius* (Fig. 1K–H'). These spiral lines are also present in juveniles of *I. maculatus phoenius* (Fig. 17D, B'–C'). The characters diagnostic between the two subspecies are the small dark spots surrounded by a clear halo, the dark thin line, and the semi-translucent and wrinkled skin in *I. maculatus phoenius* (Fig. 1K–Y). This color characteristic was the most useful character in identifying museum material (Fig. 15C–G). Some specimens, such as USNM 1080469 with almost a uniform color pattern, possess small brown spots (Fig. 15F), allowing certain identification. In contrast to *I. maculatus phoenius*, *I. maculatus maculatus* is characterized by white spot like granules on the opaque and smooth skin, as mentioned by Greeff (1882) in the original description (Fig. 1Z–H'). In addition to spiral lines, worm-like rod ossicles found in the dorsal and lateral papillae of *I. maculatus phoenius* are a shared character between the two subspecies, although less common in *I. maculatus maculatus*. They were reported by Cherbonnier (1975: 633, fig. 2o) as "rare imperforate rods". Worm-like rod ossicles can be useful in distinguishing *I. maculatus phoenius* from *I. badionotus*. These rods were observed in specimens from Colombia and Panama, and although uncommon in some specimens, they were abundantly present in the holotype (Fig. 15B).

Examination of dorsal papillae in four specimens (and several that were not measured) of *I. maculatus phoenius* with body lengths 25 to 185 mm long showed that C-shaped ossicle and table height increase with body size (Fig. 9A–B). Spines at the crown spires are thick and strong in larger specimens. Contrary to *I. badionotus*, table disc diameter and number of holes remain almost constant through growth in *I. maculatus phoenius*, with only a slight tendency to increase with size (Fig. 9C). Tables in the papillae were larger than those in the body wall (Fig. 10B). Juveniles of *I. maculatus phoenius* are not easy to distinguish from those of *I. badionotus* based on ossicles. The best character is the color pattern, especially the spiral lines (Figs 8, 17).

Separate analyses of COI-Fr1 (Barcoding region) and 16S DNA sequences confirm that *Isostichopus* sp. reported by Wen *et al.* (2011) and Vergara *et al.* (2018: Morphotype III, *Isostichopus* sp., *Isostichopus isabellae* n. sp.) is *I. maculatus phoenius*, because their sequences in GenBank cluster with ours in this subspecies (Fig. 3B, D; Table 1). Sequences of Vergara *et al.* (2018) of their Morphotype I and II of *I. badionotus*, fall in the same clade as our sequences of *I. badionotus* (Fig. 3B, D; Table 1). These molecular results, in addition to external morphology and coloration shown in several figures in various published articles, support the fact that several names used previously are also *I. maculatus phoenius*: *Stichopus* sp. (in Agudelo & Rodríguez 2015); *Isostichopus* sp. (in Vergara & Rodríguez 2015, 2016; Acosta *et al.* 2020, 2021); *Isostichopus* sp. aff *badionotus* (in Agudelo-Martínez & Rodríguez-Forero 2017; Arias-Hernández *et al.* 2017); and *Isostichopus isabellae* n. sp. (in Vergara *et al.* 2018). In addition, GenBank sequences JN207495 and JN207564 reported as *I. badionotus* by Honey-Escandón *et al*. (2012), actually belong to *I. maculatus phoenius* (Fig. 3B, D).

Vergara *et al.* (2018) presented valuable information about *Isostichopus*. Their figure 4 is useful for distinguishing *I. maculatus phoenius* from *I. badionotus*, depicting specimens of the "Light and sharp dark" color pattern (Vergara *et al.* 2018: 40, fig. 4a, c), and "Dark and White" color pattern of *I. maculatus phoenius* (most specimens in Vergara *et al.* 2018: 40, fig. 4b, e). However, some aspects of the taxonomic names they used, their morphological characterization (especially of ossicles) and the habitat information they presented create confusion: (1) they use two different names, *Isostichopus* sp. and *Isostichopus isabellae* n. sp., for the "new proposed species – Morphotype III". (2) although they mentioned a new proposed species, they also stated that "it is quite possible that the morphotype III encountered here represents a described species currently relegated into the synonymy of *I. badionotus*". (3) Vergara *et al.*'s figures 6e and 6f show a mix of ossicles from tentacles (large and thick unperforated

rods) and from pedicels from the ventral body wall (tables, rods, perforated plates and end plate), mistakenly describing them as ossicles from dorsal body wall in the figure legend.

Biology

Despite the taxonomic confusion, even as to the genus, there is recent information about reproductive biology, gametogenesis, spawning and larval development of *Isostichopus maculatus phoenius*. Agudelo & Rodríguez (2015) and Agudelo-Martínez & Rodríguez-Forero (2017) reported natural spawning in captivity from July to November during two consecutive years, concluding that *I. maculatus phoenius* has an annual reproductive cycle in Colombia, with a single spawning event during the warmer months of the year (July to November), the same cycle as reported for *I. badionotus* at other locations of the Caribbean Sea (Guzmán *et al.* 2003; Foglietta *et al.* 2004; Zacarías-Soto *et al.* 2013; Invemar 2015). Acosta *et al.* (2021) confirmed that both *I. maculatus phoenius* (named by them *Isostichopus* sp.) and *I. badionotus* around Santa Marta (Colombia) showed a reproductive season from September to November, closely related to the increase in water temperature and rainfall. These authors reported a sex ratio of 1:1, similar to *I. badionotus*. However, they reported that populations of *I. maculatus phoenius* were smaller in the average size and weight (193 ± 52 mm and 178 ± 69 g) and in size and weight at first maturity (175 mm and 155 g). Acosta *et al.* (2021) also reported one hermaphrodite individual in this subspecies. Agudelo & Rodríguez (2015) and Agudelo-Martínez & Rodríguez-Forero (2017) were able to rear larvae to the doliolaria stage, which was reached 28–30 days after hatching at 26°C. Acosta *et al.* (2020) reported 22 days to the doliolaria and juveniles of 621.8 ± 12.7 µm (± SE) in length 7 days later at 26°C, the temperature in which the highest growth rates, and survival were obtained. Measurement of the growth of *I. maculatus phoenius* under different conditions of light and different temperatures (21°C, 23°C, 25°C), indicated that growth was best promoted by darkness at 23°C for individuals of small size and at 25°C for those of medium size (Fontalvo-Martínez & Rodríguez 2017). The histology of the gut of *I. maculatus phoenius* has been described (Vergara & Rodríguez 2015: fig. 1b, as *Isostichopus* sp.). Density of 0.1 ind/km^2 (0.001 ind/ha) has been reported in Magdalena, Colombia (Invemar 2015, as *Isostichopus* sp.).

Conservation status

As a previously unrecognized species that has been overlooked and confused with *I. badionotus*, *I. maculatus phoenius* has not been included in the IUCN Red List of threatened species. However, *I. maculatus phoenius* is being fished together with *I. badionotus*. Because of its cryptic habits, artisanal fishermen search for it under rocks, or at night. Wen *et al.* (2011) found DNA sequences of this subspecies in commercial food products (frozen and dried) purchased from local retail markets in Guangzhou, China (GenBank FJ794474) (Fig. 3B). The species has also been identified in photographs of specimens harvested in Colombia (Invemar 2015; G.H. Borrero-Pérez pers. obs.). Recently, the subspecies was included in the FAO catalog of commercially important sea cucumbers of the world (Purcell *et al.* 2023, as *Isostichopus* sp. '*phoenius*') as a high-value species in Asian dried seafood markets. The average price of dried *I. maculatus phoenius* in Hong Kong is US$ 358 kg^{-1} (Purcell *et al.* 2023). Interest to include it in fishery and for aquaculture in Colombia has been mentioned by Rodríguez-Forero *et al.* (2013), Agudelo & Rodríguez (2015), Vergara & Rodríguez (2016), Agudelo-Martínez & Rodríguez-Forero (2017) and Arias-Hernández *et al.* (2017). Vergara & Rodríguez (2016) found that the chemical composition of the muscle of *I. maculatus phoenius* (as *Isostichopus* sp.) was similar to that of freshly internationally traded sea cucumbers. Arias-Hernandez *et al.* (2017) have formulated a dry-salting protocol for *I. maculatus phoenius* (as *I.* sp. aff. *badionotus*). Martínez *et al.* (2016) presented a manual for the cultivation and processing of sea cucumbers including *I. maculatus phoenius* (as *Isostichopus* sp.). As this taxon is traded as *I. badionotus*, it is subject to the same regulations in fisheries (Purcell *et al.* 2023); however, differences between this species and *I. maculatus phoenius* in size, habitat and behavior show the necessity to treat them as different species to ensure sustainable exploitation.

Isostichopus fuscus (Ludwig, 1875)
Figs 1I'–O', 3A–D, 4D, 5B, 9, 10D, 11D, 19–21; Tables 1–3

Stichopus fuscus Ludwig, 1875: 97–98.

Stichopus badionotus – Selenka 1867: 316 (partim). — Clark 1922: 56 (partim).
Stichopus fusus – Théel 1886: 256. Typographic error.
Stichopus fuscus – Ludwig 1898: 5, pl. 1 figs 1–5. — Clark 1910: 350; 1922: 45 (as unidentifiable form). — Deichmann 1937: 163; 1938: 363. — Steinbeck & Ricketts 1941: 410.
Isostichopus fuscus – Deichmann 1958: 280–281, pl. 1 figs 1–3. — Hickman 1998: 56, appendix a, p. 65. — Solís-Marín *et al.* 2009: 138, fig. 44. — Borrero-Pérez & Vanegas-González 2022: 329–334. — Purcell *et al.* 2023: 144–145.

Original name

Stichopus fuscus Ludwig, 1875.

Current status

Isostichopus fuscus (Ludwig, 1875).

Name-bearing type

Syntype ZMH E.2689.

Type locality

Manchalilla, Ecuador; proposed by Deichmann (1958) instead of Patagonia (probably wrong), as Ludwig (1898) reported the species in this locality.

Diagnosis

Reticulated, uniform chocolate brown, with stains or reddish color in the background with yellowish large wart-like dorsal papillae (Figs 1I'–O', 21); large tables with a circular spire well developed in the cloaca (Figs 11D, 19C, 20F); distributed in the East Pacific Ocean (Fig. 5B); mtDNA divergence from other species of the genus > 6.1% in COI-Fr1 (barcoding region), > 9.5% in COI-Fr2 and > 5.2% in 16S (Table 2).

Material examined

EAST PACIFIC – **Mexico** • 3 specs, Selenka's syntype of *S. badionotus* (L = 180 to 220 mm); Guerrero, Acapulco; A. Agassiz, collector number 239 leg.; MCZ HOL-743 • 1 spec. (L = 140 mm); Sonora, Pelican Point; 30 Jul. 1969; B. Burch leg.; USNM E21411 • 1 spec. (L = 210 mm); Guerrero, Acapulco; 4–6 Aug. 1982; Hassler exped.; MCZ HOL-742 • 2 specs (L = 210–230 mm); Oaxaca, Puerto Escondido; 25–26 Mar. 1940; E.F Ricketts and J Steinbeck leg.; MCZ HOL-2113 • 1 spec.; Guerrero, Zihuanejo Bay, Playa Las Gatas; depth 3 m; 14 Oct. 1995; M. Olivares leg.; rocky bottom; ICML-UNAM 5.13.52 • 1 spec.; Nayarit, Punta Mita, Corral del Mangle; 21.7700583° N, 105.5174277° W; depth 5 m; 29 Jul. 1995; C. Vizcarra leg.; rocky bottom; ICML-UNAM 5.13.54 • 2 specs; Michoacán, Faro de Bucerías; 18.3468861° N, 103.5119833° W; depth 4 m; 20 Dec. 1993; J. Mendoza. leg.; rocky bottom; ICML-UNAM 5.13.55 • 2 specs; Oaxaca, Puerto Angelito; 15.6522222° N, 96.48527777° W; depth 4 m; 25 Jan. 1995; S. Ramírez leg.; rocky bottom; ICML-UNAM 5.13.63 • 1 spec.; Michoacán, Lázaro Cárdenas municipality, Pichilinguillo; 18.0719444° N, 102.76° W; depth 6 m; Dec. 2006; rocky bottom; ICML-UNAM 5.13.69 • 4 specs; Baja California Sur, west coast of Mexico, Magdalena Bay; 24.5138889° N, 112.0066666° W; depth 4 m; 18 Oct. 1987; F. Solís-Marín leg.; rocky bottom; ICML-UNAM 5.13.73 • 1 spec.; Guerrero, Zihuanejo Bay, Playa La Pedregosa Grande; 17.6183333° N, 101.5311111° W; depth

5 m; 20 Oct. 1992; J. Vargas leg.; rocky bottom; ICML-UNAM 5.13.77 • 2 specs; Sonora, Laguna de Yavaros, La Barra pier; 31 Oct. 1970; Orbe leg.; rocky bottom; ICML-UNAM 5.13.78 • 1 spec.; Colima, Manzanillo, Peña Blanca; 4 Oct. 1993; G. Ramírez leg.; ICML-UNAM 5.13.110 • 1 spec.; Colima, Revillagigedo Archipelago, Socorro Island; 18.7249167° N, 110.9392222° W; depth 15–17 m; 29 Nov. 1997; H. Reyes leg.; ICML-UNAM 5.13.115 • 1 spec.; Nayarit, Isla Isabel; 21.8425° N, 105.8861111° W; 20 Nov. 1997; J. Carballo leg.; rocky bottom; ICML-UNAM 5.13.121 • 1 spec.; Guerrero, Caleta de Campos, El Corralón; 18.0697833° N, 102.7438333° W; depth 3 m; 2 Mar. 2010; F. Solís-Marín leg.; ICML-UNAM 5.13.126 • 1 spec.; Michoacán, Lázaro Cárdenas municipality, Mexcalhuacán; 18.049° N, 102.6591666° W; depth 6–11 m; 4 Mar. 2010; F. Solís-Marín leg.; ICML-UNAM 5.13.127 • 1 spec.; Colima, Manzanillo, Canal de Tepalces; 19.0047944° N, 104.2572305° W; depth 1 m; 15 Aug. 2010; E. Celaya leg.; ICML-UNAM 5.13.128 • 1 spec.; Jalisco, Puerto Vallarta, Majahuitas; 20.5066667° N, 105.3855° W; depth 15 m; 23 Jan. 2010; F. Solís-Marín leg.; ICML-UNAM 5.13.130. – **USA** • 1 spec. (L = 140 mm); California, San Diego; 4–6 Sep. 1982, 18–22 Aug. 1982; Hassler exped.; MCZ HOL-758. – **Colombia** • 1 spec. (L = 180 mm); Chocó, Piedra Bonita; 5.59403° N, 77.5034° W; depth 12 m; 18 Oct. 2016; G. Borrero-Pérez, Riscales2016 leg.; rocky bottom, among rocks; INV EQU4323 • 1 spec. (L = 115 mm); same data as for preceding; INV-EQU4324 • 1 spec.; Chocó, Chicocora; 6.68023° N, 77.4305° W; depth 12 m; 18 Oct. 2016; G. Borrero-Pérez, Riscales2016 leg.; rocky bottom, among rocks, IfRIC154R; INV TEJ1960 • 1 spec. (L = 120 mm); Chocó, Nuqui; 5.5691389° N, 77.52369444° W; depth 10 m; 18 Sep. 2003; G. Borrero-Pérez, Nuqui2003 leg.; rocky bottom, among rocks; INV EQU2746 • 1 spec. (L = 40 mm); Chocó, Piedra de Oswaldo; 5.54429° N, 77.51554° W; depth 15 m;19 Apr. 2016; J. Vanegas-González, Riscales2016 leg.; rocky bottom, among rocks; INV EQU4229 • 1 spec. (L = 145 mm); Chocó, Punta Arusí; 5.61111° N, 77.48512° W; depth 6 m; 24 Apr. 2016; J. Vanegas-González, Riscales2016 leg.; rocky bottom, among rocks; INV EQU4230 • 1 spec. (L = 130 mm); Chocó, Parguera; 5.60989° N, 77.50409972° W; depth 15.5 m; 20 Apr. 2016; J. Vanegas-González, Riscales2016 leg.; rocky bottom, among rocks; INV EQU4231 • 1 spec. (L = 170 mm); Chocó, Punta Faro; 6.82467° N, 77.68996° W; depth 12 m; 25 Oct. 2016; G. Borrero-Pérez, Riscales2016 leg.; rocky bottom, among rocks; INV EQU4321 • 1 spec. (L = 165 mm); same data as for preceding; INV EQU4322 • 1 spec. (L = 130 mm); Chocó, Piedra de Rodrigo; 6.78391° N, 77.69358° W; depth 19 m; 26 Oct. 2016; G. Borrero-Pérez, Riscales2016 leg.; rocky bottom, among rocks; INV EQU4325 • 1 spec.; Malpelo Island; 29 Feb. 1972; C. Birkeland leg.; USNM E23715. – **Panama** • 1 spec.; Panama, Taboguilla Island; 8.8005667° N, 79.52332777° W; depth 10 m; 31 Aug. 2015; H. Lessios and A. Calderón leg.; rocky bottom, hidden under rocks; IfTa210; Tiss-IfTa210 • 1 spec. (L = 150 mm); same data as for preceding; IfTa211; USNM 1659483 • 1 spec. (L = 200 mm); same data as for preceding; 17 Aug. 2015; IfIP322; USNM 1659482 • 1 spec. (L = 150 mm); same data as for preceding; IfTa213; USNM 1682794 • 1 spec. (L = 155 mm); same data as for preceding; If212; MBMLP-If212 • 1 spec.; Gulf of Panama; 7.6666667° N, 78.75° W; 6 Sep. 1972; ICML-UNAM 5.13.98. – **Ecuador** • 1 spec. (a piece of tegument); Galapagos Islands, San Cristobal Island; depth 15 m; 1 May 1993; P. Humann leg.; USNM 1017480 • 1 spec. (L = 57 mm); Galapagos Islands, James Island; 21 Jan. 1938; RV *Velero III*, Hancock Pacific exped.; MCZ HOL-1921 • 1 spec.; Galapagos Islands, Devil's Crown; depth 15 m; 17 Aug. 1998; Hickman, Cleveland leg.; 98-502; UF 9112 • 1 spec.; Galapagos Islands, Champion; 17 Aug. 1998; Hickman, Cleveland leg.; 98-503; UF 9651 • 1 spec.; Galapagos Islands, San Cristobal, Kicker Rock; depth 21 m; 5 May 1996; Hickman, Cleveland leg.; under rock; 96 19; UF 9672. – **Peru** • 2 specs; Isla Lobos de Afuera; 6.9666667° S, 80.75° W; depth 5 m; 10 Jun. 1999; F. Solís-Marín leg.; rocky bottom; ICML-UNAM 5.13.72.

GULF OF CALIFORNIA – **Mexico** • 1 spec. (L = 210 mm); La Paz, El Mogote; 21–22 Mar. 1940; E.F Ricketts and J Steinbeck leg.; MCZ HOL-2115 • 6 specs; Sinaloa, Mazatlán Bay, Isla de Venados; 23.3980556° N, 106.4722222° W; depth 7 m; 15 Feb. 1979; M.E. Caso. leg.; ICML-UNAM 5.13.23 • 1 spec.; Baja California Sur, La Paz Bay, Canal San Lázaro, Salvierra wreck; 24.3852778° N, 110.3008333° W; depth 20 m; 15 Aug. 1996; R. Murillo. leg.; rocky bottom; ICML-UNAM 5.13.56 • 1 spec.; Baja California Sur, La Paz Bay, Puerto Balandra; 24.3284028° N, 110.3344222° W; depth

2 m; 28 Apr. 1969; G. Mendez leg.; rocky bottom; ICML-UNAM 5.13.57 • 1 spec.; Baja California Sur, La Paz Bay, Los Islotes; 24.5858333° N, 110.3886111° W; depth 6 m; 20 Mar. 1993; C. Sánchez leg.; rocky bottom; ICML-UNAM 5.13.64 • 1 spec.; Baja California Sur, La Paz Bay, Isla Espíritu Santo, San Gabriel Bay; 24.4405167° N, 110.3744416° W; depth 3 m; 25 Nov. 1963; M. Beltrán leg.; rocky bottom; ICML-UNAM 5.13.67 • 2 specs; Baja California Sur, La Paz Bay, Puerto Balandra; 24.3283333° N, 110.3341666° W; depth 3 m; 29 Apr. 1969; M.E. Caso leg.; rocky bottom; ICML-UNAM 5.13.81 • 1 spec.; Sinaloa, Mazatlán Bay, Isla de Lobos; 23.2302778° N, 106.4619444° W; 17 Nov. 1998; L. Carballo leg.; ICML-UNAM 5.13.122 • 1 spec.; Sonora, San Carlos; 27.0156806° N, 111.0915° W; 16 Jan. 2010; F. Solís-Marín leg.; ICML-UNAM 5.13.129 • 2 specs; Baja California, Bahía de Calamajue; 29.775° N, 114.2333333° W; May 1998; D. Gonzalez leg.; ICML-UNAM 5.13.116 • 1 spec.; Baja California Sur, South of Isla Santa Catalina; 25.5148333° N, 110.778° W; depth 20–30 m; 24 Aug. 2008; F. Solís-Marín leg.; rocky bottom; ICML-UNAM 5.13.125.

Description

External appearance. Medium to large size species up to 280 mm (Solís-Marín *et al.* 2009), preserved specimens examined 40–230 mm long (n = 19). Body loaf-like, length/width ratio 3.0±0.9 (n = 19, 1.6–5.8). Living specimens convex in cross section, some specimens somewhat quadrangular, rounded in both anterior and posterior parts (Fig. 21). Body wall firm and 2–7 mm thick (MCZ HOL-743, L = 220 mm). Anus supra-terminal, circular and surrounded by large papillae. Mouth directed ventrally, encircled by a collar of large papillae and 20 peltate tentacles; tentacles 10–12 mm long, shield 9–10 mm wide with deep 3–4 mm indentions (MCZ HOL-743, 220 mm). Dorsal papillae large, not variable in shape, wart-like, even in small specimens (INV EQU4229, L = 40 mm, 2 mm high and 2.5 wide; MCZ HOL-743, L = 220 mm, 2–4 mm high and 4–5 mm wide), irregularly arranged, fewer on the dorso-lateral side (Figs 19A, 21). Lateral row papillae large and rounded, sharply defining the dorsal and ventral surface in both juveniles and adults, in living or preserved specimens (Figs 19A, 21). Preserved specimens usually with prominent papillae. Ventral surface densely covered with cylindrical pedicels, arranged in three longitudinal rows (Fig. 21).

Color and body wall appearance. Body wall smooth and opaque, nor translucent, nor rugose in live and preserved specimens more than 110 mm long (Figs 1, 21). Color highly variable, four main patterns recognized (Figs 1, 21): (1) Chocolate brown uniform pattern (BU) (Fig. 1J'): uniform chocolate brown and yellow papillae. (2) Chocolate brown and stains pattern (BS) (Fig. 1I'): chocolate brown background with clearer stains and yellow papillae. (3) Chocolate brown and reddish pattern (BR) (Fig. 1K'): chocolate brown in the dorsal side that gradually changes to reddish in the lateral and ventral sides; some small specimens reddish in the entire body. (4) Reticulated pattern (R) (Fig. 1L'–O'): beige or white background with a reticulum of darker green or brown, which may also appear as small white or beige spots on a darker green or chocolate brown background. Some small specimens of this color. Large, rounded, and yellowish papillae are common in the four-color patterns. Larger specimens preserved in alcohol retain these color patterns. Dorsal papillae in the preserved specimens brown-yellowish and conspicuous. These characteristic dorsal papillae also present in Selenka's specimens, mostly in the posterior part of the body (Fig. 19A). Small juveniles with semi translucent body wall; color in preserved juvenile (40 mm long) uniform beige (INV EQU4229, Fig. 21M), the same as that of adults in a live juvenile specimen (80 mm long) (Fig. 21N).

Internal anatomy (based on MCZ HOL-743, L = 220 mm). Calcareous ring stout, radial elements roughly quadrangular (6 mm wide and 7 mm long), with four anterior small lobes and short posterior projections in the dorsal radial plates; three ventral radial plates with shorter posterior projections; interradial elements almost as wide as radial elements and half as short (6 mm wide and 3 mm long) pointed anteriorly and concave posteriorly (Fig. 4D). Stone canal irregularly helical, about 24 mm long including the madreporite of 9 mm, attached to the mesentery, partially calcified, and pointed at the

end. Tentacle ampullae about 18–30 mm long and 2 to 2.5 mm wide. One Polian vesicle, about 25 mm long by 9 mm wide. Gonads in two tufts, one on either side of dorsal mesentery, branched in cylindrical tubes, filled with eggs (Fig. 11D). Longitudinal muscles 5–8 mm wide, divided and attached to body wall. Respiratory trees inserted near the anterior part of cloaca, a common stem present, divided in a right tree and a left shorter one.

Ossicles (based on MCZ HOL-743, MBMLP-IfTa212, INV EQU4229, INV EQU4324, INV EQU4323 and USNM 1682794 (SEM images, Fig. 19), specimens 40–220 mm long).

Dorsal papillae with tables, thin C-shaped rods, perforated plates, and large, curved rods (Figs 10D, 20A). Perforated plates not found in the 40 mm specimen, only in specimens longer than 115 mm. C-shaped deposits, few and rarely S-shaped, ranging from 46 to 109 ($\bar{x}$ = 71) µm long; usually at the papilla tip, sometimes at the papilla base, abundant or scarce even in different samples of tegument of the same specimen. No clear pattern in the C-shaped rod length in relation to body length (Fig. 9A). Numerous table ossicles 34–65 ($\bar{x}$ = 50) µm high and 42–95 ($\bar{x}$ = 63) µm across the disc. Spires composed of four pillars usually parallel, ending in triplets of blunt spines forming a wide crown and one crossbeam connecting adjacent pillars; in 40 mm long specimen a crown of many minute spines. Disc margins smooth and wide; discs with one rounded central perforation and 8 to 12 peripheral holes, usually arranged in one simple ring. Tables near the top of the papillae taller and larger, with several extra

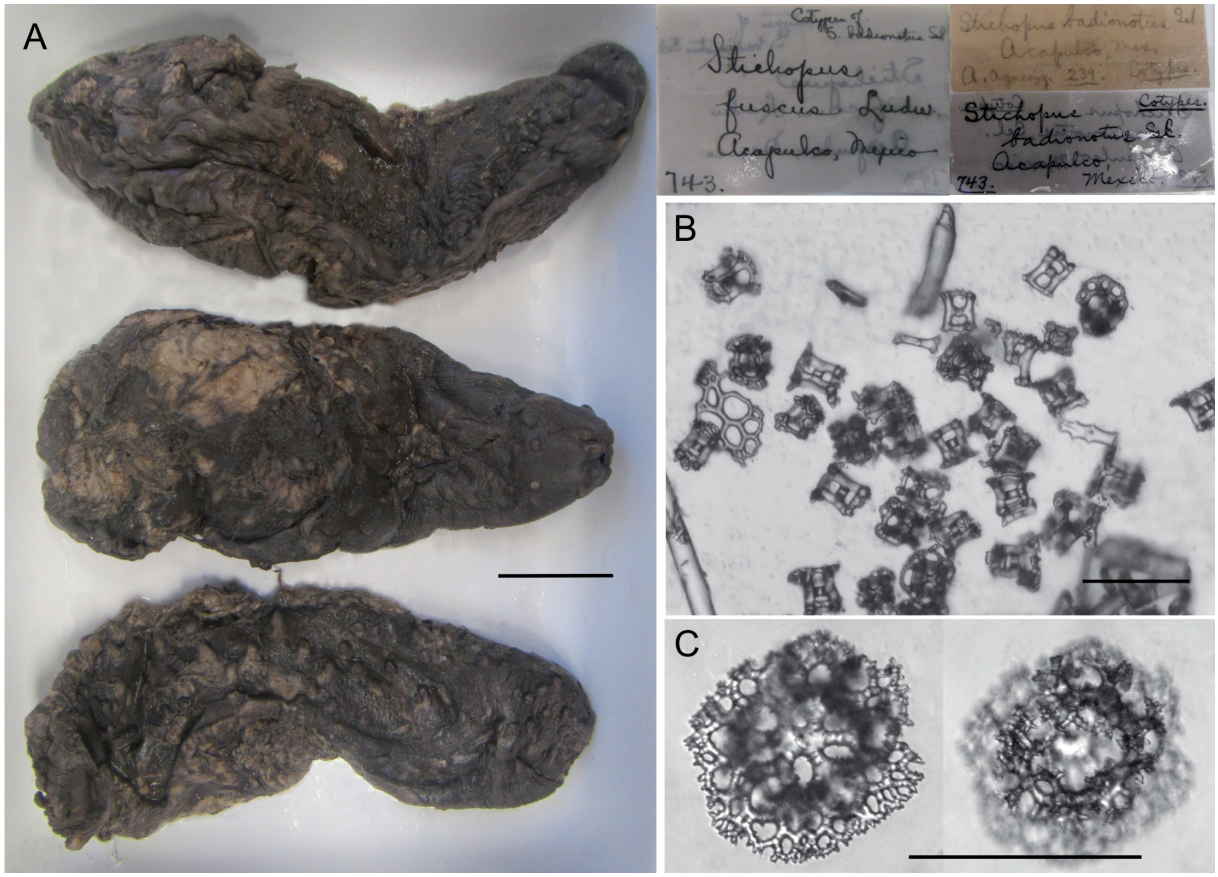

Fig. 19. Preserved specimens of *Isostichopus fuscus* (Ludwig, 1875) from Acapulco, Mexico and of Selenka's syntype of *I. badionotus* (Selenka, 1867) (MCZ HOL-743, 160–175 mm long). **A**. Dorsal view of three specimens. **B**. Ossicles from dorsal papillae. **C**. Large tables with circular spire from the anterior cloaca. Photos by G. Borrero. Scale bars: A = 30 mm; B–C = 100 µm.

perforations arranged in more than one ring, and more square than those from the body wall (Fig. 10D). Changes of tables in size and shape during growth are not pronounced; lower tables in 40 mm specimen (34–46 μm high; $\bar{x}$ = 41) than in larger specimens (41–65 μm high, $\bar{x}$ = 50) (Figs 9B, 10D); disc tables in smaller and larger specimens less wide than in those of middle size (Figs 9C, 10D). Few perforated plates, located at the papilla tip, with few large perforations, larger in the center of the plate; plates 103–151 μm across; slightly or strongly curved rods 192–329 μm long, with quadrangular projections, sometimes perforated in the central part of the rod (Fig. 20A).

Dorsal body wall with tables and few C-shaped rods, rarely S-shaped (Figs 10D, 20A). Similar in shape to tables at the papillae but narrower and smaller 33–69 ($\bar{x}$ = 47) μm high and 37–71 ($\bar{x}$ = 52) μm across the disc, with regular discs with one ring of 8–10 holes (Fig. 10D); few C-shaped rods 47–60 μm long, present only in some of the specimens.

Pedicels with tables, C-shaped rods, perforated plates, large and curved rods, and end plates (Fig. 20B). C-shaped ossicles 57–86 μm long in some specimens. Numerous table ossicles 27–45 ($\bar{x}$ = 38) μm high and 46–76 ($\bar{x}$ = 56) μm across the disc; shape of the tables similar to those from the dorsal papillae and body wall, but with the central perforation usually bigger and not rounded in some tables, 10–13 peripheral holes in a simple ring, and usually no extra perforations. Numerous elongated perforated plates, with many perforations larger and elongated in the center of the plate; plates 207–383 μm long; slightly or strongly curved rods 285–483 μm long, usually with perforated central expansions; end plates 674–678 μm across.

Ventral body wall with only tables and few C-shaped ossicles.

Tentacles with rods and tables (Fig. 20C). Table ossicles 38–61 μm across disc; spire low, composed of four pillars which can be incomplete, without crossbeams connecting adjacent pillars; discs with a large and not rounded central perforation with various peripheral holes (5 to 12) arranged in one ring; margins usually spinous. Numerous strongly or slightly curved spiny rods 91–654 μm long.

Mouth membrane with C-shaped rods, simple rods, and tables in some specimens (Fig. 11D). C-shaped ossicles 42–79 μm long; rods 73–124 μm long; some large tables 123 μm high and 164–230 μm across the disc, with well-developed spire, composed of several pillars joined at the top, forming a very dense crown of spines, without distinguishable crossbeams connecting adjacent pillars; spire usually flat. Table discs with many peripheral perforations, arranged in several rings with spinous and thin margins, sometimes reduced, same width as the spire.

Longitudinal muscles with only C-shaped ossicles 40 to 67 μm long (Fig. 20D). Posterior cloaca with C-shaped ossicles, 49–77 μm long and rods 87–191 μm long (Fig. 11D). Anterior cloaca with C-shaped ossicles 57 μm long; simple or bifurcated rods 135–234 μm long; large tables and irregular plate-like branched rods (Fig. 20E). Large tables with a well-developed spire, composed of several joined pillars; discs smooth but with spiny margins, with several central perforations and 26 to 65 or more small peripheral holes, arranged in several rings (table disc diameter 122–184 μm, spire width 26–65 μm) (Fig. 11D). Large tables with a circular well-developed spire, composed of 5 to 9 pillars, not joining at the top, with at least one crossbeam connecting adjacent pillars at the top; lateral edges of the pillars usually with pointed projections; discs and margins very spiny, discs having several central elongated perforations and 5 to 48 or more large peripheral holes, arranged in several rings (discs 90–99 μm high, 121–209 μm across disc, 59–105 μm spire width) (Figs 11D, 19C, 20F). Perforated plates symmetrically radial similar to table discs, without spire, 109–234 μm long (Fig. 11D). Respiratory trees with small tables 55 μm high and 60 μm across the disc similar to those in the body wall (Fig. 20G), and with some tables like those having circular spires from the anterior cloaca, 104–107 μm across the disc and 67–72 μm spire width. Intestine with spinose or smooth deposits in a cross shape 62–148 μm long, sometimes with bifurcated ends, and

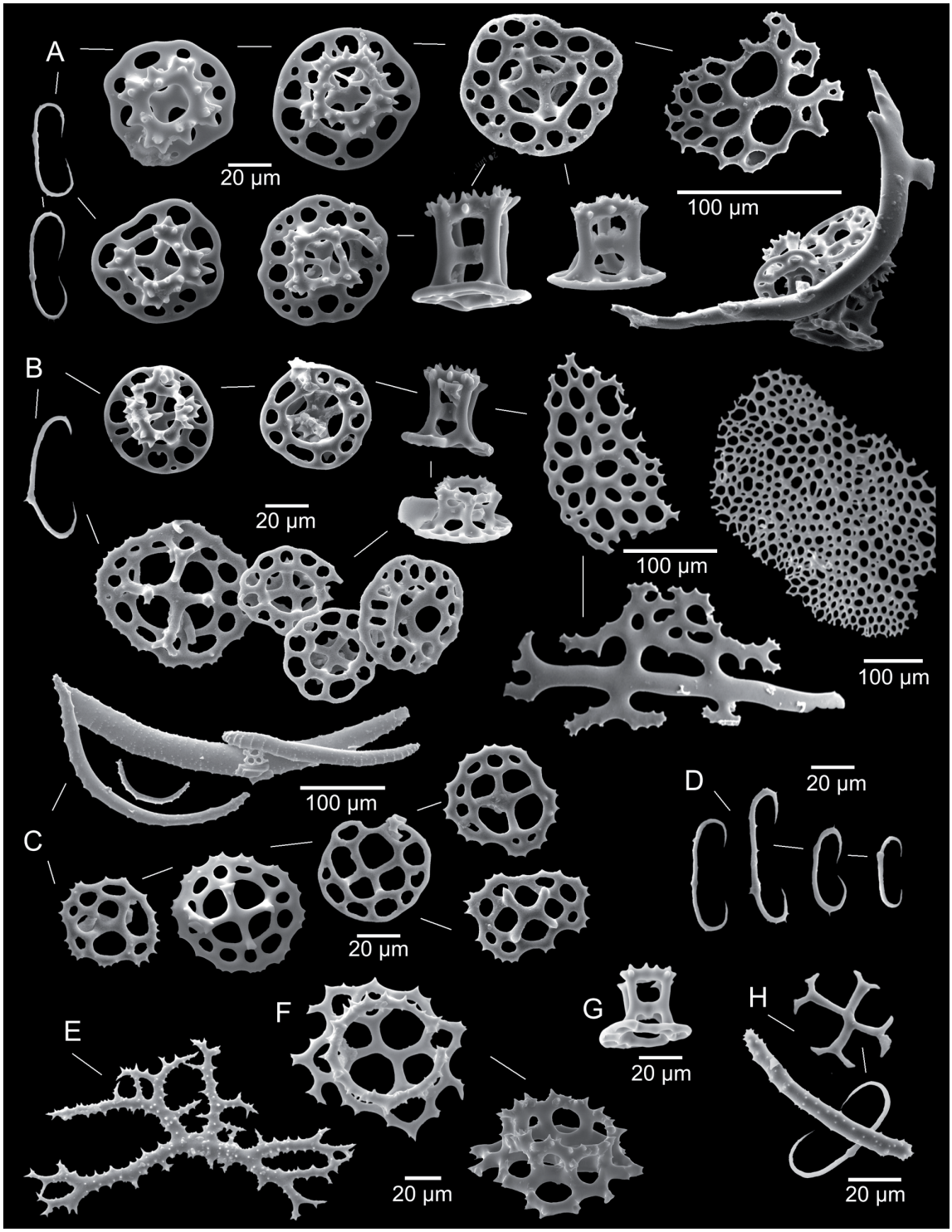

Fig. 20. *Isostichopus fuscus* (Ludwig, 1875) ossicles (specimen USNM 1682794-Ta213, 155 mm long). **A**. Thin C-shaped rods, tables, perforated plates and large, curved rods from dorsal body wall and papillae. **B**. Thin C-shaped rods, tables, perforated plates, large, curved rods and end plate (fragment) from ventral body wall and tube feet. **C**. Rods and tables from tentacles. **D**. Thin C-shaped rods from longitudinal muscles. **E**. Rods bifurcated from the cloaca. **F**. Large tables with a circular spire well developed in the anterior cloaca. **G**. Tables from respiratory trees. **H**. Rods in cross shape, simple rods, and C-shaped rods in the intestine. Photos by G. Borrero.

some C-shaped ossicles 41–99 µm long (Fig. 20H). Gonads with delicate and long rods 300–405 µm and some small tables 51–57 µm high and 54–60 µm across the disc (Fig. 11D).

Distribution

Eastern Tropical Pacific from Baja California, Mexico, to Peru, including the Gulf of California, islands and rocky reefs, including the Revillagigedos Archipelago and Socorro Island (Mexico), Isla del Coco (Costa Rica), Malpelo and Gorgona (Colombia), Galápagos (Ecuador), and Lobos de Afuera Islands (Peru) (Deichmann 1958; Maluf 1988; Hooker *et al.* 2005; Prieto-Ríos 2010; Purcell *et al.* 2023) (Fig. 5B). We examined one specimen (L = 150 mm) collected in the Western Central Pacific (Republic of the Marshall Islands, Caroline Islands, Pohnpei Island, Ponape) and deposited at the Museum of Comparative Zoology (MCZ HOL-786). The specimen was initially identified as *Stichopus variegatus* Semper, 1868 (a currently unaccepted species) but changed to *S. fuscus* (and even *S. badionotus* in some of the labels). We found that ossicles match those of *Isostichopus fuscus*, but that the large papillae characteristic of *I. fuscus* were absent. This specimen would extend the geographic distribution of *I. fuscus* to the Central Pacific, but more information is required for confirmation. Purcell *et al.* (2023: 145) include the Indo-Pacific Cocos (Keeling) Islands (possibly confusing them with Isla del Coco, Costa Rica) in the distribution of the species. This, as well as the inclusion of Patagonia in the map of the species, clearly appear to be errors (Purcell *et al.* 2023). Bathymetric distribution: shallow subtidal zone to 39 m (Deichmann 1958; Maluf 1988).

Habitat

Isostichopus fuscus is common in rocky bottoms and coralline patches along the coast. Specimens can be exposed or semi-hidden. In Baja California, it is found in coral and rocky habitats (Purcell *et al.* 2023). Along the Colombian Pacific coast, they were observed inside crevices, between rocks or semi-exposed (Borrero-Pérez pers. obs.). In the Galapagos, they prefer rocky bottoms where the seaweed *Ulva* sp. is predominant (Toral-Granda & Martínez 2007) and they are more active at night (Shepherd *et al.* 2003).

Remarks

Deichmann (1958) clarified the status of *I. fuscus* by recognizing three specimens of Selenka's cotypes of *I. badionotus* as *I. fuscus* (Fig. 19A), proposing Manchalilla, Ecuador, as the type locality, and describing the differences between *I. badionotus* and *I. fuscus*. Populations of Atlantic *I. badionotus* and Pacific *I. fuscus* have been confirmed as different species by molecular markers (Byrne *et al.* 2010). The character proposed by Deichmann (1958) to distinguish *I. fuscus* from *I. badionotus* was the proportion (profile) of the tables in lateral view, narrower tables in *I. badionotus* but almost square ones in *I. fuscus.* In our observations, comparison of the ratio of table height to width shows some differences (Fig. 10). However, table profile can be a variable and subjective character and depends on whether the tables are from the papillae or the body wall (tables of both species are more square in papillae and narrower in the body wall). *Isostichopus maculatus phoenius* and *I. maculatus maculatus* also possess tables that are more square than narrow in the papillae. Although this character could help identify individuals, for example in specimens from fishery confiscations, it is better to combine table profiles with external characters and geographic origin to identify *I. fuscus* reliably. A new diagnostic character of *I. fuscus*, not reported previously are large tables with a well-developed circular spire in the cloaca (Figs 11D, 19C, 20F).

Color variability in *I. fuscus* was also recorded by Deichmann (1958), who proposed that the "Reticulated" pattern corresponded to younger specimens and "Chocolate-brown" to adults. We found juveniles and adults with both color patterns (Fig. 21), and we also found other color patterns including a chocolate-brown and reddish pattern, as well as completely red juveniles, also recorded by Clark (1910) in a live specimen from Peru.

Examination of dorsal papillae in four specimens (and several that were not measured) of *I. fuscus*, from 40 mm to 180 mm long, showed that ossicles become more abundant in the largest specimens. The

largest C-shaped ossicles were in 155 mm long specimens. Spines at the crown spires were thick and strong in the largest specimens. Table height and disc diameter increased with body length in specimens 40 to 155 mm, but they were smaller in the 180 mm specimen (Fig. 9A–C). In contrast to *I. badionotus*, large specimens of *I. fuscus* had wide discs, similar to those of *I. maculatus phoenius*.

Biology

Commercial interest and decline of the populations of *I. fuscus* motivated studies on its ecology and biology. This information is mainly from the Gulf of California and from the Galapagos, the main localities of fishery. Information about *I. fuscus* in other areas in the Eastern Pacific is scarce. *Isostichopus fuscus* is a long-lived, slow-growing species that reaches sexual maturity in 5 years, at which point individuals are approximately 21 cm long in the Gulf of California (Herrero-Pérezrul *et al.* 1999; Herrero-Pérezrul & Reyes-Bonilla 2008). In the Galapagos, the reported size of first maturity is between 21 and 23 cm (Toral-Granda & Martínez 2004). In the Gulf of California spawning occurs between May and September, influenced by the increase in water temperature (Fajardo-León *et al.* 1995; Herrero-Pérezrul *et al.* 1999). In the Galapagos, reproductive activity has been reported throughout the year, spawning occurs every month one to four nights after the new moon, regardless of temperature (Mercier *et al.* 2007; Toral-Granda 2008b). *Isostichopus fuscus* is gonochoric, although there have been some cases of hermaphroditism, which may be related to low population densities due to overfishing (Herrero-Pérezrul *et al.* 1998). The larval pelagic period lasts from 22 to 27 days; newly settled juveniles measure 1 mm in length; at 72 days they reach 3.5 cm and at 110 days they are 8 cm long (Hamel *et al.* 2003; Mercier *et al.* 2007). The success of fertilization in sea cucumbers is a function of the spatial dispersion of the broodstock, so that minimum density is important (Bell *et al.* 2008). For populations of *I. fuscus* at Galapagos, a density of ~1.2 ind/m^2 (~12 000 ind/ha) was estimated to achieve 50% fertilization success (Shepherd *et al.* 2004). Highest population densities of *I. fuscus* were 3500 ind/ha in Galapagos in 1999, before the establishment of fishing seasons (Toral-Granda 2005). On the coast of mainland Ecuador, in the provinces of Santa Elena and South Manabí, mean density was estimated as 100 ind/ha (Aguilar *et al.* 2011, 2013). Densities were 4300 ind/ha in Jalisco, Mexico, in 1991 (Girón *et al.* 1991 in Glockner 2014) and 3780 ind/ha in Bahía de los Ángeles, Baja California, in 1992 (Salgado-Castro 1992 in Glockner 2014). Estimated densities at Gorgona Island (Colombia) ranged between 150 and 600 ind/ha (Palacios & Muñoz 2012). Along the northern Pacific mainland of Colombia, *I. fuscus* was common in 2003 and 2016 (G.H. Borrero-Pérez pers. obs.).

Hosting of the parasitic worm *Anoplodium* sp. (Platyhelminthes: Rhabditophora) was reported in *I. fuscus* (Hamel *et al.* 2017). The rate of infestation was 1 to 725 of flatworms per sea cucumber. Individuals with a high rate of infestation had gonads that were very small or absent. Combined with overfishing, the infestation by this parasite could seal the fate of *I. fuscus* in certain regions of the Eastern Pacific (Hamel *et al.* 2017).

Conservation status

Isostichopus fuscus is fished legally and/ or illegally in Ecuador, Mexico, Panama, and Peru (Purcell *et al*. 2012, 2023). Currently *Isostichopus fuscus* is included as "Endangered (EN)" in the IUCN Red List of Threatened Species (Mercier *et al.* 2013). It is the only sea cucumber species included in Appendix III of CITES proposed by Ecuador (Toral-Granda 2008b). In addition, *I. fuscus* is under special protection by Mexican law (DOF 2010 in Glockner-Fagetti *et al.* 2016) and it is included in the Red Book of Marine Invertebrates of Colombia (Borrero-Pérez & Vanegas-González 2022). *Isostichopus fuscus* is one of the most valuable species in the genus. It is sold at US$ 1.4 per fresh specimen in Ecuador and for US$ 498–527 kg^{-1} in China (Purcell *et al.* 2023). The average maximum market price for "Endangered" sea cucumbers in the IUCN red list, including *I. fuscus*, is US$ 1030 kg^{-1}. Maximum price of species listed as "Vulnerable" is US$ 158 kg^{-1}, of species listed as "Of Least Concern" is US$ 124 kg^{-1} and of species listed as "Data Deficient" is US$ 106 kg^{-1} (Purcell *et al.* 2014). These authors propose that market value is one of the factors that most drives the risk of extinction of these species.

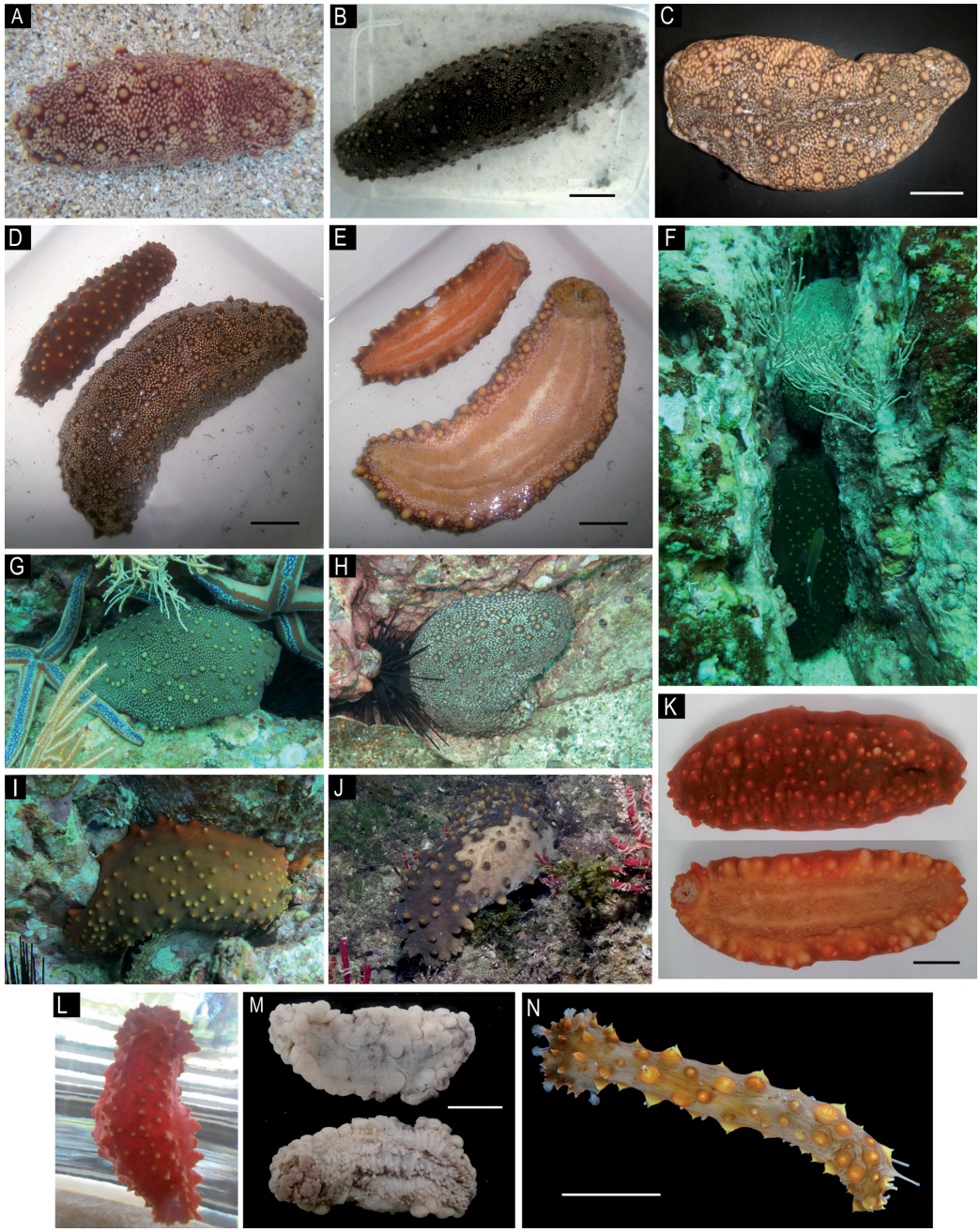

Fig. 21. Color patterns and morphological variation of *Isostichopus fuscus* (Ludwig, 1875) (DNA sequences and detailed information of some specimens are indicated in Table 1, see Photo ID column for correspondence). **A–C, D–E-bottom, F-top, G–H**. Specimens with "Reticulated" pattern from Taboguilla, Panama (Ta210) (A), Perlas Islands, Panama (B), North Chocó, Colombia (C, D–E-bottom dorsal and ventral view, F-top, G–H). **D–E-top, I, K–L**. Specimens with "Chocolate brown and reddish" pattern from North Choco, Colombia (I, D–E-top-dorsal and ventral view, K-small specimen completely red), and Perlas Islands, Panamá (L, small specimen completely red). **J**. Specimen with "Chocolate brown and stains" pattern from Mexico. **F-bottom**. Specimen with "Chocolate brown uniform" pattern from North Chocó, Colombia. **M**. Preserved juvenile from North Choco, Colombia (original coloration not recorded). **N**. Juvenile from Mexico, "chocolate brown uniform with yellow papillae" pattern. Photos: F–I by L. Chasqui; L by A. Calderón; J, N by C. Sánchez; A–E, K, M by G. Borrero. Scale bars: B, M = 10 mm; D–E = 30 mm; C, K, N = 20 mm.

Along the mainland coast of Ecuador, the commercial extraction of this species began in 1989. Two years later, due to stock depletion, it moved to the Galapagos, where a management plan was developed in 1999 (Bruckner *et al.* 2003). Currently, there is a total ban on fishing the species off continental Ecuador (Purcell *et al.* 2023). The population densities of *I. fuscus* at Galapagos ranged from 3500 ind/ha in 1999 to 500 ind/ha in 2004 (Toral-Granda 2005). These data revealed an alarming decline in population density, despite "presumably robust" populations in 1999 after a five-year fishing ban. In 2009 and 2010 there was a new moratorium on fishing as the minimum population density of 1100 ind/ha (11 ind/100 m^2), was not met (Purcell *et al.* 2023). Currently, in the Galapagos Islands there are several management strategies that include a total allowable catch, minimum catch size (20 cm fresh or 7 cm dry), no-take reserves, a two month fishing season, and access only to artisanal fishers who are permanent residents of the islands (Purcell *et al.* 2023).

In Mexico, commercial exploitation of *I. fuscus* started in 1988, on the western coast of the Baja California Peninsula (Herrero-Pérezrul 2004). In the early 90s, the demand for this resource motivated the assessment of *I. fuscus* populations at new sites with fishing potential (Glockner 2014). Population densities decreased from 1991–1992 to 2013 in localities surveyed such as Jalisco (4300 ind/ha in 1991, 60 ind/ha following years) and Bahía de los Ángeles (3780 ind/ha in 1992, 1000 ind/ha in 2005–2007, 700 ind/ha in 2013) (Girón *et al.* 1991; Girón & González 1992; Salgado-Castro 1992 all in Glockner 2014). The population density decreased by 82% during the time or evaluation and the average size of the individuals decreased by 26% (Glockner 2014). The management measures of the species, such as limits to total allowable catch, establishment of minimum catch size, and closing the fishery during the season of reproduction, have not been sufficient to ensure the sustainable extraction of this species in Bahía de los Ángeles (Herrero-Pérezrul & Reyes-Bonilla 2008; Glockner 2014). The observed values of density and mean length apparently affected reproductive success, because recruitment was low (Glockner-Fagetti *et al.* 2016). Purcell *et al.* (2023) also report several management strategies in Mexico, including the establishment of a fishing season (October–May), a minimum legal size (400 g or 20 cm), annual permits and no-take reserves where the smallest individuals are found.

Preoccupation about the conservation of this species in regions besides Galapagos and Mexico is also justified because of the incessant growth of demands by Asian markets. Of concern is also that most of the known population densities in the eastern Pacific are lower than the estimated density proposed by Shepherd *et al.* (2004). In addition, the population densities after the fishing are lower than 1100 ind/ha, the threshold reference point presented by Purcell *et al.* (2023) for *I. fuscus* in Galapagos.

In Panama, there are reports of illegal extraction of *I. fuscus* and other species of sea cucumbers at the Perlas Islands and at the island of Coiba. Between 2004 and 2005, 689 kg dry weight of sea cucumbers were exported to Hong Kong (China) from Panama (Vergara-Chen *et al.* 2015). However, Executive Decrees 157-2003 and 217-2009 instituted a ban on harvest, possession, and commercialization of this organism (Vergara-Chen *et al.* 2015). There are no fishing records on *I. fuscus* in Colombia and Peru. A first attempt to breed *I. fuscus* in land-based installations on the coast of Ecuador was reported by Mercier *et al.* (2004). Ongoing projects seeking to restore the sea cucumber population are being developed at the Provincia Santa Elena, Ecuador (https://www.eluniverso.com/vida/2017/05/21/nota/6191473/proyecto-busca-repoblar-pelado-pepinos-mar-spondylus).

Isostichopus macroparentheses (Clark, 1922)
Figs 1P'–Q', 3A–D, 4E, 5B, 9, 10E, 11E, 22–24; Tables 1–3

Stichopus macroparentheses Clark, 1922: 61–63, pl. 1 figs 1–7.

Stichopus megaparentheses – Clark 1922: 63. Typographic error.
Stichopus macroparentheses – Deichmann 1926: 21; 1930: 82–83, pl. 5 figs 37–43. — Clark 1933: 110 (as *S. macraparentheses*, typographic error).

Isostichopus badionotus – Deichmann 1957: 4–5; 1963: 106. — Miller & Pawson 1984: 54. — Cutress 1996: 105, 112. — Pawson *et al.* 2010: 34–35.
Stichopus macroparenthesis – Deichmann 1957: 4–5. Typographic error.
Isostichopus macroparentheses – Pawson 1976: 374, fig. 1d. — Solís-Marín *et al.* 1998: 524. — Hendler & Pawson 2000: 282. — Laguarda-Figueras *et al.* 2001: 28, fig. 11a–d; 2005: 119. — Alvarado & Solís-Marín 2013: 650.

Original name

Stichopus macroparentheses Clark, 1922.

Current status

Isostichopus macroparentheses (Clark, 1922).

Name-bearing type

Holotype MCZ HOL-921, MCZ HOL-225 (ossicle slide of the holotype); paratype MCZ HOL-1214.

Type locality

Montego Bay, Jamaica.

Diagnosis

C-shaped ossicles >90 µm long on average; disc tables in dorsal papillae and body wall completely reduced in adults (Figs 10E, 23A); tridimensional spheres and straight/spiky rods in the respiratory tree (Fig. 23F); semi-translucent and smooth body wall; color not variable, background of dorsal side light yellow-brown, with irregularly arranged blurred large and small darker brown spots (Figs 22A, C, 24); mtDNA divergence from other species of the genus >16.2% in COI-Fr1 (barcoding region), >16.3% in COI-Fr2 and >9.5% in 16S (Table 2).

Material examined

Holotype

JAMAICA • L = 50 mm, contracted; Montego Bay, Bogue Island; 18.46908° N, 77.931086° W; Mar. 1912; H.L. Clark leg.; MCZ HOL-921 • ossicle slide of the holotype; same data as for holotype; MCZ HOL-225.

Paratype

USA • 1 spec. (L = 65 mm); Florida, Tortugas, Bird Key; 24.6185° N, 82.8854° W; Jun. 1917; Carnegie Institute, Tortugas Laboratory leg.; MCZ HOL-1214.

Other material

GULF OF MEXICO – **Mexico** • 1 spec.; Veracruz, Isla Lobos; 21.465° N, 97.22866° W; depth 2–7 m; 16 Mar. 2011; F. Solís-Marín leg.; coral, rocky bottom; ICML-UNAM 5.88.1 • 1 spec.; Veracruz, Isla Lobos; 21.4726667° N, 97.23116° W; depth 12 m; 17 Mar. 2011; F. Solís-Marín leg.; coral, rocky bottom; ICML-UNAM 5.88.2 • 1 spec.; Veracruz, Isla Lobos; 21.4541667° N, 97.22500° W; depth 1.5 m; 13 Mar. 1976; coral, rocky bottom; ICML-UNAM 5.88.3.

CARIBBEAN SEA – **Mexico** • 1 spec.; Quintana Roo, Puerto Morelos, off Rodman shipyard; 20.87472° N, 86.85083° W; depth 2 m; 1 Jul. 1995; F. Solís-Marín leg.; rocky bottom; ICML-UNAM 5.88.0 • 1 spec.; Quintana Roo, Akumal Bay; 20.39375° N, 87.31426° W; depth 2.5 m; 25 May 2012; F. Solís-Marín leg.; rocky bottom; ICML-UNAM 11053. – **US Virgin Islands** • 1 spec. (L = 60 mm); St. Croix Island, Rod Bay; 17.733761° N, 64.614086° W; depth 0.5 m; 17 Jul. 1990; R. Aronson

leg.; USNM E40833. – **British Virgin Islands** • 1 spec. (L = 135 mm); Guana Island; 18.472111° N, 64.576794° W; depth 2 m; 1 Jun. 1997; A. Kerr leg.; USNM E47524. – **Antigua and Barbuda** • 1 spec. (L = 80 mm); Antigua Island, English Harbor; 17° N, 61.7667° W; 7 Jan. 1918; C. Nutting leg.; USNM E4391 • 1 spec. (L = 70 mm); same data as for preceding; USNM E22322 • 1 spec. (L = 50 mm); same data as for preceding; USNM 1283366. – **Curaçao** • 1 spec.; Carmabi Marine Research Station; 12.12177° N, 68.96964° W; depth 3 m; 18 Feb. 2020; G. Paulay leg.; reef shelf; BCUR-0532; UF20352. – **Belize** • 1 spec. (L = 20 mm); Tobacco Cay; 16.945997° N, 88.060744° W; depth 2 m; 10 Jun. 2016; L. Geyer and G. Borrero-Pérez leg.; rocky bottom, ImrBe99; USNM 1659484 • 1 spec. (L = 40 mm); Carrie Bow Cay; 16.803074° N, 88.081939° W; depth 2 m; 12 Jun. 2016; A. Hiller and G. Borrero-Pérez leg.; rocky bottom, ImrBe107; USNM 1659485 • 1 spec. (L = 30 mm); Belize, Carrie Bow Cay; 16.80295° N, 88.08145° W; depth 1–2 m; Apr. 1975; M. Carpenter leg.; USNM E18627 • 1 spec. (L = 25 mm); Carrie Bow Cay, near transect along wall of trough behind fore reef crest; 16.80295° N, 88.08145° W; depth 18 m; 22 Mar. 1979; G. Hendler leg.; USNM 1021529.

Description

External appearance. Small to medium size species, preserved specimens up to 135 mm long (n = 11, range 20–135 mm, holotype: 50 mm, paratype: 65 mm). Body loaf-like, length/width ratio 3.1 ± 0.5 (n = 11, range 2.4–4.1, holotype 3.8, paratype 4.1). Holotype (contracted) and paratype rounded posteriorly and anteriorly (Fig. 22A, C), similar to living specimens, which are convex/subcylindrical in cross section (Fig. 24). Body wall soft and not very thick (paratype: 0.5–1 mm; USNM E47524 (L = 135 mm): 2–4 mm). Anus supra-terminal, circular and not surrounded by large papillae. Mouth directed ventrally, encircled by a collar of medium sized papillae (paratype: 2 mm high; holotype: retracted). Nineteen large peltate tentacles in the holotype (retracted) and paratype (3–4 mm long, 2.5–3 mm wide shield, with 0.5 mm deep indentations); 20 tentacles in the largest specimen USNM E47524 (6–7 mm long; 4–4.5 mm wide shield). Large live and preserved specimens with flat and inconspicuous dorsal and lateral papillae (Fig. 24F, J–K) (USNM47524: less than 1 mm high and 2 to 5 mm wide at the base). Juvenile live specimens with medium to large dorsal papillae, rounded or pointed, ending in a thin tip, scattered irregularly; lateral papillae similar in shape to the dorsal ones, but smaller and less obvious (Fig. 24A–E). Papillae in the holotype and paratype small (Fig. 22A, C). Lateral rows not sharply defining the dorsal and ventral surface in either juveniles or adults, in living or preserved specimens (Figs 22, 24). Ventral surface in both juveniles and large specimens densely covered with cylindrical pedicels, arranged in three longitudinal rows (Figs 22, 24); most of the pedicels retracted and longitudinal rows not evident in the largest preserved specimen (USNM E47524).

Color and body wall appearance. Body wall surface smooth and semi-translucent (Figs 1, 22, 24) (see also Clark 1922: 62). Color not variable, living specimens light yellow-brown in the background on the dorsal side with irregularly arranged blurred big and small darker brown spots that do not coincide with the papillae; papillae lighter, with the distal end almost white, or at least lighter than the base of the papillae, yellow according to Clark (1922) (Fig. 1P'–Q'). Ventral surface lighter than dorsal with small spots in the same dorsal pattern, pedicels translucent white, end plate of darker brown (Fig. 24). Preserved specimens similar to live ones in color, tentacles with light brown tubes and darker shields (Fig. 24F–I). Holotype and paratype uniform whitish on the dorsal and ventral surfaces, with slightly darker tentacles (Fig. 22A, C). Living juveniles (20 mm long) similar in color as adults, tentacles translucent white (Fig. 24A–E).

Internal anatomy (based on MCZ HOL-1214 (paratype, L = 65 mm), USNM E47524 (L = 135 mm) and MCZ HOL-921 (holotype, L = 50 mm, mostly deteriorated)). Calcareous ring diameter 7 mm in the 65 mm specimen and 11 mm in the largest 135 mm one; radial elements almost as long as wide (L = 65 mm: 2 mm wide, 1.5 mm long; L = 135 mm: 5 mm wide, 4.2 mm long), with four anterior small lobes and small posterior projections that are larger in the largest specimen (1.2 mm) (Fig. 4E); interradial

elements pointed anteriorly and concave in the posterior margin, about half as wide as radial elements and somewhat shorter (L = 65 mm: 2.5 mm wide, 1.5 mm long; L = 135 mm: 2.5 mm wide, 3 mm long). Single and irregularly helical stone canal (L = 65 mm: 4 mm long; L = 135 mm: 10 mm long), attached to the mesentery, ending in a flat leaf-like madreporite, 2 mm wide in the largest specimen. Tentacle ampullae in the largest specimen 12–16 mm long, 2–3 mm long in the 65 mm specimen, and 1.5–2 mm in the holotype. One tube-like Polian vesicle in the 65 mm specimen and the holotype (both 6 mm long, 1 mm wide); two tube-like Polian vesicles in the largest specimen, one longer (15 mm long, 2.5 mm wide) than the other (9 mm long, 1.5 mm wide), streaked longitudinally, with spots and dark tips. Gonads found only in the holotype (Fig. 11E). Longitudinal muscles approximately 1.5 and 2.5 mm wide in the 65 mm specimen and the holotype, and 4 mm wide in the largest specimen (USNM E47524), divided and attached to the body wall medially and laterally. Respiratory trees insert to the cloaca arising from a common stem 13 mm long in the 135 mm specimen, the left tree extending with the intestine (L = 65 mm: 25 mm long; L = 135 mm: 65 mm long) and right tree free (19 mm and 45 mm long, respectively).

Ossicles (based on MCZ HOL-921 (holotype, L = 50 mm), MCZ HOL-225 (holotype permanent slide), MCZ HOL-1214 (paratype, L = 65 mm), USNM E47524 (L = 135 mm, SEM images (Fig. 22)); USNM 1659484 (juvenile, L = 20 mm) and USNM 1659485 (juvenile, L = 40 mm); juveniles only for dorsal papillae and body wall). Ossicles of the holotype are mostly deteriorated; however, some aspects of the remaining ossicles, the permanent slide MCZ HOL-225, and the description of Clark (1922), who only described the ossicles from papillae and pedicels, are included.

Dorsal papillae with tables, thin C-shaped rods, perforated plates, and large, curved rods (Figs 10E, 22B, 23A). All types of ossicles present in all specimens, from 20 mm to 135 mm long. Numerous C-shaped rods, a few S-shaped ones, ranging from 91 to 155 ($\bar{x}$ = 133) µm long; 2–3 times as long as tables are high, usually abundant in the papilla tip, sometimes in the base; no obvious correlation with body length (Figs 9A, 10E). Numerous tables with notable changes in shape and size during growth. Tables in 20, 40 and 65 mm specimens 31 to 48 ($\bar{x}$ = 40) µm high and with large discs with smooth and wide margins 24–77 ($\bar{x}$ = 48) µm across the disc, characterized by one large central perforation, which appears as four large and symmetrical holes, without outer holes, or usually with 4 outer smaller holes alternating with the central holes (Fig. 10E, also see Clark 1922: pl 1 fig. 2; Deichmann 1930: pl 5 fig. 39); some tables with 5 to 15 (rarely 20) holes in the disc, forming a complete outer ring, rarely with one more incomplete ring. Spires composed of four pillars usually narrowed at the tip, although also with parallel pillars, crossbeam closer to the base; crown of spire rounded without teeth or with few teeth; minute teeth on tables with larger discs. These tables with large discs disappear in individuals during growth, and are replaced with regular *Isostichopus* tables with smaller discs, ranging from 32 to 42 ($\bar{x}$ = 39) µm across the disc in the 65 mm specimen, with one rounded central perforation and 2–9 peripheral holes, always arranged in one simple ring. Similar tables scarce in the largest specimen (L = 135 mm), most of the tables with disc completely reduced, 17–27 ($\bar{x}$ = 23) µm across and spires composed of four parallel pillars slightly or strongly constricted, 29–38 ($\bar{x}$ = 34) µm high; one crossbeam near the base, pillars ending in triplets of small spines forming an expanded crown (Figs 10E, 23A). Few perforated plates, located in the papilla tip, with few large perforations, larger in the center of the plate, ranging from 82 to 127 µm across; Clark (1922) used the term "end plates" to describe these dorsal perforated plates. Slightly or strongly curved rods, usually with quadrangular projections in the central area, sometimes perforated, 41 to 289 µm long, increasing gradually in size during growth.

Dorsal body wall with tables and rare C-shaped and S-shaped rods (Figs 10E, 23A). Numerous smaller tables similar to those from the papillae, 33–50 µm ($\bar{x}$ = 40 µm) high and 23–103 µm ($\bar{x}$ = 45 µm) across disc in specimens less than 65 mm long (Fig. 10E); no tables with disc in the 135 mm specimen, disc usually completely reduced 14–19 ($\bar{x}$ = 17) µm across disc and 31–37 ($\bar{x}$ = 34) µm high (Fig. 10E).

Pedicels with tables, C-shaped rods, perforated plates, large and curved rods, and end plates (Fig. 23B). Numerous tables with one large central perforation, which appears as four symmetrical holes, with 4 to 12 outer smaller holes usually in a single ring, both in the 65 mm and 135 mm long specimens; no tables with reduced disc; tables 27–40 ($\bar{x}$ = 35) µm high and 30–55 ($\bar{x}$ = 42) µm across the disc in

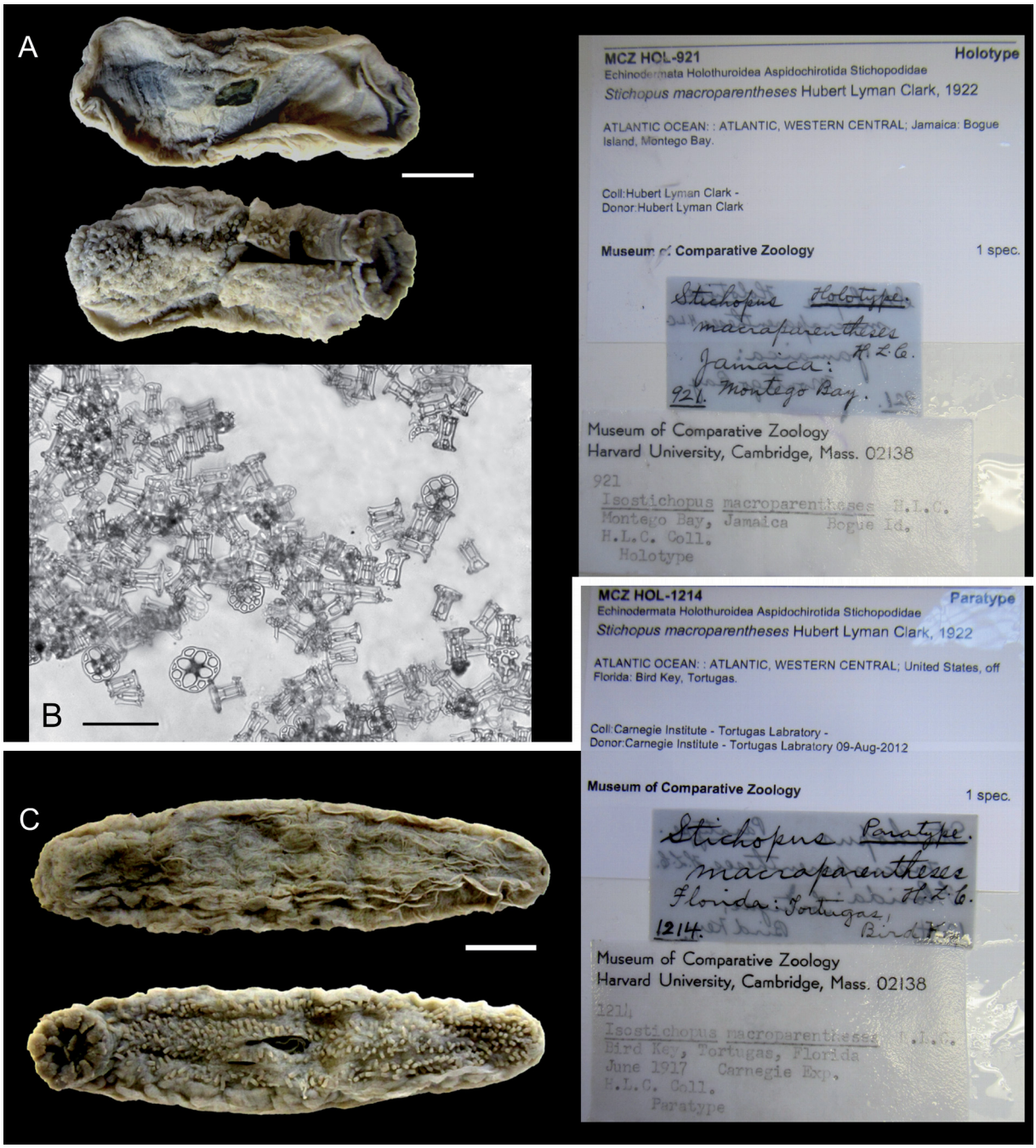

Fig. 22. Type specimens of *Isostichopus macroparentheses* (Clark, 1922). **A**. Dorsal and ventral view of the holotype from Bogue Island, Montego Bay, Jamaica (MCZ HOL-921, 50 mm long, contracted) and original labels. **B**. Holotype ossicles from dorsal papillae (slide MCZ HOL-225). **C**. Dorsal and ventral view of the paratype from Bird Key, Tortugas, Florida (MCZ HOL-1214, 65 mm long) and original labels. Photos by G. Borrero. Scale bars: A, C = 10 mm; B = 100 µm.

the 65 mm long specimen, and 22–32 ($\bar{x}$ = 27) μm high and 20–44 ($\bar{x}$ = 32) μm across the disc in the 135 mm specimen; numerous C-shaped ossicles, but not in all pedicels; C-shaped ossicles from the ventral surface much narrower, smaller than those from the dorsal side, as also mentioned by Clark (1922), 78 to 112 ($\bar{x}$ = 99) μm long in the 135 mm specimen, shorter than 165 μm reported by Clark in the type specimens. Numerous elongated perforated plates, with many perforations larger and elongated in the center of the plate 145–212 μm long in the 65 mm specimen and 228–284 μm long in the 135 mm specimen. Slightly curved rods with wide perforated expansions in the middle, 173–243 μm long in the 65 mm specimen and 268-323 μm long in the 135 mm specimen; end plate 489–569 μm across.

Ventral body wall with numerous tables similar to those from pedicels; C-shaped ossicles not present.

Tentacles with tables and rods (Fig. 23C). Few tables having smooth discs with four large central and symmetrical holes with 1 to 3 peripheral holes in the 65 mm specimen (31–41 μm across disc) and 0 to 12, mostly 4 in the 135 mm specimen (38–51 μm across disc). Spire low, composed of four incomplete pillars that usually are not joined at the top; without crossbeams connecting adjacent pillars. Numerous strongly or slightly curved spiny rods of different sizes ranging from 64 to 839 μm, increasing gradually with body size.

Mouth membrane with tables, C-shaped rods and simple rods (Fig. 11E); tables larger than those from dorsal and ventral sides, having spinous discs with one large central perforation, which appears as four symmetrical holes usually with 4 to 7 peripheral holes, not forming a complete ring in the 65 mm specimen (46–82 μm high, 62–101 μm across the disc) and with one or two rings of 4 to 14 perforations in the first and 2 to 8 perforations in the second ring in the 135 mm specimen (50–97 μm high, 43–108 μm across the disc); spires low, with four incomplete pillars not joined at the top, or composed of a variable number of pillars that are joined in a slender reticulate spire, cross beams not distinguishable; numerous C-shaped ossicles 37–71 μm long in the 65 mm specimen and 33–89 μm long in the 135 mm specimen; numerous small rods 54–108 μm long in the 65 mm specimen and 35–71 μm long in the 135 mm specimen.

Longitudinal muscles with small rods 33–63 μm long; few tables 35–38 μm high and 29–38 μm across the disc in the 135 mm specimen (Fig. 23D). Posterior cloaca with numerous C-shaped ossicles 54–93 μm long in the 65 mm specimen and 61–89 μm long in the 135 mm specimen (Fig. 23E). Anterior cloaca in the 135 mm specimen with spinous simple or bifurcated rods 78–112 μm long; large tridimensional spheres 141–195 μm across and tables similar to those of the dorsal papillae and body wall 25–30 μm high and 15–32 μm across the disc (Fig. 11E); muscle ossicles not found in the 65 mm specimen. Respiratory trees with strongly spinous straight or cross-shaped rods 178–283 μm long in the 65 and the 135 mm long specimens; large tridimensional spheres 157–250 μm across in the 135 mm long specimen (Fig. 23F); one table with a reduced disc (30 μm high, 18 μm across disc) in the 65 mm specimen. Intestine with spinose or smooth deposits in a cross shape, sometimes with bifurcated ends 51–71 μm long in the holotype, 31–43 μm in the paratype and 53-114 μm in the 135 mm long specimen (Fig. 23G). Gonads with delicate and large rods 102–233 μm long in the holotype (Fig. 11E); gonads not found in the paratype or in the 135 mm specimen.

Distribution

Thus far, *I. microparentheses* is only known from the Gulf of Mexico and the Caribbean Sea, in few disjunct localities shown in Fig. 5B, including Bird Key, Florida Keys; Veracruz and Quintana Roo, Mexico; Carrie Bow Cay and Tobacco Cay, Belize; English Harbor, Antigua Island; Guana island, British Virgin Islands; St. Croix, US Virgin Islands; Bogue Island, Jamaica and Curaçao. The record from Sarasota, West Florida is from a juvenile (15 mm total length), which was not confirmed as

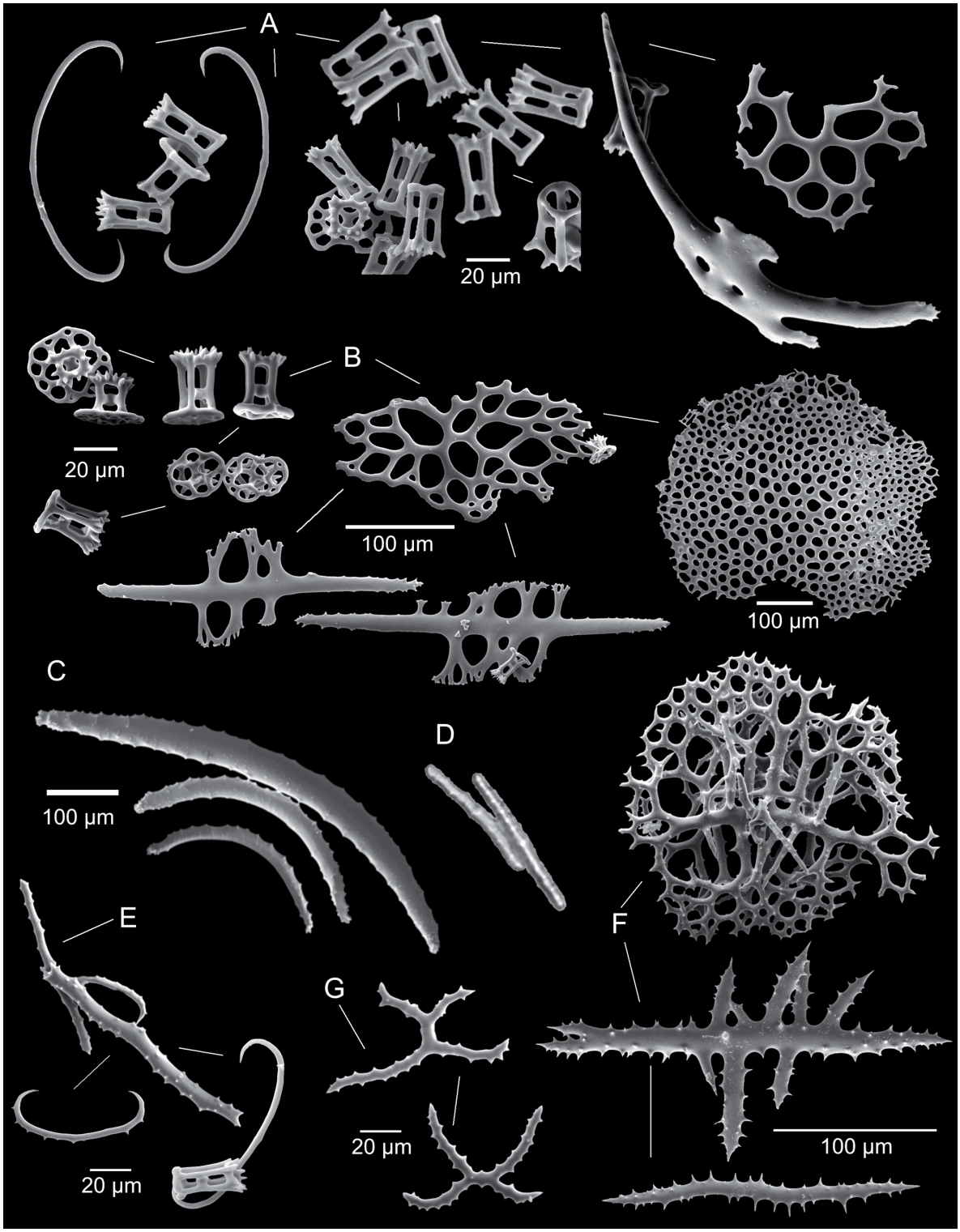

Fig. 23. *Isostichopus macroparentheses* (Clark, 1922), ossicles (specimen USNM E47524, 135 mm long). **A**. Thin C-shaped rods, tables, perforated plates, and large rods from the dorsal body wall and papillae. **B**. Tables, perforated plates, large rods and end plate from the ventral body wall and tube feet. **C**. Rods from tentacles. **D**. Rods from longitudinal muscles. **E**. Rods and C-shaped rods from the cloaca. **F**. Tridimensional sphere and straight rods from respiratory trees. **G**. Cross-shaped ossicles from intestine. Photos by G. Borrero.

Fig. 24. Color patterns and morphological variation of *Isostichopus macroparentheses* (Clark, 1922) (DNA sequences and detailed information of some specimens are indicated in Table 1, see Photo ID column for correspondence). **A–B**. Dorsal and ventral view of juvenile USNM 1659484-Be99 from Belize. **C–D**. Dorsal and ventral view of juvenile USNM 1659485-Be107 from Belize. **E**. Dorsal view of juvenile UF 20352 from Curaçao. **F**. Dorsal and ventral view of preserved specimens from British Virgin Islands (USNM E47524). **G**. Dorsal and ventral view of preserved specimens from US Virgin Islands (USNM E40833). **H**. Dorsal view of preserved specimen from English Harbor, Antigua Island (USNM E4391). **I**. Lateral view of preserved specimen from Carrie Bow Cay, Belize (USNM E18627). **J–K**. Dorsal and ventral view of specimen from Mexico. Photos: A–D, F–I by G. Borrero; J–K by F. Solís-Marín; E by Florida Museum of Natural History Data Collection. Scale bars: F = 20 mm; G = 10 mm; H–I = 1 mm each line.

I. macroparentheses (USNM E10473). We only collected this species in Belize. Bathymetric distribution 0.5 to 18 m. The unconfirmed juvenile USNM E10473 was collected at 48 m depth.

Habitat

Unlike the other species and subspecies of the genus, *I. macroparentheses* is not common or abundant, and most of the collected specimens are juveniles. There is little information about the habitat of the species. According to the collection data and literature references, juveniles and adults of this species live under or among rocks in the back reef, reef crest, and fore reef (Clark 1922, 1933; Deichmann 1930; Pawson 1976). According to Deichmann (1930) and Clark (1933) some specimens collected in Antigua were found on sand among eel-grass.

Remarks

Clark (1922) described this species from two juvenile specimens (holotype L = 50 mm, contracted; paratype L = 65 mm). The species was also reviewed by Deichmann (1930), who amended its diagnostic characters. However, due to changes during growth and the natural variability of ossicles, doubts about its validity as a separate species arose. Deichmann (1957) considered *S. macroparentheses* a synonym of *S. badionotus*, proposing that specimens with large C-shaped ossicles were juveniles of *S. badionotus*. Pawson (1976), however, argued that the difference between the C-shaped ossicles between the species is "dramatic, particularly when one compares juveniles of *I. macroparentheses* with *I. badionotus*". However, Miller & Pawson (1984), Cutress (1996) and Pawson *et al.* (2010), accepted the species as a synonym of *I. badionotus*. Laguarda-Figueras *et al.* (2005) and Alvarado & Solís-Marín (2013) have considered *I. macroparentheses* as a valid species in taxonomic lists. Prior to the present study there has been no detailed review setting the differences of *I. macroparentheses* from *I. badionotus*. Furthermore, adult specimens of *I. macroparentheses* had not been examined, so the characteristics of the species were based only on the two small specimens designated as types by Clark (1922). We conclude that *I. macroparentheses* is the species of *Isostichopus* that is best differentiated from the others. It exhibits several diagnostic characteristics, among which those related to the ossicles stand out, i.e. the size of the C-shaped ossicles, the disc tables in dorsal papillae and body wall, and the three-dimensional spheres and straight/spiky rods in the respiratory tree.

Cutress (1996) found that one adult specimen of *I. badionotus* (196 mm long) had few C-shaped ossicles longer than 100 μm in the dorsal median body wall. She concluded that the large size of C-shaped ossicles described in *I. macroparentheses* fell within the range of variation of *I. badionotus*, accepting *I. macroparentheses* as a synonym of *I. badionotus*. However, the average size of C-shaped ossicles in the dorsal side of this *I. badionotus* specimen was 74 μm (range 52 to 124 μm) and 71 μm (48 to 90 μm) in the ventral side; while these ossicles in dorsal papillae of *I. macroparentheses* are 91–142 μm ($\bar{x}$ = 113 μm) long, and in pedicels 78 to 112 μm ($\bar{x}$ = 99 μm) long, clearly larger than that of the other *Isostichopus* (Fig. 9A).

Examination of dorsal papillae in four 20–135 mm long specimens (and several that were not measured) of *I. macroparetheses*, showed that this species displays pronounced changes during growth in table height, disc diameter and number of holes in table discs The disc of the tables from dorsal papillae presented in Fig. 10E (USNM 1669484, MCZ HOL-1214), and drawn by Clark (1922: pl. 1 figs 1–2) and described as diagnostic by Deichmann (1957), can be useful to distinguish juveniles or specimens of intermediate sizes (holotype and paratype) from other species. These structures, however, can be scarce in some individuals, and disc of tables with more holes can be more abundant. In larger specimens (L = 135 mm), the table discs are completely reduced. Ossicles are less abundant in the largest specimens than in middle sized specimens. C-shaped ossicle size does not change during growth.

Biology

There is no information available on population status and ecology.

Conservation status

Currently *Isostichopus macroparentheses* is included in the IUCN Red List of Threatened Species in the category of "Data Deficient". "There is little to no information available on the population status, habitat, ecology, major threats, or conservation measures occurring to this species" (Samyn 2013).

Key to the species of the genus Isostichopus Deichmann, 1958

1. C-shaped ossicles >90 µm on average and 2–3 times as long as the tables are high; disc tables in dorsal papillae and body wall completely reduced in adults (Figs 2C, 10E, 23A); tridimensional spheres and straight/spiky rods in the respiratory trees (Fig. 23F); color not variable, dorsal side light yellow-brown in background, with irregularly arranged blurred large and small darker brown spots (Fig. 24); distributed in the Gulf of Mexico and Caribbean Sea, confirmed in few localities (Fig. 5B), not a common species ..... ***I. macroparentheses*** (Clark, 1922)
– C-shaped ossicles <90 µm on average; disc tables in dorsal papillae and body wall with complete ring of holes, not reduced in adults; color highly variable; common and abundant species 2

2. Table ossicles from top of the dorsal papillae in two shapes (Figs 10C, 13A), large, regular *Isostichopus* tables 58–86 µm (average = 71 µm) (Fig. 2B) and modified "*maculatus*" tables 60–108 µm (average = 86 µm) (Fig. 2D); whitish spot-like granules on the skin (Figs 1, 14); distributed in the Mid and East Atlantic (Fig. 5A) ..... ***I. maculatus maculatus*** (Greeff, 1882)
– Table ossicles from top of the dorsal papillae only regular *Isostichopus* tables 29–70 µm (average = 47 µm) 3

3. Large wart-like dorsal papillae (Figs 19, 21); table ossicles from top of the dorsal papillae only regular *Isostichopus* tables squarer than narrow in profile (Figs 10D, 20A); large tables with a circular spire well developed in the cloaca (Figs 11D, 19C, 20F); distributed in the East Pacific Ocean (Fig. 5B) ..... ***I. fuscus*** (Ludwig, 1875)
– Dorsal papillae variable in size and shape; table ossicles from top of the dorsal papillae only regular *Isostichopus* tables square or narrow in profile; distributed in the West Atlantic Ocean 4

4. Semi-translucent and rugose body wall; spiral lines in dorsal and lateral papillae (Figs 1, 17); worm-like rod ossicles in dorsal papillae (Figs 15B, 16A); calcareous ring with dorsal radial plates with short posterior projections (Fig. 4B) in large specimens (L = 185 mm); adult specimens living hidden during day associated with live corals, sponges, rubble, and rocks, exposed for only short time (Fig. 18) ..... ***I. maculatus phoenius*** (Clark, 1922)
– Opaque and smooth body wall; no spiral lines in dorsal and lateral papillae (Figs 1, 8); no worm-like rod ossicles in dorsal papillae (Fig. 7A); calcareous ring with dorsal radial plates with long posterior projections turned inwards (Fig. 4A) in larger individuals (L = 160–235 mm); adult specimens living exposed on muddy, sandy, rocky substrates, seagrass beds and mixed bottoms (Fig. 8) ..... ***I. badionotus*** (Selenka, 1867)

Discussion

Concern about the state of the stocks of sea cucumbers worldwide has motivated several initiatives aimed to improve understanding of this resource and its fishing industry and to provide technical information for conservation and sustainable exploitation (Samyn 2000; Lovatelli *et al.* 2004; Bruckner 2006; Toral-Granda 2008a, 2008b; Toral-Granda *et al.* 2008; Purcell 2010; Purcell *et al.* 2012). In the Caribbean Sea, increasing economic importance and growing concern about the overexploitation of sea cucumbers

has generated efforts in several countries to characterize natural populations for fishery management and to farm in aquiculture some valuable species, such as *Isostichopus*. As a result, new and useful information has been generated, but taxonomic confusion has also arisen. Here, based on evidence from mitochondrial DNA, morphology, habitat preference, and distribution have concluded that the genus *Isostichopus* includes four species: *I. badionotus*, *I. macroparentheses*, *I. fuscus* and *I. maculatus*; the last one with the subspecies *I. maculatus maculatus* and *I. maculatus phoenius*.

Barcoding, based on the mitochondrial COI gene, has proven useful in species delimitation and discovery of echinoderms, especially sea cucumbers (Uthicke *et al.* 2010; Byrne *et al.* 2010; Michonneau 2015; Borrero-Pérez & Vanegas-González 2019). It has aided in the present work to distinguish cryptic species, and it has clarified the taxonomic status of *I. badionotus*, providing a reference for adding new evidence, such as habitat and distribution, as indicative of species limits. It has also formed the basis of evaluating external and internal morphology and coloration patterns to support the Operational Taxonomic Units recovered by molecular evidence. Most of the characters reviewed here were previously considered by Clark (1922); however, without molecular evidence it would have been almost impossible to clarify patterns of variation in coloration and external morphology of the species of *Isostichopus*, or to define differences among the species in ossicles that change during growth. Traditionally, sea cucumber taxonomy is based on the shape and size of ossicles. However, several cases have been reported where focusing on ossicle shape to distinguish species has led to an underestimation of diversity (Michonneau 2015). We now know that in *Isostichopus* ossicles may be diagnostic in some species, but external morphology (especially coloration patterns), habitat and distribution are the most useful characteristics for identification. This evidence will result in easier and correct species identifications, and thus will be a useful tool for the characterization of natural populations, fishery management and aquaculture.

No evidence was found to support the presence of the genus *Stichopus* in the Caribbean Sea. The records of *S. herrmanni* and *S. variegatus* reported by Rodríguez-Forero *et al.* (2013), Agudelo & Rodríguez (2015) and Koike *et al.* (2015) are in reality records of *I. badionotus*. Records of *Stichopus* sp. by Agudelo & Rodríguez (2015) and Vergara & Rodríguez (2015) belong to *I. maculatus phoenius*. The *Stichopus* names of species in the Atlantic Ocean appearing in the literature before Deichmann (1958) erected the genus *Isostichopus* currently correspond to *Isostichopus*. *Stichopus ecnomius* Clark, 1922, listed as nomen dubium in WoRMS (2020), is a synomym of *Astichopus multifidus* (Sluiter, 1910). We agree wtih Cutress (1996) after examining the type of *A. multifidus* (MCZ HOL-890), a juvenile 6 mm long, with aberant tables as described by Cutress (1996: 103, fig. 36).

Coloration is considered diagnostic of species in many invertebrates and fish (Knowlton 1993; McMillan *et al*. 1999; Malay & Paulay 2010), including echinoderms. A cryptic species of the "*Holothuria hilla*" complex was discovered, with color as the best diagnostic character (Borrero-Pérez & Vanegas-González 2019). However, all of the species and subspecies of *Isostichopus*, except *I. macroparentheses*, are highly variable in color. All color variants can be present sympatrically, e.g., in Bocas del Toro in Panama, where all color forms of *I. badionotus* and *I. maculatus phoenius* are common. However, only one-color pattern of *I. badionotus* was present or predominant at other localities, such as La Guajira in Colombia (G.H. Borrero-Pérez pers. obs.), or Bermuda (Clark 1942). We found a slight genetic differentiation in mtDNA between most (but not all) individuals of Chips-Uniform color patterns and individuals of Reticulated-Black and Yellow color patterns of *I. badionotus*. We found different habitat preferences between these two groups. These differences suggest that there may be non-random mating, the first step in speciation. Additional genetic, geographic, and habitat data on coloration patterns are needed to determine the significance of this variation. Genetic variation between color variants was reported in *Apostichopus japonicus*, in which microsatellite analysis indicated that they were reproductively isolated (Kanno & Kijima 2003; Kanno *et al.* 2006).

Clark (1942) noted that pigmentation in echinoderms deserves careful and exhaustive study. The subject remains poorly explored, especially with regard to the function of color in sea cucumbers. It is possible that species-specific color patterns may be determined by natural selection (Michonneau 2015). As sea cucumbers cannot see, the mechanisms of assortative mating by color need to be investigated. The association of color patterns with habitat could result in assortative mating that promotes pre-zygotic reproductive barriers. Gamete recognition proteins, such as the protein molecule bindin, as yet unreported in sea cucumbers but found in sea urchins and sea stars (Zigler & Lessios 2003; Lessios 2007, 2011; Zigler *et al.* 2012; Sunday & Hart 2013; Popovic *et al.* 2014) could play a role. Such isolation could apply to the sympatric species *I. badionotus* and *I. maculatus phoenius*, given the evidence that both show a reproductive season from September to November (Acosta *et al.* 2021).

Although species differentiation based on ossicles is not easy in *Isostichopus*, it is not impossible. Many misidentifications of sea cucumbers stem from a lack of examination of ossicles, as confusion between genera or species with completely different ossicles exist. This is the case of confounding *Stichopus* and *Isostichopus*, which currently are easy to recognize based on the presence of rosettes in *Stichopus* (Deichmann 1958; Purcell *et al.* 2012). The use of ossicles for species identification is rather simple, and a good option when molecular analyses are lacking (Toral-Granda 2006; McNab & Rogers 2017). Ossicles are a valuable character for distinguishing the most common harvested species in the Caribbean Sea, such as the species of *Isostichopus*, *Astichopus multifidus*, *Holothuria mexicana*, *H. thomasi* Pawson & Caycedo, 1980, and *Actinopyga agassizii* (Selenka, 1867) (Borrero-Pérez *et al.* 2012; Purcell *et al.* 2012; McNab & Rogers 2017). Characterization of ossicles should take into account the variability within and between individuals and the location of the ossicles in the body of each specimen. The present paper provides a guide for the morphological characterization of species of *Isostichopus*. Ossicles should be the second character to examine in live animals after external morphology and color patterns.

All branches of biology, including conservation, need correct taxonomy. In this study, we tried to follow the best practices for species identification/documentation, as discussed by Tsang *et al.* (2018). These include the use of a broad range of morphological, genetic, and ecological data to reach conclusions about species delimitation and to help with species identifications. We hope that this detailed revision will be useful for biologists, and raise awareness about the implications of incorrect identification, especially in commercially important groups.

Acknowledgments

This work would not have been possible without the help of many colleagues, researchers, curators and collection managers from different institutions, and help during field trips, collection of specimens, information, photos, DNA sequences, as well as administrative and logistic support. We thank specially E. Montoya, A. Merchán, M. Martelo, A. Fernández, J. Vanegas, N. Rincón, K. Mejía, L. Chasqui, D. Alonso (BEM – Invemar, Colombia); M. Santos, J. Gómez, G. Ospina, E. Acosta, E. Ortíz (VAR – Invemar); F. Arias (DGI – Invemar); A. Calderón, L. Rivera, L. Geyer, A. Hiller (STRI, Panama); A. Castillo, E. Petrou, I. Pedroarena-Leal, P. Gondola (Bocas del Toro Research Station, STRI); J. Ceballos (SEM images, STRI); L. Camacho, J. Maté (Scientific Permit Office, STRI), Z. Foltz (Carrie Bow Marine Field Station, Belize), C. Vergara-Chen (Universidad Tecnológica de Panama, Panama), M. González-Wangüemert (CUMFISH Project, Cod. PTDC/MAR/119363/ 2010, CCMAR, Portugal); R. Haroun (Universidad de las Palmas de Gran Canaria, España); N. Ardila, D. Báez (Ecomares, Colombia); S. Zea (Unal, Colombia); J.F. Lazarus (UniValle, Colombia); C. Sánchez (Universidad Autónoma de Baja California Sur, Mexico); C. Walter, K. Ahlfeld, J. Norenburg, C. Meyer (National Museum of Natural History-NMNH, Smithsonian, USA); P. Benson, A. Baldinger (Museum of Comparative Zoology-MCZ, USA); A. Cabrinovic, N. Santodomingo (Natural History Museum London, UK); Colección Nacional de Equinodermos-CNE, UNAM; M. González-Wangüemert and P. Antón (16S and COI-Fr1 sequences obtained through the Project "Improved understanding of the Sea cucumber fisheries situation

in Liberia", Cod. TCP/LIR/3801/C1 2021, FAO Representation in Liberia); Gustav Paulay (COI-Fr1 sequences obtained in the Florida Museum of Natural History, USA); N. Vasco-Rodrigues (MARE IP Leiria); T. Collison (Blue Ventures) and P. Wirtz. Financial support for this project was provided by L'Oréal-UNESCO International Fellowships for Young Women in Life Sciences – 2012 (GHBP), General Research funds from STRI, and Invemar through the projects "Caracterización Biótica de los Arrecifes Rocosos (Riscales y Morros) en el Chocó Norte, Pacífico Colombiano 2016–2018" and "Obtención del código de barras del ADN (Barcoding) para los grupos de fauna y flora marinos– 2016, 2017" (Code BPIN: 2014011000405 and 2017011000113), and "Elementos técnicos y generación de capacidad para el ordenamiento, conservación y manejo de los espacios y recursos marinos, costeros e insulares de Colombia. Code: Act-VAR-001-013. 4. Caracterizar poblaciones de pepinos de mar" (Convenio Interadministrativo 57 MADS – Invemar). This is the contribution of INVEMAR No. 1376.

References

Acosta E.J., Rodríguez-Forero A., Werding B. & Kunzmann A. 2020. Effect of density, temperature and diet on the growth, survival and development of larvae and juveniles of *Isostichopus* sp. *Aquaculture Research* 52: 611–624. https://doi.org/10.1111/are.14918

Acosta E.J., Rodríguez-Forero A., Werding B. & Kunzmann A. 2021. Ecological and reproductive characteristics of holothuroids *Isostichopus badionotus* and *Isostichopus* sp. in Colombia. *PLoS ONE* 16 (2): e0247158. https://doi.org/10.1371/journal.pone.0247158

Agudelo V. & Rodríguez A. 2015. Advances on spontaneous captive breeding and culture conditions of Caribbean Sea cucumber *Stichopus* sp. *SPC Beche-de-mer Information Bulletin* 35: 50–57.

Agudelo-Martínez V. & Rodríguez-Forero A. 2017. Gametogenesis, spawning and larval development of *Isostichopus* sp. aff *badionotus*. *SPC Beche-de-mer Information Bulletin* 37: 65–74.

Aguilar F., Revelo W., Chicaiza D., Mendívez W. & Hill D. 2011. Estado poblacional del pepino de mar *Isostichopus fuscus* (Ludwig, 1875) en la provincia de Santa Elena y Sur de Manabí. *Revista de Ciencia del Mar y Limnología* 5 (1): 1–10.

Aguilar F., Revelo W., Chicaiza D., Mendívez W. & Hill1 D. 2013. Distribución y densidad poblacional del pepino de mar *Isostichopus fuscus* (Ludwig, 1875) en la provincia de Santa Elena y sur de Manabí. *Boletín Científico y Técnico* 23 (1): 73–98.

Alfonso I. 2006. Report on the conservation of sea cucumbers in the families Holothuridae and Sticopodidae in Cuba. *In*: Bruckner A.W. (ed.) *Proceedings of the CITES Workshop on the Conservation of Sea Cucumbers in the Families Holothuriidae and Stichopodidae*: 141–144. NOAA Technical Memorandum NMFSOPR 34, Silver Spring, USA.

Alfonso I., Frías M.P., Aleaga L. & Alonso C.R. 2004. Current status of the sea cucumber fishery in the south eastern region of Cuba. *In*: Lovatelli A., Conand C., Purcell S., Uthicke S., Hamel J-F. & Mercier A. (eds) *Advances in Sea Cucumber Aquaculture and Management*: 151–159. Food and Agriculture Organization (FAO), Rome.

Alfonso I., Frías M.P., Castelo R. & Blás Y. 2008. Situación de la pesquería del pepino de mar *Isostichopus badionotus* al norte de la Isla de la Juventud, Cuba. *Revista Cubana de Investigaciones Pesqueras* 25 (1): 20–26.

Alvarado J.J. & Solís-Marín F.A. (eds) 2013. *Echinoderm Research and Diversity in Latin America*. Springer, Berlin. https://doi.org/10.1007/978-3-642-20051-9

Ancona Lopez A.A. 1957. Sobre holoturias do litoral sul Brasileiro. *Boletim da Faculdade de Filosofia Ciencias e Letras Universidade de São Paulo Serie Zoologia* 21: 1–50.

Arias-Hernández O., Alcendra-Pabón E., Carreño-Montoya O.J., Cabrera-Durán E., Corvacho-Narváez R.O. & Rodríguez-Forero A. 2017. Sea cucumber (*Isostichopus* sp. aff. *badionotus*) dry-salting protocol design. *Natural Resources* 8: 278–289. https://doi.org/10.4236/nr.2017.83016

Bell F.J. 1883. Studies on the Holothuroidea. II. Descriptions of new species. *Proceedings of the Zoological Society of London* 51 (1): 58–69. https://doi.org/10.1111/j.1469-7998.1883.tb06643.x

Bell J.D., Purcell S.W. & Nash W.J. 2008. Restoring small-scale fisheries for tropical sea cucumbers. *Ocean & Coastal Management* 51: 589–593. https://doi.org/10.1016/j.ocecoaman.2008.06.011

Borrero-Pérez G.H. & Vanegas-González M.J. 2019. *Holothuria (Mertensiothuria) viridiaurantia* sp. nov. (Holothuriida, Holothuriidae), a new sea cucumber from the Eastern Pacific Ocean revealed by morphology and DNA barcoding. *ZooKeys* 893: 1–19. https://doi.org/10.3897/zookeys.893.36013

Borrero-Pérez G.H. & Vanegas-González M.J. 2022. *Isostichopus fuscus*. *In*: Chasqui V.L., Alvarado-Chacón E.M., Ardila N., Borrero-Pérez G.H., Campos N.H. & Mejía-Quintero K. (eds) *Libro Rojo de Invertebrados marinos de Colombia*: 329–334. Serie de publicaciones generales de INVEMAR No. 122, Instituto de Investigaciones Marinas y Costeras INVEMAR, Ministerio de Ambiente y Desarrollo Sostenible. Santa Marta, Colombia.

Borrero-Pérez G.H., Santos-Acevedo M. & Ortiz-Gómez E. 2006. Perspectives and present situation of sea cucumber fisheries in the Colombian Caribbean Sea. *In*: Harris L.G., Böttger S.A., Walker C.W. & Lesser M.P. (eds) *Echinoderms: Durham. Proceedings of the 12th International Echinoderm Conference*: 588. Durham, NH.

Borrero-Pérez G.H., Benavides-Serrato M. & Díaz-Sanchez C.M. 2012. *Equinodermos del Caribe colombiano II: Echinoidea y Holothuroidea*. Serie de Publicaciones Especiales 30, Instituto de Investigaciones Marinas y Costeras, Santa Marta.

Borrero-Pérez G.H., Reyes-Sánchez F., López-Navarro J., Ortiz-Gómez E. 2022. *Isostichopus badionotus*. *In*: Chasqui V., Alvarado-Chacón E.M., Ardila N., Borrero-Pérez G.H., Campos N.H. & Mejía-Quintero K. (eds) *Libro Rojo de Invertebrados Marinos de Colombia*: 180–186. Instituto de Investigaciones Marinas y Costeras INVEMAR, Ministerio de Ambiente y Desarrollo Sostenible, Serie de publicaciones generales de INVEMAR No. 122. Santa Marta, Colombia.

Bruckner A.W. (ed.) 2006. *Proceedings of the CITES Workshop on the Conservation of Sea Cucumbers in the Families Holothuriidae and Stichopodidae.* NOAA Technical Memorandum NMFSOPR 34, Silver Spring, USA.

Bruckner A.W., Johnson K.A. & Field J.D. 2003. Conservation strategies for sea cucumbers: can a CITES Appendix II listing promote international trade? *SPC Beche-de-mer Information Bulletin* 18: 24–33.

Byrne M., Rowe F. & Uthicke S. 2010. Molecular taxonomy, phylogeny and evolution in the family Stichopodidae (Aspidochirotida: Holothuroidea) based on COI and 16S mitochondrial DNA. *Molecular Phylogenetics and Evolution* 56: 1068–1081. https://doi.org/10.1016/j.ympev.2010.04.013

Caycedo I.E. 1978. Holothuroidea (Echinodermata) de aguas someras en la Costa Norte de Colombia. *Anales del Instituto de Investigaciones Marinas de Punta Betín* 10: 149–198. https://doi.org/10.25268/bimc.invemar.1978.10.0.512

Cherbonnier G. 1975. Note sur la présence, dans le golfe de Guinée de l'holothurie Aspidochirota *Stichopus badionotus* Selenka (= *S. maculatus* Greeff). *Bulletin du Muséum national d'Histoire naturelle, 3e sér., nº 300, Zoologie* 210: 603–630.

Clark H.L. 1899. Further notes on the Echinoderms of Bermuda. *Annals of the New York Academy of Sciences* 12: 117–138. https://doi.org/10.1111/j.1749-6632.1899.tb54988.x

Clark H.L. 1910. The echinoderms of Peru. *Bulletin of the Museum of Comparative Zoology at Harvard College* 52: 321–358. https://doi.org/10.5962/bhl.title.24250

Clark H.L. 1922. The holothurians of the genus *Stichopus*. *Bulletin of the Museum of Comparative Zoology at Harvard College* 65 (3): 39–74.
Available from https://www.biodiversitylibrary.org/page/4774250 [accessed 16 Apr. 2024].

Clark H.L. 1933. A handbook of the littoral echinoderms of Porto Rico and the other West Indian Islands. *Scientific Survey of Porto Rico and the Virgin Islands* 16 (1): 1–147.

Clark H.L. 1942. The echinoderm fauna of Bermuda. *Bulletin of the Museum of Comparative Zoology at Harvard College* 89: 367–391. Available from https://www.biodiversitylibrary.org/page/2792395 [accessed 16 Apr. 2024].

Conand C. 2006. Sea cucumber biology, taxonomy, distribution and conservation status. *In*: Bruckner A.W (ed.) *Proceedings of the CITES Workshop on the Conservation of Sea Cucumbers in the Families Holothuriidae and Stichopodidae*: 33–50. NOAA Technical Memorandum NMFSOPR 34, Silver Spring, USA.

Crozier W.J. 1918. The amount of bottom material ingested by holothurians (*Stichopus*). *Journal of Experimental Zoölogy* 26 (2): 379–389. https://doi.org/10.1002/jez.1400260207

Cutress B.M. 1996. Changes in dermal ossicles during somatic growth in Caribbean littoral sea cucumbers (Echinodermata: Holothuroidea: Aspidochirotida). *Bulletin of Marine Science* 58 (1): 44–116.

Deichmann E. 1926. Report on the holothurians collected by the Barbados-Antigua Expedition of the University of Iowa. *University of Iowa Studies in Natural History* 11: 9–31.

Deichmann E. 1930. The holothurians of the western part of the Atlantic Ocean. *Bulletin of the Museum of Comparative Zoology at Harvard College* 71 (3): 43–226.
Available from https://www.biodiversitylibrary.org/page/2798795 [accessed 14 Apr. 2024].

Deichmann E. 1937. 10. The Templeton Crocker Expedition. IX. Holothurians from the Gulf of California, the west coast of Lower California and Clarion Island. *Zoologica: scientific contributions of the New York Zoological Society* 22 (2): 161–176. https://doi.org/10.5962/p.184685

Deichmann E. 1938. 18. Eastern Pacific Expeditions of the New York Zoological Society. XVI. Holothurians from the western coasts of Lower California and Central America, and from Galapagos Islands. *Zoologica: Scientific Contributions of the New York Zoological Society* 23 (18): 361–387.
https://doi.org/10.5962/p.184698

Deichmann E. 1940. Report on the holothurians, collected by the Harvard-Havana expeditions 1938 and 1939, with a revision of the molpadonia of the Atlantic Ocean. *Memorias de la Sociedad Cubana de Historia Natural* 14 (3): 183–240.

Deichmann E. 1954. The holothurians of the Gulf of México. *U.S. Fish and Wildlife Service Fishery Bulletin* 55: 381–409.

Deichmann E. 1957. The littoral holothurians of the Bahama Islands. *American Museum Novitates* 1821: 1–20. Available from https://www.biodiversitylibrary.org/page/63294879 [accessed 16 Apr. 2024].

Deichmann E. 1958. The Holothuroidea collected by the VELERO III and IV during the years 1932 to 1954. Part II. Apsidochirota. *Allan Hancock Pacific Expeditions* 11(2): 253–349.
Available from https://www.biodiversitylibrary.org/page/5215760 [accessed 16 Apr. 2024].

Deichmann E. 1963. Shallow water holothurians known from the Caribbean waters. *Studies on the Fauna of Curaçao and other Caribbean islands* 63: 100–118.
Available from https://repository.naturalis.nl/pub/506106 [accessed 16 Apr. 2024].

Entrambasaguas L. 2008. *Estudio Faunístico y Ecológico de los Equinodermos del Archipiélago de Cabo Verde*. PhD Thesis, Universidad de Murcia, España.

Entrambasaguas L., Pérez-Ruzafa A., García Charton J.A., Stobart B. & Bacallado J.J. 2008. Abundance, spatial distribution and habitat relationships of echinoderms in the Cabo Verde Archipelago (eastern Atlantic). *Marine and Freshwater Research* 59 (6): 477–488. https://doi.org/10.1071/MF07109

Fajardo-León M., Michel-Guerrero E., Singh-Cabanillas J., Vélez-Barajas J. & Massó-Rojas A. 1995. Estructura poblacional y ciclo reproductor del pepino de mar *Isostichopus fuscus* en Santa Rosalía, BCS, México. *Ciencia Pesquera* 11 (1): 45–53.

Fan S., Hu C., Wen J. & Zhang L. 2011. Characterization of mitochondrial genome of sea cucumber *Stichopus horrens*: a novel gene arrangement in Holothuroidea. *Science China. Life Sciences* 54 (5): 434–441. https://doi.org/10.1007/s11427-011-4168-8

Felaco L. & Olvera-Novoa M. 2017. Determining ideal stocking density for the cultivation of sea cucumber (*Isostichopus badionotus*) juveniles in integrated multitrophic aquaculture (IMTA). *Book of Abstracts Latin American & Caribbean Aquaculture 2017*: 86. Mazatlán, Mexico.

Foglietta L.M., Camejo M.I., Gallardo L. & Herrera F.C. 2004. A maturity index of holothurians exhibiting asynchronous development of gonad tubules. *Journal of Experimental Marine Biology and Ecology* 300: 19–30. https://doi.org/10.1016/j.jembe.2003.10.019

Fontalvo-Martínez A. & Rodríguez A. 2017. Evaluación del crecimiento de pepino de mar *Isostichopus* sp. aff *badionotus* bajo condiciones de luz/oscuridad y a diferentes temperaturas. *Book of Abstracts Latin American & Caribbean Aquaculture 2017*: 95. Mazatlán, Mexico.

Fuente-Betancourt M.G., Jesús-Navarrete A., Sosa-Cordero E. & Herrero-Pérezrul M.D. 2001. Assessment of the sea cucumber (Echinodermata: Holothuroidea) as potential fishery resource in Banco Chinchorro, Quintana Roo, Mexico. *Bulletin of Marine Science* 68 (1): 59–67.

FWC (Florida Fish and Wildlife Conservation Commission) 2014. Sea cucumber management changes take effect June 11 [http://myfwc.com/].
Available from http://myfwc.com/news/news-releases/2014/june/04/sea-cucumber/ [accessed 4 Jun. 2014].

Glockner A. 2014. *Ecología Poblacional y Pesquería del Pepino de Mar Isostichopus fuscus en Bahía de los Ángeles, Baja California, México.* MSc Thesis, Centro de Investigación Científica y de Educación Superior de Ensenada, Ensenada, Baja California, México.

Glockner-Fagetti A., Calderón-Aguilera L.E. & Herrero-Pérezrul M.D. 2016. Density decrease in an exploited population of brown sea cucumber *Isostichopus fuscus* in a biosphere reserve from the Baja California peninsula, Mexico. *Ocean & Coastal Management* 121: 49–59.
https://doi.org/10.1016/j.ocecoaman.2015.12.009

Gómez-Maduro M.C. & Hernández-Ávila I. 2011. Equinodermos de la bahía de Tunantal, Estado Sucre, Venezuela. *Boletín del Instituto Oceanográfico de Venezuela* 50 (2): 209–231.

Greeff R. 1882. Echinodermen, beobachtet auf einer Reise nach der Guinea-Insel São Tomé. *Zoologischer Anzeiger* 5: 114–120, 135–139, 156–159.
Available from https://www.biodiversitylibrary.org/page/9734185 [accessed 16 Apr. 2024].

Guzmán H.M. & Guevara C. 2002. Population structure, distribution and abundance of three commercial species of Sea Cucumber (Echinodermata) in Panama. *Caribbean Journal of Science* 38 (3–4): 230–238.
Available from https://repository.si.edu/handle/10088/1618 [accessed 16 Apr. 2024].

Guzmán H.M., Guevara C.A. & Hernández I.C. 2003. Reproductive cycle of two commercial species of sea cucumber (Echinodermata: Holothuroidea) from Caribbean Panamá. *Marine Biology* 142: 271–279.
https://doi.org/10.1007/s00227-002-0939-x

Hamel J., Ycaza-Hidalgo R. & Mercier A. 2003. Larval development and juvenile growth of the Galapagos sea cucumber *Isostichopus fuscus*. *SPC Beche-de-mer Information Bulletin* 18 (1):3–8.

Hamel J.F., Eeckhaut I. & Mercier A. 2017. New host for the parasitic worm *Anoplodium* sp. (Rhabditophora: Platyhelminthes) found in the sea cucumber *Isostichopus fuscus* (Holothuroidea: Echinodermata). *SPC Beche-de-mer Information Bulletin* 37: 75–78.

Hammond L.S. 1983. Nutrition of deposit-feeding holothuroids and echinoids (Echinodermata) from a shallow reef lagoon, Discovery Bay, Jamaica. *Marine Ecology Progress Series* 10:297–305. https://doi.org/10.3354/meps010297

Heilprin A. 1888. Contributions to the natural history of the Bermuda Islands. *Proceedings of the Academy of Natural Sciences of Philadelphia* 40: 302–328.
Available from https://www.biodiversitylibrary.org/page/1963690 [accessed 16 Apr. 2024].

Hendler G. & Pawson D.L. 2000. Echinoderms of the Rhomboidal cays, Belize: Biodiversity, distribution, and ecology. *Atoll Research Bulletin* 466–480: 275–302.
Available from https://repository.si.edu/handle/10088/33941 [accessed 16 Apr. 2024].

Hendler G., Miller J.E., Pawson D.L. & Kier P.M. 1995. *Echinoderms of Florida and the Caribbean. Sea Stars, Sea Urchins and Allies*. Smithsonian Institution Press, Washington.

Hernández-Flores A.D., Condal A., Poot-Salazar A. & Espinoza-Méndez J.C. 2015. Geostatistical analysis and spatial modeling of population density for the sea cucumbers *Isostichopus badionotus* and *Holothuria floridana* on the Yucatan Peninsula, Mexico. *Fisheries Research* 172: 114–124. https://doi.org/10.1016/j.fishres.2015.07.005

Hernández-Flores A., Cuevas-Jiménez A., Poot-Salazar A., Condal A. & Espinoza-Méndez J.C. 2018. Bioeconomic modeling for a small-scale sea cucumber fishery in Yucatan, Mexico. *PLoS ONE* 13 (1): e0190857. https://doi.org/10.1371/journal.pone.0190857

Herrero-Pérezrul M.D. 2004. *Análisis de la Pesquería de Pepino de Mar en la Península de Baja California, México*. PhD Thesis, Instituto Politécnico Nacional, La Paz, Baja California Sur, México.

Herrero-Pérezrul M.D. & Reyes-Bonilla H. 2008. Weight-length relationship and relative condition of the holothurian *Isostichopus fuscus* at Espíritu Santo Island, Gulf of California, México. *Revista de Biología Tropical* 56: 273–280.

Herrero-Pérezrul M.D., Reyes-Bonilla H. & García-Domínguez F. 1998. Casual hermaphroditism in gonochoric *Isostichopus fuscus* (Ludwig, 1875) (Echinodermata: Holothuroidea) of the southern Gulf of California, Mexico. *Bulletin of Marine Science* 63 (3): 611–615. https://doi.org/10.1007/s002270050653

Herrero-Pérezrul M.D., Reyes-Bonilla H., García-Domínguez F. & Cintra-Buenrostro C.E. 1999. Reproduction and growth of *Isostichopus fuscus* (Echinodermata: Holothuroidea) in the southern Gulf of California, México. *Marine Biology* 135: 521–532. https://doi.org/10.1007/s002270050653

Hickman C.P. 1998. *A Field Guide to Sea Stars and Other Echinoderms of Galapagos. Galapagos Marine Life Series*. Sugar Spring Press, Lexington, VA.

Hoareau T.B. & Boissin E. 2010. Design of phylum-specific hybrid primers for DNA barcoding: addressing the need for efficient COI amplification in the Echinodermata. *Molecular Ecology Resources* 10 (6): 960–967. https://doi.org/10.1111/j.1755-0998.2010.02848.x

Honey-Escandón M., Laguarda-Figueras A. & Solís-Marín F.A. 2012. Molecular phylogeny of the subgenus *Holothuria* (Selenkothuria) Deichmann, 1958 (Holothuroidea: Aspidochirotida). *Zoological Journal of the Linnean Society* 165 (1): 109–120. https://doi.org/10.1111/j.1096-3642.2011.00794.x

Hooker Y., Solís-Marín F.A. & Lleellish M. 2005. Equinodermos de las Islas Lobos de Afuera (Lambayeque, Perú). *Revista Peruana de Biología* 12 (1): 77–82.

ICZN 1999. *International Code of Zoological Nomenclature. Fourth Edition*. The International Trust for Zoological Nomenclature, London, UK. Available from https://www.iczn.org/the-code/the-code-online/ [accessed 16 Apr. 2024].

Invemar 2013. *Elementos técnicos y generación de capacidad para el ordenamiento y manejo de los espacios y recursos marinos, costeros e insulares de Colombia. Pepinos de mar.* Informe técnico final convenio MADS-Invemar 57, Santa Marta, Colombia.

Invemar 2014. *Elementos técnicos que permitan establecer medidas de manejo, control, uso sostenible y restauración de los ecosistemas costeros y marinos del país. Componente N° 4. Evaluar el estado de los recursos hidrobiológicos asociados a los ecosistemas marinos, costeros e insulares de Colombia: Caracterización de la población y uso del recurso pepino de mar en el departamento de Córdoba.* Informe técnico final convenio MADS-Invemar, Santa Marta, Colombia.

Invemar 2015. *Manejo para la conservación de los recursos hidrobiológicos, Actividad: Lineamientos para el manejo, uso y conservación del recurso pepino de mar de la Guajira y Córdoba con base a la información disponible (Componente 2)*. Informe Técnico Final MADS- Invemar 275, Santa Marta, Colombia.

Jesús-Navarrete A., May-Poot M.N. & Medina-Quej A. 2018. Density and population parameters of sea cucumber *Isostichopus badionotus* (Echinodermata: Stichopodidae) at Sisal, Yucatan. *Latin American Journal of Aquatic Research* 46 (2): 416–423. https://doi.org/10.3856/vol46-issue2-fulltext-17

Kanno M. & Kijima A. 2003. Genetic differentiation among three color variants of Japanese sea cucumber *Stichopus japonicus*. *Fisheries Science* 69: 806–812. https://doi.org/10.1046/j.1444-2906.2003.00690.x

Kanno M., Suyama Y., Li Q. & Kijima A. 2006. Microsatellite analysis of Japanese sea cucumber, *Stichopus* (*Apostichopus*) *japonicus*, supports reproductive isolation in color variants. *Marine Biotechnology* 8: 672–685. https://doi.org/10.1007/s10126-006-6014-8

Katoh K., Misawa K., Kuma K. & Miyata T. 2002. MAFFT: a novel method for rapid multiple sequence alignment based on fast Fourier transform (describes the FFT-NS-1, FFT-NS-2 and FFT-NS-i strategies). *Nucleic Acids Research* 30: 3059–3066. https://doi.org/10.1093/nar/gkf436

Kerr A.M., Janies D.A., Clouse R.M., Samyn Y., Kuszak J. & Kim J. 2005. Molecular phylogeny of coral-reef sea cucumbers (Holothuriidae: Aspidochirotida) based on 16S mitochondrial ribosomal DNA sequence. *Marine Biotechnology* 7 (1): 53–60. https://doi.org/10.1007/s10126-004-0019-y

Kimura M. 1980. A simple method for estimating evolutionary rates of base substitutions through comparative studies of nucleotide sequences. *Journal of Molecular Evolution* 16: 111–120. https://doi.org/10.1007/BF01731581

Knowlton N. 1993. Sibling species in the sea. *Annual Review of Ecology and Systematics* 24: 189–216. https://doi.org/10.1146/annurev.ecolsys.24.1.189

Koike H., Usseglio P. & Ramos F. 2015. Baseline assessment of virgin biomass of sea cucumbers in Old Providence and Santa Catalina, Western Caribbean. *SPC Beche-de-mer Information Bulletin* 35:42–49.

Kumar S., Stecher G. & Tamura K. 2016. MEGA7: Molecular Evolutionary Genetics Analysis version 7.0 for bigger datasets. *Molecular Biology and Evolution* 33 (7):1870–1874. https://doi.org/10.1093/molbev/msw054

Kumar S., Stecher G., Li M., Knyaz C. & Tamura K. 2018. MEGA X: Molecular Evolutionary Genetics Analysis across computing platforms. *Molecular Biology and Evolution* 35: 1547–1549. https://doi.org/10.1093/molbev/msy096

Lacerda-Miceli M.L. & Scott P.C. 2005. Estimativa preliminar do estoque da holotúria *Isostichopus badionotus* no entorno da Ilha Grande, RJ apoiado em Sistemas de Informação Geográfica e Sensoriamento Remoto. *Anais XII Simpósio Brasileiro de Sensoriamento Remoto*: 3659–3665. Goiânia, Brasil.

Laguarda-Figueras A., Solís-Marín F.A., Durán-González A., Hernández Pliego P. & Del Valle García R. 2001. Holoturoideos (Echinodermata: Holothuroidea) del Caribe mexicano: Puerto Morelos. *Avicennia* 14: 7–46.

Laguarda-Figueras A., Solís-Marín F.A., Durán-González A., Gust-Ahearn C., Buitrón-Sánchez B.E. & Torres-Vega J. 2005. Equinodermos (Echinodermata) del Caribe Mexicano. *Revista de Biología Tropical* 53 (3): 109–122.

Lessios H.A. 2007. Reproductive isolation between species of sea urchins. *Bulletin of Marine Science* 81: 191–208.

Lessios H.A. 2011. Speciation genes in free-spawning marine invertebrates. *Integrative and Comparative Biology* 51 (3): 456–465. https://doi.org/10.1093/icb/icr039

Lima P.N., Ventura R. & Campos S.L. 2003. Gonad morphology and gametogenesis of the sea cucumber *Isostichopus badionotus* from southeast Brazil. *Sixth European Conference on Echinoderms (ECE)*, Banyuls-sur-Mer, France.

Lloyd F.E. 1900. New York Academy of Sciences. Section of Biology. *Science* 12: 885. https://doi.org/10.1126/science.12.310.885

Lopez-Rocha J.A. 2011. Distribución y abundancia del pepino de mar *Isostichopus badionotus* frente a la Costa de Sisal Yucatán. *Proceedings of the 64th Gulf and Caribbean Fisheries Institute*: 153–160. Puerto Morelos, Mexico.

Lovatelli A., Conand C., Purcell S., Uthicke S., Hamel J-F. & Mercier A. (eds) 2004. *Advances in Sea Cucumber Aquaculture and Management.* FAO Fisheries Technical Paper 463, Food and Agriculture Organization (FAO), Rome.

Ludwig H. 1875. Beiträge zur Kenntniss der Holothurien. *Arbeiten aus dem Zoologisch-Zootomischen Institut in Würzburg* 2: 77–118. Available from https://www.biodiversitylibrary.org/page/34381203 [accessed 16 Apr. 2024].

Ludwig H. 1898. Holothurien. *Ergebnisse der Hamburger Magalhaensischen Sammelreise* 1: 1–98. https://doi.org/10.5962/bhl.title.63772

Luna-Fontalvo J., Rodríguez-Forero A. & Sarmiento-Rodríguez J. 2014. Microbiota aislada del pepino de mar (*Isostichopus badionotus*) nativo de la bahía de Taganga, Caribe colombiano. *INTROPICA* 9: 75–83. https://doi.org/10.21676/23897864.1441

Malay M.C.M.D. & Paulay G. 2010. Peripatric speciation drives diversification and distributional pattern of reef hermit crabs (Decapoda: Diogenidae: *Calcinus*). *Evolution* 64: 634–662. https://doi.org/10.1111/j.1558-5646.2009.00848.x

Maluf L.Y. 1988. Composition and distribution of the central eastern Pacific echinoderms. *Natural History Museum Los Angeles County, Technical Report* 2: 1–242.

Martínez V., Hernández W., Turizo M., Caro L. & Rodríguez A. 2016. *Manual para el Cultivo y Procesamiento de Pepino de Mar.* Editorial Universidad del Magdalena, Santa Marta, Colombia. https://doi.org/10.2307/j.ctt1zgwmmb

Martins L., Souto C., Braga J. & Tavares M. 2016. Echinoidea and Holothuroidea (Echinodermata) of the Trindade and Martin Vaz Archipelago, off Brazil, with new records and remarks on taxonomy and species composition. *Journal of the Marine Biological Association of the United Kingdom* 98 (3): 521–555. https://doi.org/10.1017/S0025315416001569

McMillan W.O., Weigt L.A. & Palumbi S.R. 1999. Color pattern evolution, assortative mating, and genetic differentiation in brightly colored butterflyfishes (Chaetodontidae). *Evolution* 53: 247–260. https://doi.org/10.2307/2640937

McNab J. & Rogers A. 2017. Holothuroidea species found in Belizean waters. *SPC Beche-de-mer Information Bulletin* 37: 111–114.

Medina-Lambrano K., Ortiz E. & Rodríguez-Forero A. 2017. Variación de la composición proximal del pepino de mar *Isostichopus* sp. aff *badionotus*, en el Caribe colombiano. *Book of Abstracts Latin American & Caribbean Aquaculture 2017*: 175. Mazatlán, México.

Mercier A., Hidalgo R.Y. & Hamel J.F. 2004. Aquaculture of the Galapagos sea cucumber *Isostichopus fuscus*. *In*: Lovatelli A., Conand C., Purcell S., Uthicke S., Hamel J-F. & Mercier A. (eds) *Advances in Sea Cucumber Aquaculture and Management*: 347–358. Food and Agriculture Organization (FAO), Rome.

Mercier A., Ycaza R.H. & Hamel J.F. 2007. Long-term study of gamete release in a broadcast-spawning holothurian: predictable lunar and diel periodicities. *Marine Ecology Progress Series* 329 (1):179–189. https://doi.org/10.3354/meps329179

Mercier A., Hamel J.F., Toral-Granda V., Alvarado J.J., Ortiz E.P. & Benavides M. 2013. *Isostichopus fuscus*. *The IUCN Red List of Threatened Species* 2013: e.T180373A1621878. Available from: http://doi.org/10.2305/IUCN.UK.2013-1.RLTS.T180373A1621878.en [accessed 2 Mar. 2020].

Michonneau F. 2015 (unpublished). Cryptic and not-so-cryptic species in the complex *Holothuria (Thymiosycia) impatiens* (Forsskål, 1775) (Echinodermata: Holothuroidea). *bioRxiv (The preprint server for biology)*. https://doi.org/10.1101/014225

Miller J.E. & Pawson D.L. 1984. Holothurians (Echinodermata: Holothuroidea). *Memoirs of the Hourglass Cruises* 7 (1): 1–79.

Miller A.K., Kerr A.M., Paulay G., Reich M., Wilson N.G., Carvajal J.I. & Rouse G.W. 2017. Molecular phylogeny of extant Holothuroidea (Echinodermata). *Molecular Phylogenetics and Evolution* 111: 110–131. https://doi.org/10.1016/j.ympev.2017.02.014

Netto L.F. 2006. *Echinodermata do Canal de São Sebastião (São Sebastião, SP)*. MSc Thesis, Instituto de Biociências, Universidade de São Paulo, Brasil.

Netto L.F., Hadel V.F. & Tiago C.G. 2005. Echinodermata from São Sebastião Channel (São Paulo, Brazil). *Revista de Biología Tropical* 53 (3): 207–218.

Nuno A., Metcalfe K., Godley B.J. & Broderick A.C. 2015. *Marine Conservation Priorities São Tomé and Príncipe Scoping Report*. University of Exeter.

Ortega M. 2015. *Evaluación de la Pesquería del Pepino de mar Isostichopus badionotus (Aspidochirotida: Stichopodidae), al Norte de la Isla de la Juventud, Cuba.* MSc Thesis, Instituto Politécnico Nacional, Cuba.

Ortega M. & Alfonso I. 2011. Abundancia y distribución del pepino de mar *Isostichopus badionotus* (Aspidochirotida: Stichopodidae), en seis localidades de pesca al norte de la Isla de la Juventud, Cuba. *Revista Cubana de Investigaciones Pesqueras* 28 (2): 8–14.

Palacios M.M. & Muñoz C.G. 2012. *Caracterización ecológica de 11 Sitios de Buceo en el Parque Nacional Natural Gorgona en el Marco del Estudio para la Determinación de la Capacidad de Carga Turística.* The Nature Conservancy, Parques Nacionales Naturales de Colombia y Aviatur, Colombia.

Palumbi S.R. 1996. Nucleic acids II: the polymerase chain reaction. *In*: Hillis D.M., Moritz C.M. & Mable B.K. (eds) *Molecular Systematics*: 205–247. Sinauer Associates, Sunderland, MA.

Pawson D.L. 1976. Shallow-water sea cucumber (Echinodermata: Holothuroidea) from Carrie Bow Cay, Belize. *Proceedings of the Biological Society of Washington* 89 (31): 369–382. Available from https://www.biodiversitylibrary.org/page/34553807 [accessed 16 Apr. 2024].

Pawson D.L. 1978. The echinoderm fauna of Ascension Island, South Atlantic Ocean. *Smithsonian Contributions to the Marine Sciences* 2: 1–31. https://doi.org/10.5479/si.01960768.2.1

Pawson D.L., Pawson D.J. & King R.A. 2010. A taxonomic guide to the Echinodermata of the South Atlantic Bight, USA: 1. Sea cucumbers (Echinodermata: Holothuridea). *Zootaxa* 2449: 1–48. https://doi.org/10.11646/zootaxa.2449.1.1

Pelegrín-Morales E., Siam-Lahera C., Arencibia-Carballo G. & Álvarez-Capote J.S. 2009. Valoración de la Bahía de Cabañas para el cultivo de pepino de mar *Isostichopus badionotus* en Cuba. *Revista electrónica de Veterinaria* 10 (10): 1–9.

Pérez-Ruzafa A., Entrambasaguas L. & Bacallado J.J. 1999. Fauna de equinodermos (Echinodermata) de los fondos rocosos infralitorales del archipiélago de Cabo Verde. *Revista de la Academia Canaria de Ciencias* 11 (3–4): 43–62.

Pérez-Ruzafa A., Entrambasaguas L., Marcos C., Bacallado J.J. & García-Charton J.A. 2003. Spatial relationships of the echinoderm fauna of Cabo Verde islands: a multi-scale approach. *In*: Féral J.-P. & David B. (eds) *Echinoderm Research 2001*: 31–39. Sweets & Zeitlinger, Lisse.

Pires-Nogueira R.L., Freire C.B., Rezende C.R. & Campos-Creasey L.S. 2001. Reproductive cycle of the sea cucumber *Isostichopus badionotus* (Echinodermata) from Baía da Ilha Grande, Rio de Janeiro, Brazil (abstract). *Abstracts of the 9th International Congress of Invertebrate Reproduction and Development*: 15–20. Rhodes University, Grahamstown, South Africa.

Poot-Salazar A., Hernández-Flores A. & Ardisson P.L. 2015. Indicadores de sostenibilidad para la evaluación de las pesquerías de pepino de mar en la península de Yucatán, México. *Ciencia Pesquera* 23 (2): 11–24.

Popovic I., Marko P.B., Wares J.P. & Hart M.W. 2014. Selection and demographic history shape the molecular evolution of the gamete compatibility protein bindin in *Pisaster* sea stars. *Ecology and Evolution* 4: 1567–1588. https://doi.org/10.1002/ece3.1042

Prata J., Manso C.L.C. & Christoffersen M. 2014. Aspidochirotida (Echinodermata: Holothuroidea) from the northeast coast of Brazil. *Zootaxa* 3889: 127–150. https://doi.org/10.11646/zootaxa.3889.1.8

Prieto-Ríos E. 2010. *Taxonomía de Holothuroidea (Echinodermata) del Mar del Perú.* BSc thesis, Universidad Nacional Mayor de San Marcos, Lima, Perú.

Puentes V., Escobar F.D., Polo C.J. & Alonso J.C. 2014. *Estado de los principales recursos pesqueros de Colombia – 2014.* Serie Recursos Pesqueros de Colombia – AUNAP, Oficina de generación del conocimiento y la información, Autoridad Nacional de Acuicultura y Pesca.

Purcell S.W. 2010. *Managing Sea Cucumber Fisheries with an Ecosystem Approach.* FAO Fisheries Technical Paper 520, Food and Agriculture Organization (FAO), Rome.

Purcell S.W., Samyn Y. & Conand C. 2012. *Commercially Important Sea Cucumbers of the World*. FAO Species Catalogue for Fishery Purposes 6, Food and Agriculture Organization (FAO), Rome.

Purcell S.W., Polidoro B.A., Hamel J.F., Gamboa R.U. & Mercier A. 2014. The cost of being valuable: predictors of extinction risk in marine invertebrates exploited as luxury seafood. *Proceedings of the Royal Society B* 281: 20133296. https://doi.org/10.1098/rspb.2013.3

Purcell, S.W., Lovatelli, A., González-Wangüemert, M., Solís-Marín, F.A., Samyn, Y. & Conand, C. 2023. *Commercially Important Sea Cucumbers of the World – Second edition*. FAO Species Catalogue for Fishery Purposes No. 6, Rev. 1. Rome, FAO. https://doi.org/10.4060/cc5230en

Reyes-Sánchez F.J., Puentes-Cañón G.M., Ramírez J.G., Ortiz-Gómez E.P. 2011. Primer registro de capturas de *Holothuria mexicana* y *Isostichopus badionotus*, mediante la pesquería artesanal en la zona de la media Guajira del Caribe colombiano, entre los meses comprendidos de junio de 2006 a junio de 2011. *Resúmenes Primer Congreso Latinoamericano de Equinodermos*: 174. Puerto Madryn, Argentina.

Rodríguez-Forero A., Agudelo-Martínez V.Y. & Vergara-Hernández W.O. 2013. First insight into Colombian Caribbean sea cucumbers and sea cucumber fishery. *SPC Beche-de-mer Information Bulletin* 33: 9–13.

Rodríguez-Gil L.A., Reyes-Sosa C.F., Giorgana-Figueroa J.L., Nahuat-Dzib S., Molina-Durán O.A. & Pérez-López I.A. 2015. La pesca del pepino de mar en Yucatán, México y el análisis del recurso desde su captura hasta su comercialización en dos cooperativas pesqueras. *Book of Abstracts 68th Annual Gulf and Caribbean Fisheries Institute*: 227. Panama City, Panama.

Rogers A. 2013. Density, abundance and distribution of sea cucumbers in Belize. *Proceedings of the 66th Gulf and Caribbean Fisheries Institute*: 1–4. Corpus Christie, TX.

Rogers A. 2018. Cultivo de pepino de mar *Holothuria floridana* y *Isostichopus badionotus* en antiguos estanques de camarones, un estudio de caso de Belice. *Book of Abstracts 71st Annual Gulf and Caribbean Fisheries Institute*: 233. San Andres Island, Colombia.

Rogers A., Hamel J.F. & Mercier A. 2017. From life-sustaining to life-threatening: the case of the sea cucumber fishery in Nicaragua. *SPC Beche-de-mer Information Bulletin* 37: 48–50.

Ronquist F. & Huelsenbeck J.P. 2003. MrBayes 3: Bayesian phylogenetic inference under mixed models. *Bioinformatics* 19: 1572–1574. https://doi.org/10.1093/bioinformatics/btg180

Samyn Y. 2000. Conservation of aspidochirotid holothurians in the littoral waters of Kenya. *SPC Beche-de-mer Information Bulletin* 13: 12–17.

Samyn Y. 2013. *Isostichopus macroparentheses*. *The IUCN Red List of Threatened Species* 2013: e.T180313A1613882.
Available from https://doi.org/10.2305/IUCN.UK.2013-1.RLTS.T180313A1613882.en [accessed 2 Mar. 2020].

Samyn Y., Appeltans W. & Kerr A. 2005. Phylogeny of *Labidodemas* and the Holothuriidae (Holothuroidea: Aspidochirotida) as inferred from morphology. *Zoological Journal of the Linnean Society* 144: 103–120. https://doi.org/10.1111/j.1096-3642.2005.00158.x

Samyn Y., VandenSpiegel D. & Massin C. 2006. *Taxonomie des holothuries des Comores*. AbcTaxa 1, Série de Manuels dédiés aux Renforcements des Capacités en Taxonomie et en Gestion des Collections, Royal Belgian Institute of Natural Sciences, Brussels, Belgium.

Sarkis S. 2015. Culturing the four-sided sea cucumber, *Isostichopus badionotus*, in Bermuda: a tool for conserving its natural populations. *Book of Abstracts 68th Annual Gulf and Caribbean Fisheries Institute*: 243. Panama City, Panama.

Schneider C.A., Rasband W. S. & Eliceiri K.W. 2012. NIH Image to ImageJ: 25 years of image analysis. *Nature Methods* 9 (7): 671–675. https://doi.org/10.1038/nmeth.2089

Selenka E. 1867. Beiträge zur Anatomie und Systematik der Holothurien. *Zeitschrift für wissenschaftliche Zoologie* 17 (2): 291–374. Available from https://www.biodiversitylibrary.org/page/45007590 [accessed 16 Apr. 2024].

Semper C. 1867–1868. Holothurien. *In*: Semper C. (ed.) *Reisen im Archipel der Philippinen. Zweiter Theil. Wissenschaftliche Resultate. Erster Band*. W. Engelmann, Leipzig. https://doi.org/10.5962/bhl.title.11687

Shepherd S.A., Toral-Granda M.V. & Edgar G.J. 2003. Estimating the abundance of clustered and cryptic marine macro-invertebrates in the Galapagos with particular reference to sea cucumbers. *Noticias de Galápagos* 62: 36–39.

Shepherd S.A., Martínez P., Toral-Granda M.V. & Edgar G.J. 2004. The Galapagos sea cucumber fishery: management improves as stocks decline. *Environmental Conservation* 31 (2): 102–110. https://doi.org/10.1017/S0376892903001188

Shiell G. 2004. Field observations of juvenile sea cucumbers. *SPC Beche-de-mer Information Bulletin* 20: 6-11.

Sluiter C.P. 1910. Westindische Holothurien. *Zoologische Jahrbücher Jena Supplement* 11: 331–342.

Solís-Marín F.A., Arriaga-Ochoa J.A., Laguarda-Figueras A., Frontana-Uribe S.C. & Durán-González A. 2009. *Holoturoideos (Echinodermata: Holothuroidea) del Golfo de California*. Jiménez Editores e Impresores, Distrito Federal, México.

Steinbeck J. & Ricketts E. 1941. *Sea of Cortez. A Leisurely Journal of Travel and Research.* The Viking Press, New York.

Sunday J.M. & Hart M.W. 2013. Sea star populations diverge by positive selection at a sperm-egg compatibility locus. *Ecology and Evolution* 3: 640–654. https://doi.org/10.1002/ece3.487

Tagliafico A., Rangel M.S. & Rago N. 2011. Distribución y densidad de dos especies de holoturoideos en la isla de Cubagua, Venezuela. *Revista de Biología Tropical* 59 (2): 843–852. https://doi.org/10.15517/rbt.v0i0.3144

Théel H. 1886. Report on the Holothurioidea dredged by H.M.S. Challenger during the years 1873–76, Part II. *Report on the Scientific Results of the Voyage of H.M.S. Challenger during the years 1873–76 Zoology* 14 (39): 1–290. https://doi.org/10.5962/bhl.title.6513

Thompson J.D., Higgins D.G. & Gibson T.J. 1994. CLUSTAL W: improving the sensitivity of progressive multiple sequence alignment through sequence weighting, position-specific gap penalties and weight matrix choice. *Nucleic Acids Research* 22 (22): 4673–4680. https://doi.org/10.1093/nar/22.22.4673

Tikasingh E.S. 1963. The shallow water Holothurians of Curaçao, Aruba and Bonaire. *Studia Fauna Curaçao* 14: 77–99.

Toral-Granda M.V. 2005. Requiem for the Galapagos sea cucumber fishery? *SPC Beche de-Mer Information Bulletin* 21: 5–8.

Toral-Granda M.V. 2006. Fact sheets and identification guide for commercial sea cucumber species. *SPC Beche-de-mer Information Bulletin* 24: 49–52.

Toral-Granda M.V. 2008a. Population status, fisheries and trade of sea cucumbers in Latin America and the Caribbean. *In*: Toral-Granda V., Lovatelli A. & Vasconcellos M. (eds) *Sea Cucumbers. A Global Review of Fisheries and Trade*: 213–229. Food and Agriculture Organization (FAO), Rome.

Toral-Granda M.V. 2008b. Galapagos Islands: a hotspot of sea cucumber fisheries in Central and South America. *In*: Toral-Granda V., Lovatelli A. & Vasconcellos M. (eds) *Sea Cucumbers. A Global Review of Fisheries and Trade*: 231–253. Food and Agriculture Organization (FAO), Rome.

Toral-Granda M.V. & Martínez P.C. 2004. Population density and fishery impacts on the sea cucumber (*Isostichopus fuscus*) in the Galapagos marine reserve. *In*: Lovatelli A., Conand C., Purcell S., Uthicke S., Hamel J-F. & Mercier A. (eds) *Advances in Sea Cucumber Aquaculture and Management*: 91–100. Food and Agriculture Organization (FAO), Rome.

Toral-Granda M.V. & Martínez P.C. 2007. Reproductive biology and population structure of the sea cucumber *Isostichopus fuscus* (Ludwig, 1875) (Holothuroidea) in Caamaño, Galapagos Islands, Ecuador. *Marine Biology* 151: 2091–2098. https://doi.org/10.1007/s00227-007-0640-1

Toral-Granda M.V., Lovatelli A. & Vasconcellos M. (eds) 2008. *Sea Cucumbers. A Global Review of Fisheries and Trade*. FAO Fisheries Technical Paper 516, Food and Agriculture Organization (FAO), Rome.

Toral-Granda M.V, Alvarado J.J., Hamel J.-F., Mercier A., Benavides M. & Paola Ortiz E. 2013. *Isostichopus badionotus* (errata version published in 2016). *The IUCN Red List of Threatened Species* 2013: e.T180519A102420305. https://doi.org/10.2305/IUCN.UK.2013-1.RLTS.T180519A1642750.en

Tsang S.M., Cirranello A.L., Bates P.J.J. & Simmons N.B. 2018. The roles of taxonomy and systematics in bat conservation. *In*: Voigt C.C. & Kingston T. (eds) *Bats in the Anthropocene: Conservation of Bats in a Changing World*: 503–538. Springer, Cham. https://doi.org/10.1007/978-3-319-25220-9_16

Uthicke S., Byrne M. & Conand C. 2010. Genetic barcoding of commercial bêche-de-mer species (Echinodermata: Holothuroidea). *Molecular Ecology Resources* 10 (4): 634–646. https://doi.org/10.1111/ j.1755-0998.2009.02826

Vergara W. & Rodríguez A. 2015. Histología del tubo digestivo de tres especies de pepino de mar *Isostichopus badionotus*, *Isostichopus* sp. y *Stichopus hermanni* (Aspidochirotida: Stichopodidae). *Revista de Biología Tropical* 63 (4): 1021–1033. https://doi.org/10.15517/rbt.v63i4.16887

Vergara W. & Rodríguez A. 2016. Nutritional composition of sea cucumber *Isostichopus* sp. *Natural Resources* 7: 130–137. https://doi.org/10.4236/nr.2016.73013

Vergara W., Agudelo V. & Rodríguez A. 2016. Observations of *Carapus bermudensis* (Carapidae) in *Isostichopus badionotus* (Stichopodidae) from Taganga Bay, Colombia. *SPC Beche-de-mer Information Bulletin* 36: 90–91.

Vergara W., Agudelo V., Castro L.R. Rodríguez A. & Eeckhaut I. 2018. Morphological and molecular characterization of *Isostichopus* sp. in the Colombian Caribbean Sea. *Journal of Basic and Applied Genetics* 29 (2): 33–48. https://doi.org/10.35407/bag.2018.29.02.04

Vergara-Chen C., Guerra Z. & Collado G.N. 2015. El pepino de mar, *Isostichopus fuscus*, recurso marino en peligro con altas necesidades de manejo. *Tecnociencias* 17 (2): 21–41.

Wakida-Kusunoki A.T., Poot-Salazar A. & Mena-Loria J.D.R. 2016. First record of albinism in three-rowed sea cucumber, *Isostichopus badionotus*. *Bulletin of Marine Science* 92: 285–290. https://doi.org/10.5343/bms.2015.1051

Wen J., Hu C., Zhang L. & Fan S. 2011. Genetic identification of global commercial sea cucumber species on the basis of mitochondrial DNA sequences. *Food Control* 22: 72–77. https://doi.org/10.1016/j.foodcont.2010.06.010

Wirtz P., Menut T., Bérenger L., Prat M., Louisy P. & Roquefort C. 2020. New records of marine invertebrates from the coast of Gabon, Eastern Atlantic. *Les Cahiers de la Fondation Biotope* 32: 1–41.

WoRMS 2020. *Stichopus ecnomius* Clark, 1922. Available from https://www.marinespecies.org/aphia.php?p=taxdetails&id=529219 [accessed 2 Mar. 2020].

Zacarías-Soto M., Olvera-Novoa M.A., Pensamiento-Villarauz S. & Sánchez-Tapia I. 2013. Spawning and larval development of the four-sided sea cucumber, *Isostichopus badionotus* (Selenka, 1867), under controlled conditions. *Journal of the World Aquaculture Society* 44 (5): 694–705. https://doi.org/10.1111/jwas.12061

Zetina C., Ríos G., Hernández I., Guevara M., Ortiz E. & Pool J. 2002. *Catálogo de Especies de Pepinos de Mar Comercializables del Estado de Yucatán*. Ediciones de la Universidad Autónoma de Yucatán, Mérida, Yucatán, Mexico.

Zigler K.S. & Lessios H.A. 2003. Evolution of bindin in the pantropical sea urchin *Tripneustes*: comparisons to bindin of other genera. *Molecular Biology and Evolution* 20: 220–231. https://doi.org/10.1093/molbev/msg020

Zigler K.S., Byrne M., Raff E.C., Lessios H.A. & Raff R.A. 2012. Natural hybridization in the sea urchin genus *Pseudoboletia* between species without apparent barriers to gamete recognition. *Evolution* 66 (6): 1695–1708. https://doi.org/10.1111/j.1558-5646.2012.01609.x

Manuscript received: 30 January 2024
Manuscript accepted: 9 February 2024
Published on: 30 August 2024
Topic editor: Magalie Castelin
Section editor: Didier VandenSpiegel
Desk editor: Pepe Fernández